Adv Polym Sci (2011) 235: 33–110
DOI:10.1007/12_2009_48

Published online: 23 March 2010

Conjugated Organosilicon Materials for Organic Electronics and Photonics

Sergei A. Ponomarenko and Stephan Kirchmeyer

Abstract In this chapter different types of conjugated organosilicon materials possessing luminescent and/or semiconducting properties will be described. Such macromolecules have various topologies and molecular structures: linear, branched and hyperbranched oligomers, polymers, and dendrimers. Specific synthetic approaches to access these structures will be discussed. Special attention is devoted to the role of silicon in these structures and its influence on their optical and electrical properties, leading to their potential application in the emerging areas of organic and hybrid electronics.

Keywords Anthradithiophene · Dendrimer · Electroluminescence · Oligothiophene · Organic field-effect transistor (OFET) · Organic light-emitting diode (OLED) · Organic solar cells · Pentacene · Photoluminescence · Poly(1 · 4-phenylene vinylene) · Silafluorene · Silole

Contents

S.A. Ponomarenko
Enikolopov Institute of Synthetic Polymeric Materials of Russian Academy of Sciences (ISPM RAS), Profsoyuznaya st. 70, Moscow 117393, Russia
e-mail: ponomarenko@ispm.ru

S. Kirchmeyer (✉)
H.C. Starck Clevios GmbH, Chempark Leverkusen, Building B 202, Leverkusen 51368, Germany
e-mail: stephan.kirchmeyer@hcstarck.com

Abbreviations

[C70]PCBM	([6,6]-Phenyl C71-butyric acid methyl ester)
2T	2,2′-Bithiophene
3AC	Anthracene
3D	Three-dimensional
3T	2,2′ : 5′,2″-Terthiophene
4AC	Tetracene
4T	2, 2′:5′, 2″:5″, 2‴-Quaterthiophene
5AC	Pentacene
5T	2,2′:5′, 2″ : 5″, 2‴:5‴, 2⁗-Quinquethiophene
6T	2,2′:5′, 2:5″, 2‴:5‴, 2⁗:5⁗, 2⁗′-Sexithiophene
7T	2,2′:5′, 2″:5″, 2‴:5‴, 2⁗:5⁗, 2⁗′:5⁗′, 2⁗″-Septithiophene
η_{EL}	External electroluminescence quantum efficiency
Φ_F	Luminescence quantum yield
Ac	Acetyl
ADT	Anthradithiophene
AFM	Atomic force microscopy
AIE	Aggregation induced emission
Alq_3	Tris(8-quinolinolato) aluminum(III) complex
BS	Dibenzosilole
Bu	*n*-Butyl
*t*Bu	*tert*-Butyl
n-BuLi	*n*-Butyl lithium
t-BuLi	*tert*-Butyl lithium
CEE	Cooling-enhanced emission
CIE	International Commission on Illumination
CV	Cyclic voltammogram
Cz	Carbazolyl
D–A complex	Donor–acceptor complex
Dec	*n*-Decyl
DFT	Density functional theory
DMS	Dimethylsilyl
DMSO	Dimethyl sulfoxide
DSC	Differential scanning calorimetry
EDOT	3,4-Ethylenedioxythiophene

EL	Electroluminescence
Et	Ethyl
ET	Electron transport
eV	Electron volt
$Fe(acac)_3$	Iron(III) acetylacetonate
FET	Field-effect transistor
FF	Fill factor
HB	Hyperbranched
Hex	*n*-Hexyl
HOMO	Highest occupied molecular orbital
HTL	Hole-transporting layer
IP	Ionization potential
I_{sc}	Short circuit current
ITO	Indium tin oxide
LDA	Lithium di(iso-propyl)amide
LEC	Light-emitting electrochemical cell
LOPV	Ladder oligo(*p*-phenylenevinylene)
LUMO	Lowest unoccupied molecular orbital
MALDI–TOF	Matrix assisted laser desorption ionization–time-of-flight mass spectrometry
Me	Methyl
MEH-PPV	Poly[2-methoxy-5-(2′-ethyl-hexyloxy)-1,4-phenylene vinylene]
M_n	Number-averaged molecular weight
M_w	Weight-averaged molecular weight
$NiCl_2$(dppe)	1,2-Bis(diphenylphosphino)ethane nickel(II) chloride
NIR	Near infrared
NPB	N,N'-Bis(1-naphthyl)-N,N'-diphenylbenzidine
NPD	4,4′-Bis[*N*-1-naphthyl-*N*-phenylamino]-biphenyl
Oct	*n*-Octyl
OEt	Ethoxy
OFET	Organic field-effect transistor
OLED	Organic light-emitting diode
OligoT	Oligothiophene
OMe	Methoxy
OPV	Organic photovoltaics
OTFT	Organic thin film transistor
P3HT	Poly(3-hexylthiophene)
PBD	2-(4-Biphenylyl)-5-(4-*tert*-butylphenyl)-1,3,4-oxadiazole
PCBM	[6,6]-Phenyl C61-butyric acid methyl ester
PCE	Power conversion efficiency
PEDOT	Poly(3,4-ethylenedioxythiophene)
PF	Polyfluorene
Ph	Phenyl
PL	Photoluminescence
PMMA	Poly(methyl methacrylate)

PPV	Poly(1,4-phenylene vinylene)
ppy	2-Phenylpyridine
PS	Polystyrene
PSS	Poly(styrene sulfonate)
PTV	Polythiophenevinylene
PVK	Poly(*N*-vinyl carbazole)
Py	Pyridyl
SAM	Self-assembled monolayer
SAMFET	Self-assembled monolayer field-effect transistor
SBAr	Silicon-bridged biaryl
SCE	Saturated calomel electrode
SiF	Silafluorene
T	Thienyl
TES	Triethylsilyl
TGA	Thermal gravimetric analysis
TIPS	Triisopropylsilyl
TMS	Trimethylsilyl
TPD	N,N'-Diphenyl-N,N'-di(*m*-tolyl)biphenyl-4,4′-diamine
TPS	Triphenylsilyl
TPSppy	2-(4′-(Triphenylsilyl)biphenyl-3-yl)pyridine
TS	Dithienosilole
TVS	Trivinylsilyl
Und	*n*-Undecyl
UV-vis	Ultraviolet-visible
V_{oc}	Open-circuit voltage

1 Introduction

Organic electronics has been a fast growing field of science and technology since the beginning of the twenty-first century [1, 2]. It is designed for cost efficient and flexible lightweight large area devices, the basic units of which are organic field-effect transistors (OFETs), also known as organic thin film transistors (OTFTs) [3], organic light-emitting diodes (OLEDs) [4], and organic photovoltaic cells (OPVs) or solar cells [5–7]. They can also be combined with sensing elements [8] lasers, etc. In general, these devices are not intended to outperform contemporary inorganic (silicon) electronics. They will have lower performance due to material limitations, e.g., reduced charge carrier mobility in OTFT will limit the ability to process high frequencies. However, organic electronics will have its own market niche based on its flexibility, low weight, and, eventually, low cost as a result of substitution of expensive lithography, wet processing, and other technologies used in conventional silicon electronics by cheap roll-to-roll, ink-jet, gravure, or other printing techniques.

A major difference between silicon and organic electronics concerns the electronic structure of the semiconducting materials employed. Silicon as semiconductor is doped with elements like boron or phosphorus, which determines the type

of charge carrier by introduction of excess electrons or holes. In organic intrinsic (undoped) semiconductors HOMO–LUMO energy levels and their relative positions to the corresponding energy levels of the electrodes – ionization potentials (IPs) determine the type of the main charge carriers. As a consequence, the chemical structure of the organic semiconductor strongly influences whether an organic semiconductor is p-type (hole conducting) or n-type (electron conducting).

Conjugated organosilicon materials with semiconducting properties resemble a broad class of "organic" rather than silicon semiconductors. As typical for intrinsic organic semiconductors, the introduction of silicon atoms into the conjugated organic structure changes the HOMO–LUMO energy levels and influences their optical and semiconducting properties. Prerequisite is a direct covalent linkage between the silicon atom and the organic conjugated core. Nevertheless, in addition to conjugated structural parts, most organic semiconductors contain nonconjugated groups, which influence solubility, aggregation, crystallization, and film-forming properties. Therefore, another option is to attach organosilicon fragments to units which do not interact electronically with the chromophore but improve self-organization and morphology of the semiconductor during processing. Such an approach might be especially important for solution processing techniques. Direct conjugated linkage of silicon to chromophores might also impact the morphology, especially in the case of (hyper)branched or dendritic molecules, where silicon acts as the branching centers, but in comparison to electronic effects morphology effects are usually less dominant.

In the following, different types of conjugated organosilicon materials will be discussed which differ in topology and molecular structure: linear, branched, and hyperbranched (HB) polymers, oligomers, and dendrimers. This will comprise all materials containing conjugated organosilicon or organic units as well as silicon atoms or organosilicon fragments in the same molecular structure without direct electronic interaction.

2 Linear Conjugated Organosilicon Oligomers

Among linear conjugated organosilicon oligomers, two classes of molecules can be distinguished, which were widely investigated and show promising semiconducting and luminescent properties: (1) silicon-containing thiophene oligomers and (2) organosilicon oligoacene derivatives. It should be noted that oligothiophenes and oligoacenes (especially pentacene) themselves are among the best organic semiconductors [9, 10]. Modification with silicon will add specific features to their properties which will be discussed in the following. Apart from that, the introduction of silicon into aromatic structures creates a new building block which can be used to construct conjugated oligomers and polymers: a silacyclopentadiene also called "silole." Oligomers based on silole itself as well as its most important derivatives, such as dibenzosilole (BS) and dithienosilole (TS) and more recently developed silicon analogs of oligo(*p*-phenylenevinylenes), also open opportunities for new electronic properties.

2.1 Silicon-Containing Thiophene Oligomers

The synthesis of silicon-containing thiophene oligomers was comprehensively reviewed in 1997 [11]. In the scope of this chapter we will consider recent and most important examples of these materials and their application in organic electronics and photonics.

In contrast to benzene, thiophene itself shows no luminescence, but it's oligomers starting from 2,2′-bithiophene (2T) are luminescent and may find applications in organic photonics and electronics. Among α,α′-oligothiophenes the luminescence quantum yield (Φ_F) increases with increasing conjugation length and is accompanied by a significant red shift of the luminescence maximum. The addition of silylene or disilylene units to the α,α′-position will significantly increase Φ_F of linear 2T- and 3T-derivatives, but decreases Φ_F for 6T-derivatives as compared to pristine oligothiophenes. Hadziioannou and coworkers have reported a series of trimethylsilyl- and pentamethyldisilanyl-oligothiophenes (Fig. 1) [12]. The fluorescence quantum yield Φ_F for these molecules reached 23% for Me_3Si-T2-Si_2Me_5 compared to 1–2% measured for 2T; in contrast, the Φ_F for 6T (32%) exceeded the value for Me_3Si-T6-Oct_2SiMe_3 (25%) (Fig. 2). Bearing in mind that the fluorescence maxima of oligothiophenes strongly depend on their conjugation length, substitution of the oligothiophenes with organosilicon units may help to tune its spectral characteristics and efficiency.

α-Trimethylsilyl groups can be easily cleaved from oligothiophene units either chemically to the corresponding oligomers [13] or electrochemically to yield polymers [14, 15]. Silyl substituents with longer alkyl groups seem to be more

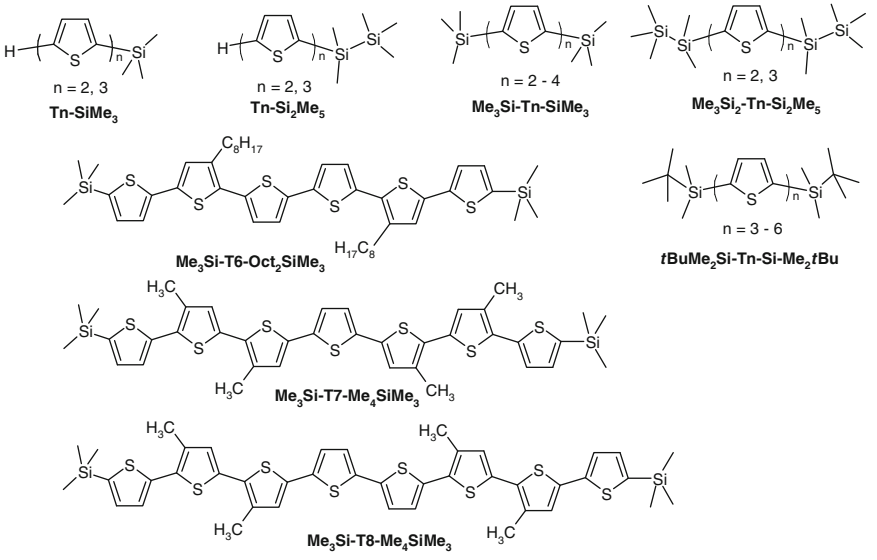

Fig. 1 Silylated oligothiophenes

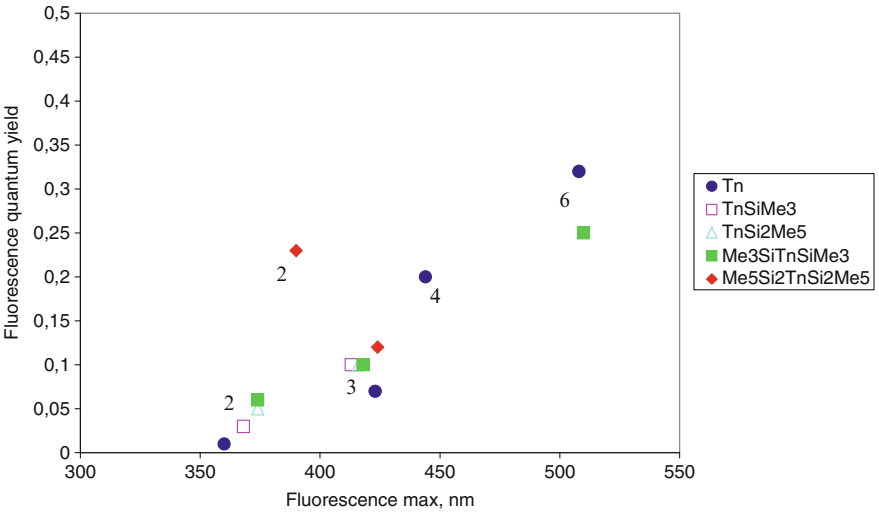

Fig. 2 Fluorescence quantum yield Φ_F vs fluorescence wavelength maximum for a series of oligothiophenes and their organosilicon derivatives (based on data from [12]). Number of conjugated thiophene units is marked on the chart near the corresponding data set

stable: a series of α,α'-bis(dimethyl-*tert*-butylsilyl) oligothiophenes *t*BuMe$_2$Si-Tn-Si-Me$_2$*t*Bu (n = 3–6) was reported by Barbarella et al. (Fig. 1) [16]. The quater- and sexithienylsilanes were prepared by Fe(acac)$_3$ (iron(III) acetylacetonate) mediated oxidative coupling of corresponding lithium derivatives, while quinquethienylsilane was obtained by the Stille reaction. All oligomers were highly soluble in most organic solvents which allowed their easy synthesis and purification. Vacuum-evaporated thin films of the oligomers with n = 4–6 displayed field-effect transistor activity, with charge mobilities increasing with the substrate deposition temperatures. The best OFET performance was achieved from the quinquethiophenesilane *t*BuMe$_2$Si-T5-Si-Me$_2$*t*Bu, which was characterized to have a mobility up to $2 \times 10^{-4}\,cm^2\,V^{-1}\,s^{-1}$ and an on/off ratio greater than 10^3 combined with good device stability in air for several months. The lower mobility of these oligomers compared to α,α'-dialkyloligothiophenes (i.e., $0.5\,cm^2\,V^{-1}\,s^{-1}$ for Dec-6T-Dec [17] or $1.1\,cm^2\,V^{-1}\,s^{-1}$ for Et-6T-Et) [18] can be explained by a significant steric hindrance caused by bulky triisopropylsilyl groups. This is evidenced by unusual triclinic crystallization of these compounds, in which the conjugated backbone shows strong deviation from coplanarity [19].

Many examples reported in the literature evidence an improved solubility of organosilicon modified oligothiophenes when compared to their unmodified derivatives. It was found that α-trimethylsilyl substituents will increase the solubility of bi-, ter-, and quaterthiophenes. More bulky α-dimethyl-*tert*-butylsilyl substituents improve the solubility up to a chromophore length of sexithiophenes. In order to synthesize soluble oligothiophenes with longer chromophores (i.e., septi- and octithiophenes, see Fig. 1), additional modifications will be necessary, e.g., by adding

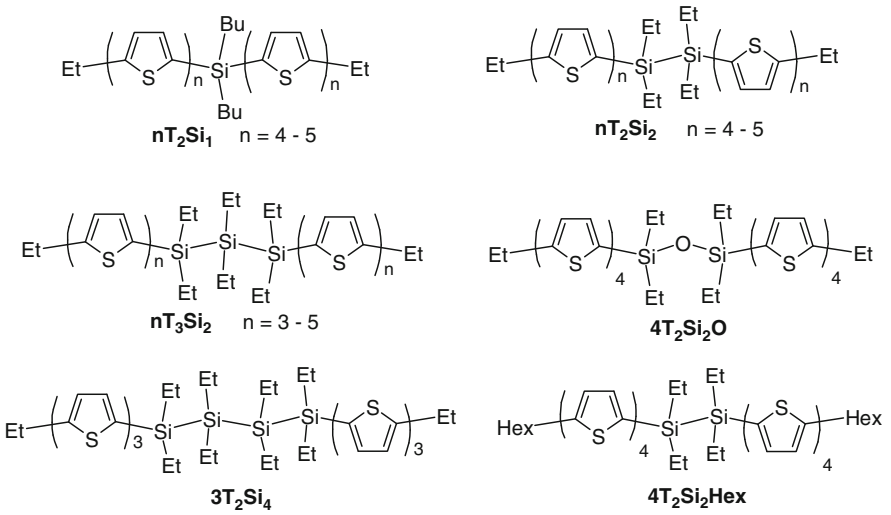

Fig. 3 Oligothiophenesilane dimers

several additional 3-methylsubstituents to the thiophene rings. However, adjacent trimethylsilyl groups to 3-methylthien-2,5-diyl units will quickly cleave from the core unit [13].

Ohshita et al. have reported on a series of oligothiophenesilane dimers bridged by mono-, bi-, or trisilanylene units with the intention to trace the influence of σ–π conjugation between the oligothiophene units and the silanylene bridge on the semiconducting properties of these materials (Fig. 3) [20, 21]. The FET mobilities of vapor-deposited films in top contact OFETs were found to be enhanced with the oligothiophene chain length and reached $5.1 \times 10^{-2}\,\mathrm{cm^2\,V^{-1}\,s^{-1}}$ for $5T_2Si_3$. This tendency follows the trend of unmodified oligothiophenes, which behave similarly [22]. In summary the influence of the silylene units is not well pronounced. On the one hand, in a series of quinquethiophenesilane dimers with different silylene bridges ($5T_2Si_x$) no clear influence of the Si-chain length on the charge carrier mobility was found. On the other hand, in a series of quaterthiophenes the charge carrier mobility of films was increased in the row $4T_2Si_3 < 4T_2Si_2O < 4T_2Si_2$. This indicates a σ–π conjugation between the oligothiophene units and the silanylene bridge of lesser importance than it was expected, and a major influence of other factors, such as film morphology and molecular alignment in the solid film. Quaterthiophenesilane dimers were sufficiently soluble in organic solvents in order to make solution-processed OFETs by spin-coating. While $4T_2Si_3Hex$ did not yield any FET mobility, the mobilities of wet coated films of $4T_2Si_3$ were an order of magnitude higher than for vapor evaporated films ($\mu = 4.1 \times 10^{-3}$ and $2.9 \times 10^{-4}\,\mathrm{cm^2\,V^{-1}\,s^{-1}}$, respectively). Quinquethiophenesilanes were hardly soluble in organic solvents, making it impossible to process films by spin-coating.

Another type of linear silicon-containing thiophene oligomers are monochlorosilyl derivatives of dialkyloligothiophenes Cl-Si-Spacer-OligoT-End (Fig. 4) [23, 24].

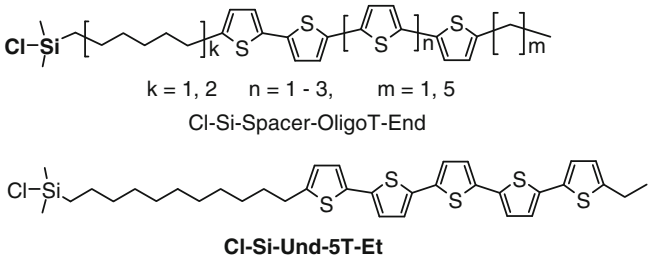

Fig. 4 Monochlorosilyl derivatives of dialkyloligothiophenes: general structure and the most promising material

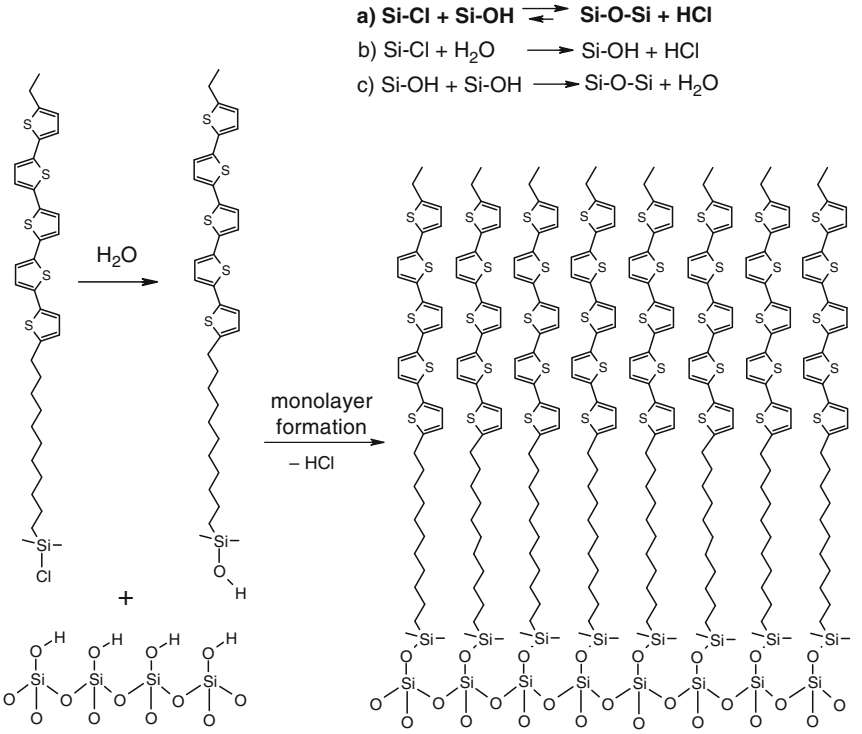

Scheme 1 Schematic representation of a SAM formation by Cl-Si-Und-5T-Et on SiO_2

Each of these structures contains the reactive monochlorosilyl group Si–Cl, attached to a semiconducting oligothiophene unit OligoT via flexible aliphatic spacers. Such molecular structures allow crystalline self-assembling monolayers (SAMs) to form on dielectric hydroxylated silicon dioxide [25] or even on oxidated polymer surfaces [26] by self-assembly from solution. A schematic representation of the SAM formation is shown in Scheme 1. Obviously the following factors play crucial roles: (1) the reversibility of the reaction of monochlorosilane with silanole, (2) a strong

π–π interactions between the oligothiophene chromophores, and (3) the presence of the aliphatic spacers between the reactive group and the oligothiophene cores, which facilitates crystallization.

The oligothiophene SAMs reveal excellent semiconducting properties similar to those of bulk oligothiophenes. Even under ambient conditions SAM semiconductors assembled from solution to form monolayers and yield field-effect transistors (SAMFETs) with a mobility of up to $0.04\,cm^2\,V^{-1}\,s^{-1}$ and on/off ratio up to 1×10^8 for 40 μm channel length devices [25]. In a series of the molecules with the structure Cl-Si-Spacer-OligoT-End the mobility increased by a factor of 10 from 4T to 5T oligothiophene units and by a factor of 2–3 with increasing spacer length [24]. It should be noted that the first oligothiophene SAMFETs prepared from nonsilicon-containing bifunctional ter- or quaterthiophenes on organosilicon modified silica or alumina surfaces worked for submicron channel length transistors only, and only in a few cases showed reasonable mobility: $0.0035\,cm^2\,V^{-1}\,s^{-1}$ for quaterthiophene and $8 \times 10^{-4}\,cm^2\,V^{-1}\,s^{-1}$ for terthiophene, with the on/off ratio up to 1,800 [27]. However, the more recent approach using Cl-Si-Und-5T-Et assembled on silica was proven to be highly efficient: it was possible to make fully functional SAMFET-based functional 15-bit Code Generators containing over 300 SAMFETs (Fig. 5) with all SAMFETs working simultaneously and with equal (or at least very close) electrical characteristics [28].

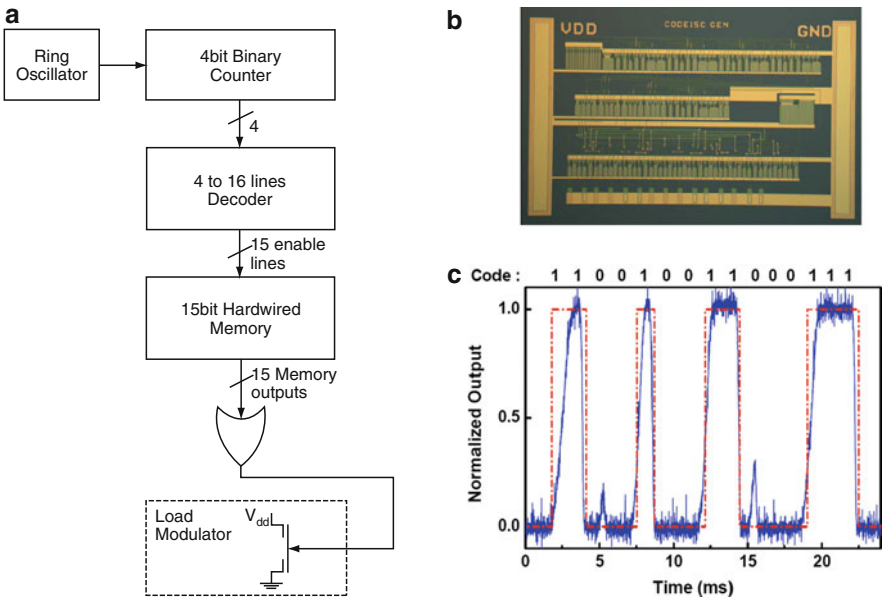

Fig. 5 SAMFET-based functional 15-bit code generator: block diagram (**a**), optical microphotograph (**b**), and output characteristics (**c**). The bit rate was about $1\,kBit\,s^{-1}$ at a supply voltage of −40 V. The outputted code is indicated at the top and by the *red line* [28]

In all types of linear Si-containing thiophene oligomers, a strong influence of silicon atoms on electronic and optical properties of the oligothiophenes was found, especially for oligomers with shorter chromophores such as bi- and terthiophenes. The introduction of silicon substituents has a more pronounced influence on their solubility and thin film morphology, independent of the presence of electronic coupling between the Si atom and oligothiophene core. Unique properties of organosilicon SAM oligothiophenes pave the way to bottom up organic electronics.

2.2 Organosilicon Oligoacene Derivatives

Various oligoacene derivatives have been modified with organosilicon units by Anthony and other groups [29]. Unlike oligothiophenes with the most reactive protons at the α positions, oligoacenes have reactive sites at the center benzene units, which can be easily modified with various organosilicon groups. In order to release steric interactions between the bulky silane groups and the chromophoric oligoacenes, the silane groups are usually attached via acelylenic extension units.

Anthracene and its derivatives are known for their good luminescence properties. Anthracene can be substituted at 9,10-positions to yield the triisopropylsilylethynyl derivative TIPS-3AC (Fig. 6). This compound crystallizes in films, which can be used as emitter in simple OLED devices showing an intense blue emission with a maximum luminance of 1,000 $cd\,m^{-2}$, an efficiency of 1.7 $cd\,A^{-1}$ at a luminance of 100 $cd\,m^{-2}$ and a bias voltage of 7.8 V [30]. Attachment of two methoxy groups to the chromophore of TIPS-3AC leads to the crystalline compound TIPS-3AC-OMe_2. The decreased π–π interaction increases the stacking distance from 3.7 to 5.7 Å, which surprisingly does not significantly alter the OLED performance (1.4 $cd\,A^{-1}$ at a brightness of 100 $cd\,m^{-2}$ and bias voltage of 7.0 V). When the triisopropylsilylethynyl substituents are shifted to 1,4-positions in the anthracene

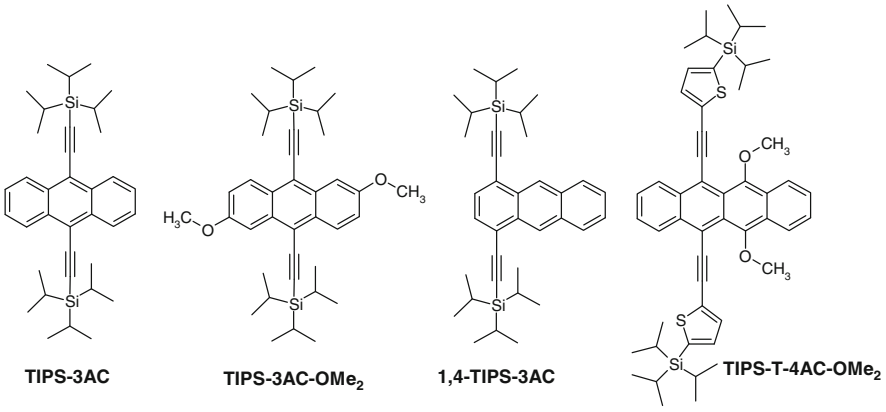

Fig. 6 Triisopropylsilyl-modified oligoacenes for OLEDs

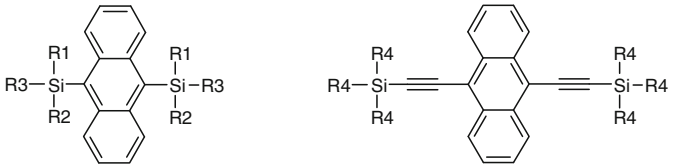

M3S-3AC: R1=R2=R3=Me
M2PS-3AC: R1=R2=Me, R3=Ph
MP2S-3AC: R1=Me, R2=R3=Ph
P3S-3AC: R1=R2=R3=Ph

TMS-3AC: R4 = Me
TPS-3AC: R4 = Ph

Fig. 7 Silylsubstituted anthracene derivatives with bulky phenyl groups

core unit (compound 1,4-TIPS-3AC in Fig. 6) the film is hindered from crystallization, and OLEDs only exhibit a weak green emission ($0.4\,\mathrm{cd\,A^{-1}}$ at a brightness of $100\,\mathrm{cd\,m^{-2}}$). Tetracene derivatives with more bulky organosilicon substituents in the 5,6-positions and electron-donating methoxy groups in the 11,12-positions (compound TIPS-T-4AC-OMe_2 in Fig. 6) emit red light in OLEDs [31]. These examples demonstrate how structural design and fine tuning can significantly change phase behavior and electronic properties of the materials that consequently influence the device performance.

Karatsu et al. have reported on photo- and electrooptical investigation of a series of silylsubstituted anthracene derivatives with bulky phenyl groups (Fig. 7) [32]. They showed efficient blue fluorescence with the quantum yield of 77–92% (compared with 36% for the parent anthracene). With an increasing number of phenyl radicals the Stokes shift for phenylsilyl compounds significantly increases from $891\,\mathrm{cm^{-1}}$ for M3S-3AC to $1,582\,\mathrm{cm^{-1}}$ for P3S-3AC, but slightly decreases for phenylsilylethynyl compounds from $208\,\mathrm{cm^{-1}}$ for TMS-3AC to $202\,\mathrm{cm^{-1}}$ for TPS-3AC. Multilayered EL devices were prepared using these compounds as a dopant (up to 5%) in a $4,4'-N,N'$-dicarbazolyl-biphenyl (CBP) host which emitted a pure blue color, with the best characteristics for P3S-3AC (CIE coordinates 0.145, 0.155)[1].

Pentacene is a benchmark as semiconductor for thin-film OFETs, showing a mobility in the good quality devices up to $5\,\mathrm{cm^2\,V^{-1}\,s^{-1}}$ [33]. However, its drawbacks are insolubility and low oxidation and thermal stability, which may be improved by incorporation of appropriate organosilicon substituents. Pentacenes substituted at the 6,13-positions are easily accessible from pentacenequinone by synthetic methods known since the 1940s [34]. Anthony et al. prepared a series of trialkylsilylethynyl pentacene derivatives from pentacenequinone and corresponding Grignard reagents (Scheme 2) [35, 36]. All derivatives proved to be soluble in common organic solvents, which allow preparation of OFETs by solution processing. The most promising semiconducting properties revealed 6,13-bis(triisopropyl-

[1] Coordinated within the CIE 1931 color space chromaticity diagram. CIE – the International Commission on Illumination (abbreviation comes from French “Commission internationale de l’éclairage”).

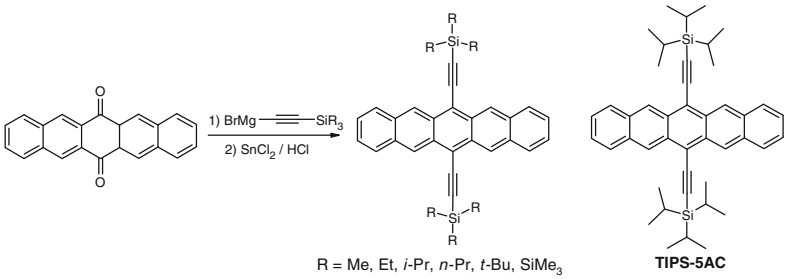

Scheme 2 Synthetic route to organosilicon 6,13-disubstituted pentacene and chemical formula of the most promising derivative for OFETs – TIPS-5AC

silylethynyl) pentacene (TIPS-5AC), although its mobility significantly depended on the preparation method [37]. In the case of thermally evaporated films, the highest hole mobility measured in OFETs was $0.4\,cm^2\,V^{-1}\,s^{-1}$. Solution-deposited TIPS-5AC yields films of significantly higher quality since slow evaporation of the solvent allows the material to self-assemble into large π-stacked arrays. Fast evaporation during spin-casting leads to a lower hole mobility of $0.2\,cm^2\,V^{-1}\,s^{-1}$ with on/off current ratios of 10^6. During drop-casting the solvent is allowed to evaporate slowly and hole mobilities greater than $1\,cm^2\,V^{-1}\,s^{-1}$ and on/off current ratios of greater than 10^7 have been achieved [38]. Electronic properties and electron transfer characteristics of TIPS-substituted oligoacenes have been studied in detail, both experimentally and theoretically [39, 40].

The unique combination of outstanding electrical performance and good solubility of TIPS-5AC was rationalized by favorable 2D π-stacking in the "bricklayer" crystal lattice of this material (Fig. 8a), which is different both from 1D π-stacking in the "slipped-stack" arrangement of some other organosilicon 6,13-disubstituted pentacenes (i.e., triethylsilylethynyl pentacene TES-5AC, Fig. 8b) and from the herringbone structure of pentacene (Fig. 8c). It is well-known that the device performance clearly depends on the crystal packing of the employed semiconductor. Moreover, apparently TIPS-substituents have just the right size for the efficient "bricklayer" packing, since smaller ethyl or larger *n*-propyl attachment groups lead to 1D "slipped-stack" arrangements, while the largest trimethylsilyl radicals lead to a herringbone structure.

Attempts have been made to deposit TIPS-pentacene from solution as the functional layer in a pentacene/C60 bilayer photovoltaic device. Careful optimization of deposition conditions, optimal concentration of mobile ion dopants, thermal postfabrication annealing, and the addition of an exciton-blocking layer yielded a device with a moderate white-light PCE of 0.52% [41]. Since TIPS-pentacene derivatives rapidly undergo a Diels–Alder reaction with fullerene, the assembly of potentially more efficient bulk-heterojunction photovoltaic devices from TIPS-pentacene and fullerene derivatives were not possible [42]. The energy levels of the TIPS-pentacene-PCBM adduct (PCBM is [6,6]-phenyl C61-butyric acid methyl ester) ineffectively supports the photoinduced charge transfer.

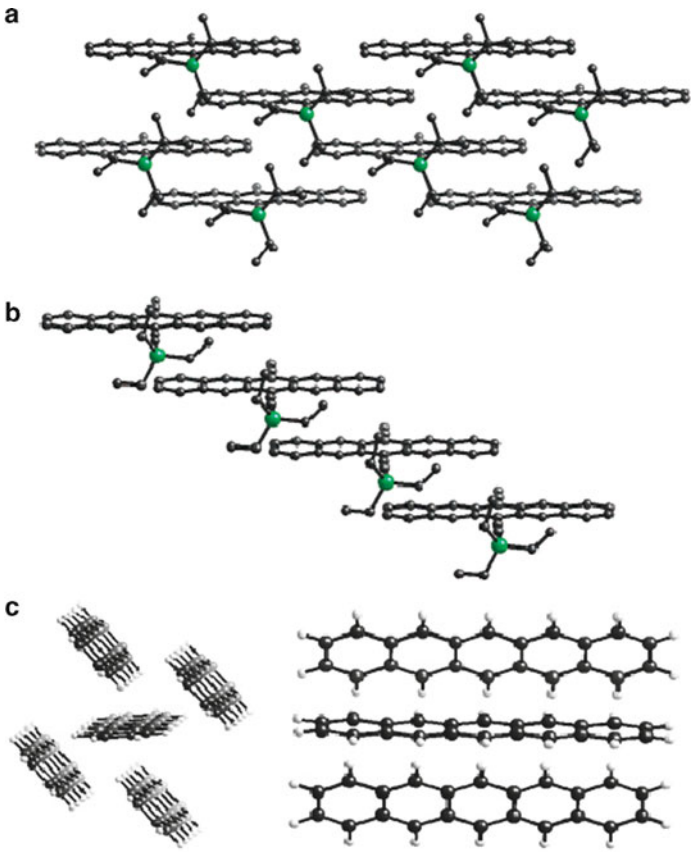

Fig. 8 Solid state ordering of TIPS-5AC (**a**), TES-5AC (**b**), and pentacene (**c**) – reproduced with permission of the American Chemical Society from [29]

Introduction of fluorine substituents into the conjugated core is known as a powerful method to change the polarity of the main charge carriers in organic semiconductors. Some fluorine derivatives of pentacene and TIPS-pentacene have also have been reported (Fig. 9). Solely perfluorinated pentacene 5AC-F14 exhibited n-type behavior with an electron mobility up to $0.22\,cm^2\,V^{-1}\,s^{-1}$ [43, 44]. Contrary to expectation, the partially fluorinated TIPS-pentacene derivatives TIPS-5AC-F4 and TIPS-5AC-F8 showed only p-type mobility, $0.014\,cm^2\,V^{-1}\,s^{-1}$ and $0.045\,cm^2\,V^{-1}\,s^{-1}$, respectively [45]. Devices were prepared by vacuum sublimation and compared to TIPS-5AC (mobility of $0.001\,cm^2\,V^{-1}\,s^{-1}$, deposited under the same conditions). An increasing mobility with an increasing degree of fluorination of TIPS-pentacene was explained by a decreasing π–π interlayer spacing in the crystal packing due to aryl–fluoroaryl interactions (from 3.43 Å for TIPS-5AC to 3.36 Å for TIPS-5AC-F4 and 3.28 Å for TIPS-5AC-F8), while the overall packing arrangement was almost the same for all these compounds.

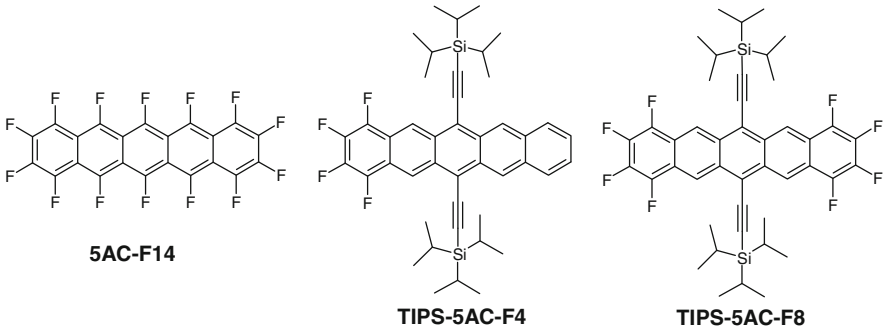

Fig. 9 Fluorosubstituted pentacene and TIPS-pentacene

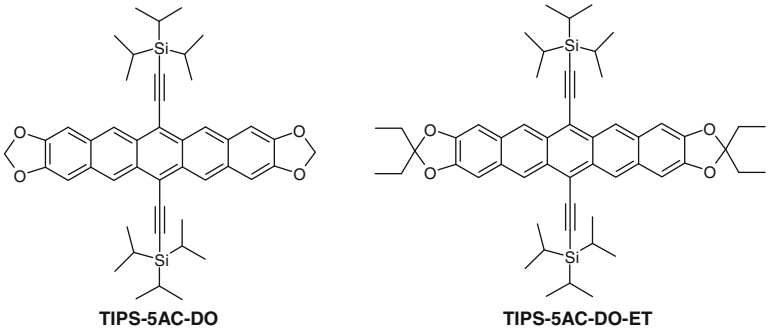

Fig. 10 Dioxolane derivatives of TIPS-pentacene

Some dioxolane derivatives of TIPS-pentacene were successfully applied in OLEDs (Fig. 10). TIPS-5AC-DO used as a guest emitter in the tris(8-quinolinolato) aluminum(III) complex (Alq_3) and 4,4′-bis[*N*-1-naphthyl-*N*-phenylamino]-biphenyl (NPD) host matrices (common hole-transport materials used in OLEDs) showed efficient energy transfer and bright red photoemission at very low concentrations (less than 0.5 mol%) [46]. However, a higher dopant concentration led to aggregate emissions that motivated the synthesis of the more bulky derivative TIPS-5AC-DO-ET (functionalized with ethyl groups at the dioxolane ring). This compound has an increased chromophore stacking distance in the crystal (5.5 Å vs 3.4 Å for TIPS-5AC-DO) and allowed a concentration up to 2% of dopant in both Alq_3 and NPD matrixes without formation of aggregates. OLEDs prepared from such composites showed bright red emission with an external electroluminescence quantum yield of 3.3% [47], close to the theoretical maximum and also very close to the highest value reported (3.6%) [48] for a small-molecule red-emissive OLED.

Heterocyclic analogs of pentacene–anthradithiophenes (ADT) are another type of promising semiconductors (with a mobility up to $0.09\,cm^2\,V^{-1}\,s^{-1}$ for vacuum sublimed film of parent ADT and up to $0.15\,cm^2\,V^{-1}\,s^{-1}$ for its dialkyl-substituted analogs), despite the fact that they can only be prepared as mixture of

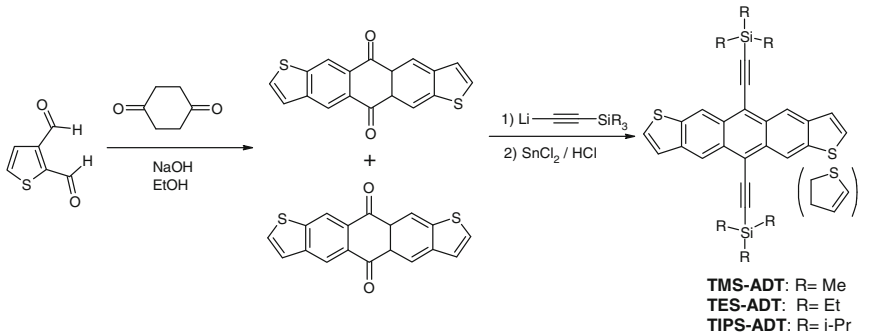

Scheme 3 Synthetic route to silylethynyl-functionalized anthradithiophenes

syn- and *anti*-isomers which cannot be separated [49]. The same problem arises for silylethynyl-functionalized ADTs, a series of which was prepared starting from thiophene-2,3-dicarboxaldehyde and 1,4-cyclohexanedione (Scheme 3) [50]. These compounds showed remarkable solubility when compared to parent ADT, but their semiconducting properties are highly dependent on the substituent groups attached to the central silicon atom. Solution-deposited films of TMS-ADT did not show any field-effect mobility due to lack of π–π-stacking, TIPS-ADT exhibited a relatively low mobility ($<10^{-4}\,cm^2\,V^{-1}\,s^{-1}$), while the mobility up to $0.19\,cm^2\,V^{-1}\,s^{-1}$ was reported for TES-ADT [51]. The mobility improved when TES-ADT was deposited by drop-casting, which yielded devices with mobilities as high as $1.0\,cm^2\,V^{-1}\,s^{-1}$ and on/off current ratios of 10^7. This dramatic improvement of semiconducting properties was associated with 2D π-stacking of TES-ADT, similar to TIPS-pentacene.

2,8-Diethyl-5,11-bis(triethylsilylethynyl)anthradithiophene (TES-ADT-ET) was synthesized by a similar synthetic route and successfully used in bulk-heterojunction solar cells in mixture with PCBM [52]. Solvent vapor annealing of these blends leads to the formation of spherulites, which consist of a network of ADT crystallites dispersed in an amorphous matrix primarily of fullerene (Fig. 11). It was shown that the coverage of a device with spherulites directly correlates with its performance. Devices with 82% spherulite coverage reach a PCE of 1%.

Significant improvements in stability and crystallinity were achieved by partial fluorination of silylethynyl-functionalized ADTs (Fig. 12) [53]. These fluorinated materials still behave as p-type semiconductors, but compared to the nonfluorinated derivatives the fluorine introduces a dramatic increase in thermal stability and photostability. TES-ADT-F2 forms highly crystalline films even from spin-cast solutions, leading to devices with maximum hole mobility greater than $1.0\,cm^2\,V^{-1}\,s^{-1}$. TIPS-ADT-F2 forms large, high-quality crystals that could even serve as a substrate for transistor fabrication. For this compound, a mobility up to $0.1\,cm^2\,V^{-1}\,s^{-1}$ was measured on the free-standing crystals. Recently single-crystal field-effect transistors prepared on the surface of TES-ADT-F2 exhibited outstanding electronic properties: a mobility as high as $6\,cm^2\,V^{-1}\,s^{-1}$, large current on/off ratios ($I_{on}/I_{off} = 1 \times 10^8$),

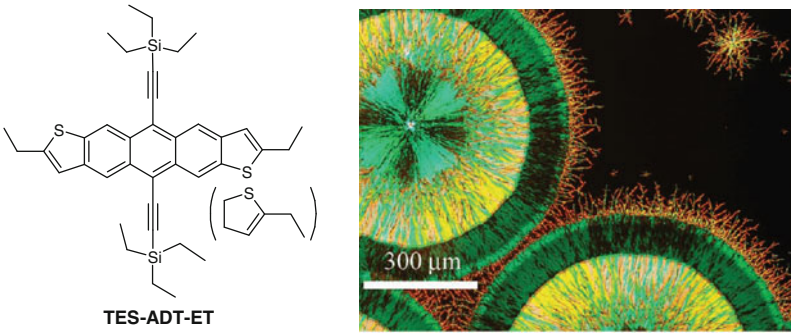

Fig. 11 2,8-Diethyl-5,11-bis(triethylsilylethynyl)anthradithiophene (TES-ADT-ET) and optical image of its blend with PCBM used in efficient photovoltaic devices – reproduced with permission of the American Chemical Society from [52]

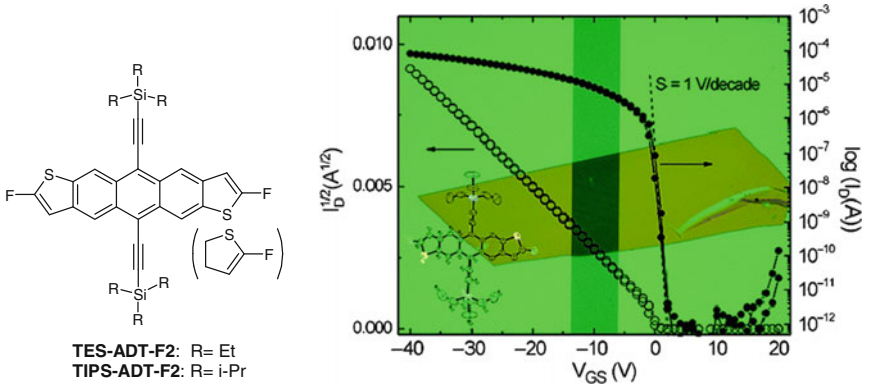

Fig. 12 Partially fluorinated silylethynyl-functionalized anthradithiophenes (*left*). Single crystal of TES-ADT-F2 and its electrical characteristics (*right*) – reproduced with permission of the American Chemical Society from [53]

a small subthreshold slopes ($S = 1\,\mathrm{V\,dec^{-1}}$), and extremely small hysteresis in the current-voltage characteristics [54]. Optical, fluorescent, and (photo)conductive properties of this and other silylethynyl-functionalized pentacene and ADT derivatives have recently been studied in detail [55]. Soluble silylethynyl-functionalized higher acenes (hexacene and heptacene) [56] and acenedithiophenes with six and seven fused rings [57] have also been reported.

Thus, linear soluble organosilicon oligoacenes have demonstrated a high technological potential for organic electronics. Their application as semiconductors have been demonstrated in OTFTs, OPVs, and in OLEDs. Both the chromophore and the attachments groups influence electronic and morphological properties for the most part in a way that will not be easily predicted and will require subsequent empirical fine tuning of structures and deposition methods to obtain materials with optimal performance.

2.3 Silole-Based Oligomers

Silole (silacyclopentadiene) and its derivatives contain a unique electronic structure leading to excellent photophysical properties [58]. Siloles have a low LUMO energy level combined with a relatively high HOMO level in comparison to other heterocyclic rings commonly used for creation of π-conjugated oligomers and polymers: pyrrole, furan, thiophene, and pyridine (Fig. 13a). The σ^*–π^* conjugation in the silole ring, arising from interactions of the σ^* orbital of the silylene moiety with the π^* orbital of the butadiene significantly lowers its LUMO energy (Fig. 13b). As a result 2,5-difunctionalized silole-containing oligomers and polymers exhibit a low band gap when used as structural unit in the conjugated backbone. Indeed, 2,5-disubstituted disilol 2,5-2SEP has an absorption maximum at 417 nm and 2,5-disubstituted quatersilole 2,5–4SEP has a λ_{max} at 443 nm (Fig. 14) [59]. These values are significantly red-shifted compared to a λ_{max} at 301, 351, and 385 nm for bi-, ter-, and quaterthiophenes [12]. In contrast, 1,1-substituted ter- and quatersiloles 1,1–3SMP and 1,1–4SMP have a λ_{max} at 280–290 nm only due to lack of electronic overlap between silicon and the conjugated rings [60].

2,5- and 1,1-Difunctionalized siloles can be prepared by intramolecular reductive cyclization of diethynylsilanes. Starting from these functionalized siloles a number of oligo(2,5-silole)s and oligo(1,1-silole)s have been successfully synthesized [59–61]. However, more often 2,5-difunctional silole monomeric units are combined with other heterocycles, i.e., thiophene, pyrrole, pyridine, etc. A series of thiophene-silole co-oligomers and copolymers have been prepared by Tamao et al. [62]. All oligomers showed a bathochromic (red) shift in the absorption maxima when compared to oligothiophenes, which tends to shift to longer wavelengths with an increasing number of silole units incorporated. In contrast, the conductivity

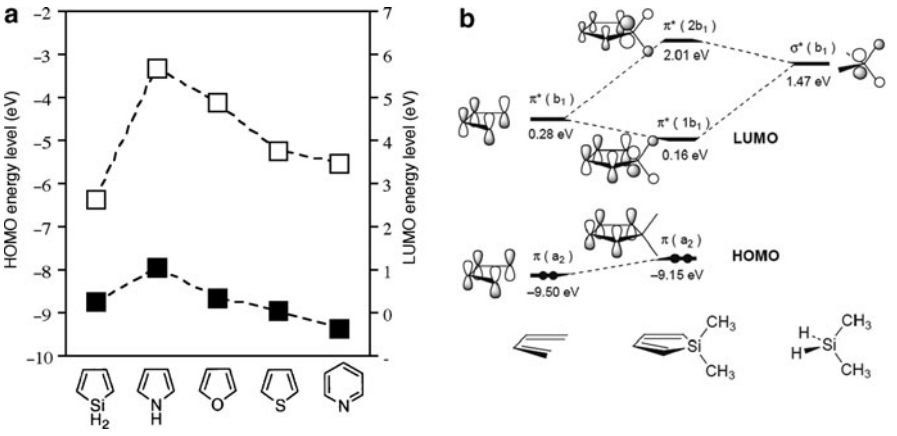

Fig. 13 Relative HOMO and LUMO levels for silole and other heterocycles, based on HF/6–31G* calculations (**a**) and orbital correlation diagram for 1,1-dimethylsilole, based on the PM3 calculations (**b**). Reproduced by permission of The Royal Society of Chemistry [58]

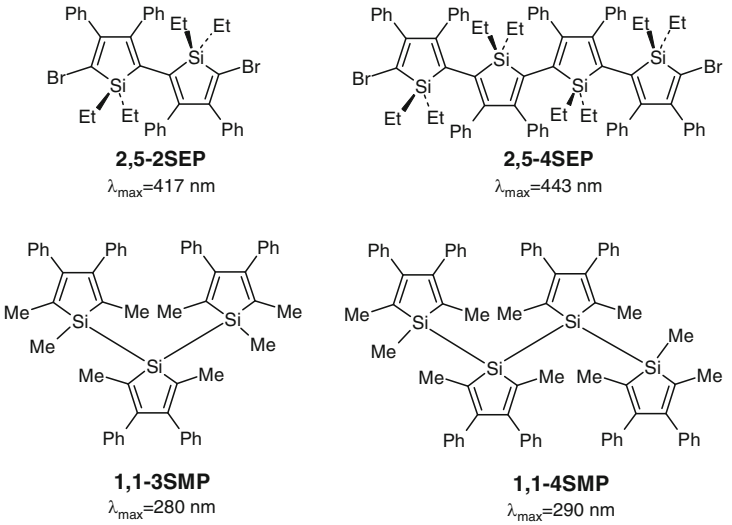

Fig. 14 Examples of oligo(2,5-silole)s and oligo(1,1-silole)s

of the resulting oligomers tends to increase with the number of thiophene units, reaching a maximum of $2.4\,\mathrm{S\,cm^{-1}}$ after doping with iodine. X-ray structural analysis revealed a high coplanarity of the thiophene and silole rings in the co-oligomers. This is not the case for co-oligomers of silole with the more electron rich pyrrole, in which a highly twisted conformation of the three rings of 2,5-dipyrrolylsilole was found [63].

Silole-containing oligomers have been used as electron transporting layers and as emitters to build efficient OLEDs (Fig. 15) [64, 65]. In OLEDs the performance of 2,5-di(2-pyridyl)-1,1-dimethyl-3,4-diphenylsilacyclopentadiene (PySPy) as electron transport (ET) material was found to be enhanced over Alq_3, which is one of the best performing electron transporting materials so far [64]. 2,5-Bis-(2′,2″-bipyridin-6-yl)-1,1-dimethyl-3,4-diphenylsilacyclopentadiene (2PyS2Py), used as ET layer, exhibited an electron mobility of $2 \times 10^{-4}\,\mathrm{cm^2\,V^{-1}\,s^{-1}}$ at a field strength of $0.64\,\mathrm{MV\,cm^{-1}}$ measured by the time-of-flight technique. Incorporation of phenylene and thiophene moieties allowed tuning of the emission color in OLEDs: silole derivatives PSP, SiTSTSi, and TTSTT emitted greenish blue, yellowish-green, and reddish orange light, respectively. 2,5-Di-(3-biphenyl)-1,1-dimethyl-3,4-diphenylsilacyclopentadiene (2PS2P) exhibits a blue fluorescence ($\lambda_{\max} = 476\,\mathrm{nm}$) with a high solid state photoluminescence quantum yield of 85% [66]. In multilayer OLED devices 2PS2P showed emission at 495 nm due to an exciplex formation with *N*,*N*′-diphenyl-*N*,*N*′-(2-naphthyl)-(1,1′-phenyl)-4,4′-diamine used in the hole-transporting layer (HTL). Interestingly, all these compounds show very weak luminescence in dilute solutions ($\Phi_F = 10^{-2}$–10^{-4}) [67].

1,2-Bis(1-methyl-2,3,4,5-tetraphenyl silacyclopentadienyl)ethane (2PSP) emits a blue–green fluorescence with an absolute quantum yield of 97% as vapor-deposited film [65]. Devices using 2PSP show a very low operating voltage, an

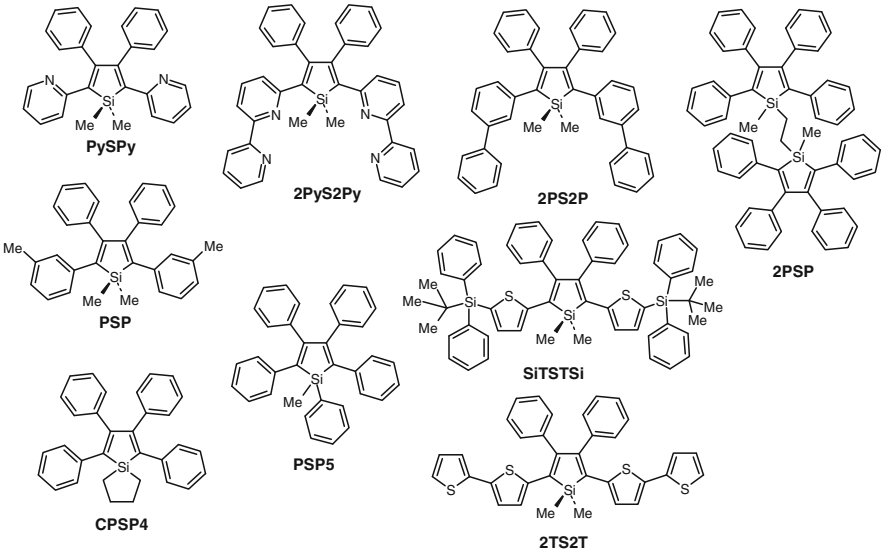

Fig. 15 Silole-containing oligomers used for OLEDs

external electroluminescence quantum efficiency η_{EL} of 4.8%, and an impressive luminous power efficiency of $9\,\mathrm{lm\,W^{-1}}$ at a brightness of $100\,\mathrm{cd\,m^{-2}}$. Unfortunately, these siloles easily crystallize due to their low glass transition temperatures (T_g). This strong tendency for crystallization contributes to device degradation when these materials are incorporated in OLED structures [68].

1-Methyl-1,2,3,4,5-pentaphenylsilole [69] (PSP5) was reported as the first compound with a huge aggregation induced emission (AIE) – a rare phenomenon, where efficiency of photoluminescence increases by two orders of magnitude upon aggregation [70]. This phenomenon was explained by restricted intramolecular rotations of the phenyl rings in the nanoaggregates (with a large contribution to the nonradiative transition process found in solutions) [71] and observed for a series of similar phenylsiloles [72, 73] as well as for other bulky molecules [74]. PSP5 and other 1,1-disubstituted siloles can be synthesized in a convenient one-pot reaction by lithiation of dithenylacetylene followed by treatment with corresponding dichlorosilane [75]. Multilayer OLED devices, prepared with PSP5 as emitter, showed a blue light emission at 496 nm with a low turn-on voltage (3.4 V), high emission efficiencies ($9,234\,\mathrm{cd\,m^{-2}}$, $12.6\,\mathrm{lm\,W^{-1}}$, and $12\,\mathrm{cd\,A^{-1}}$), and high external quantum yield (8%). Further optimization allowed raising the power efficiency of the devices to a record for blue emission value of $20\,\mathrm{lm\,W^{-1}}$ [70]. Among a series of spiro-silacycloalkyl tetraphenylsiloles prepared by Son et al., 1,1′-silacyclopentyl-2,3,4,5-tetraphenylsilole (CPSP4) has shown the most promising properties in OLEDs. A three layer device, comprising *N*,*N*′-bis(1-naphthyl)-*N*,*N*′-diphenylbenzidine (NPB) as the hole-transport layer, CPSP4 as the emitting layer, and Alq_3 as the ET layer, displayed a brightness of $11,000\,\mathrm{cd^{-2}}$ at 11 V with a current efficiency of $2.71\,\mathrm{cd\,A^{-1}}$ [73].

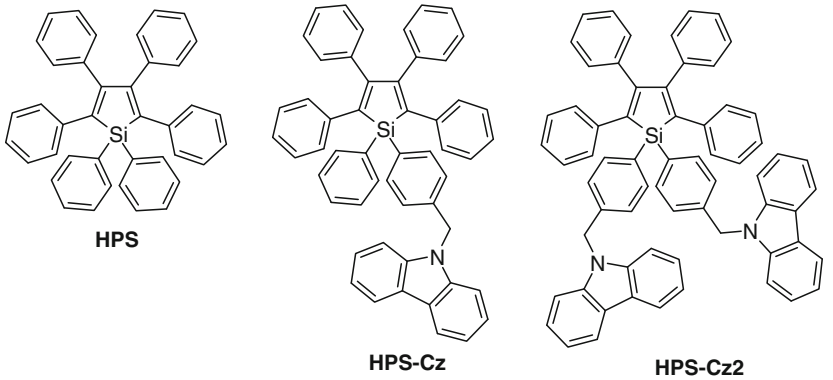

Fig. 16 Hexaphenylsilole (HPS) and its carbazole derivatives

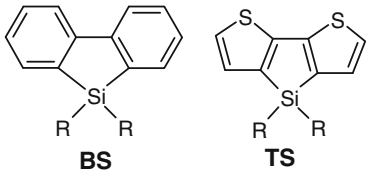

Fig. 17 Important silole-based building blocks are dibenzosilole (BS) and dithienosilole (TS)

Attaching one or two carbazolyl (Cz) groups to a hexaphenylsilole (HPS) [72] leads to thermally and morphologically stable carbazolylsiloles, HPS-Cz and HPS-Cz2, respectively (Fig. 16), which were tested on OLEDs and OPV cells [76]. These molecules, like their HPS parent, are also AIE-active. Obviously due to the formation of donor–acceptor (D–A) complexes for the asymmetrically substituted HPS-Cz the photoluminescent quantum yield of aggregated HPS-Cz (56%) was 2.4-fold higher than that of HPS-Cz2 (23%). As a result, OLEDs prepared from HPS-Cz were found to be more efficient with a turn-on voltage of 5 V, and emit light with maximal current efficiency of $2.6\,\mathrm{cd\,A^{-1}}$ at 8.5 V. HPS-Cz2 revealed a higher efficiency in photovoltaic cells. The best devices exhibited a short-circuit current density of $96.5\,\mathrm{mA\,cm^{-2}}$, an open-circuit voltage of 1.7 V, and a fill factor of 0.21. Although the structure of the cell was far from being optimized, it showed an external photovoltaic efficiency as high as 2.19% (irradiated with 365 nm UV light at $15\,\mathrm{mW\,cm^{-2}}$).

Two important silole-based building blocks are BS [77, 78] and TS [79, 80]. The first is also known as silafluorene (SiF), in which a silicon atom replaces the carbon atom in the 9-position of fluorene; the second is the silicone-bridged bithiophene (Fig. 17). In both structures the LUMO energy level is lowered by a σ^*–π^* conjugation within the silole ring.

A series of diphenyl-, dithienyl-, and dipyridylsubstituted TSs and their trimethylsilyl derivatives have been reported by the Ohshita and Kunai group [81] (Fig. 18). TS with trimethylsilylpyridyl substituents $TSPy_2$ have shown good ET

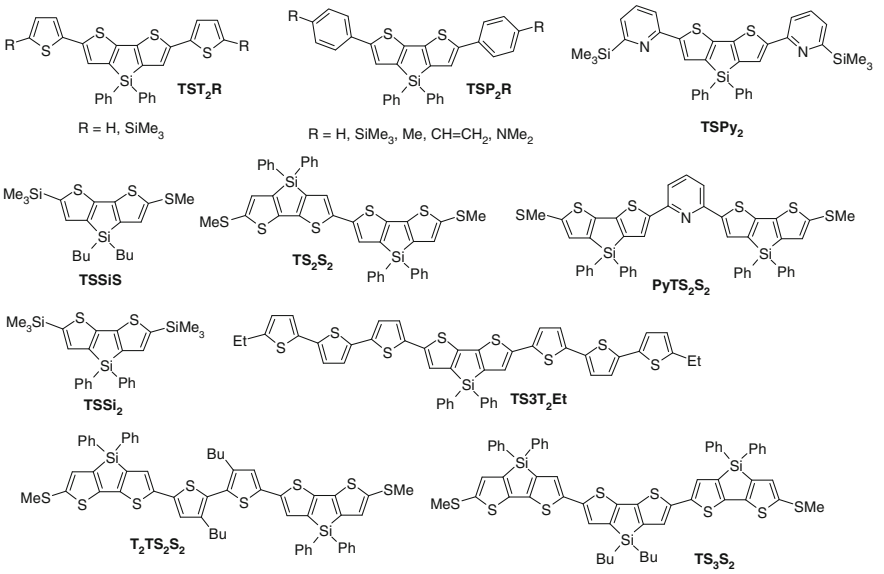

Fig. 18 Dithienosilole-based oligomers

properties in OLEDs: a device with the structure of ITO/TPD/Alq_3/$DTSPy_2$/Mg-Ag, where Alq_3 acted as the emitter and TPD (*N*,*N*′-diphenyl-*N*,*N*′-di(*m*-tolyl)biphenyl-4,4′-diamine) as hole-transporting material, emitted a strong green light with the maximum luminance of 16,000 cd m^{-2}. Lee et al. reported on the synthesis of TS derivatives containing *para*-substituted phenyl with methyl, vinyl, or dimethylamino groups [82]. TSP_2Me, TSP_2Vin, and TSP_2NMe_2 emit light with a maximum emission at 512, 517, and 560 nm, which correspond to green to yellowish-green light. At a voltage of 10 V the luminance of advanced multilayered OLED devices using these TS derivatives as emitters were found to be 680, 515, and 250 cd m^{-2}, respectively. The group of Ohshita and Kunai reported on a series of TS-containing oligomers with different conjugation lengths (2–8 conjugated aromatic rings, see Fig. 18). Attached electron-donating methylthio groups raise the HOMO energy, thus leading to oligomers with smaller HOMO–LUMO energy gaps [83]. Hence, compared to oligomers with the same π-conjugated chain length but without silole subunits, their optical absorption (395–498 nm) and the emission (498–576 nm) spectra maxima are shifted to longer wavelengths. Emission colors of these oligomers cover the whole visual spectral range from violet to red (Fig. 19) despite their moderate efficiency (Φ_F ranges from 0.02 for $T_2TS_2S_2$ to 0.22 for $PyTS_2S_2$). Solely $TS3T_2Et$, the oligomer containing eight conjugated aromatic rings, was found to be active as semiconductor in OTFT, vapor-deposited films as well as spin-coated films of which exhibiting a hole mobility of $\mu = 2.6 \times 10^{-5}$ cm^2 V^{-1} s^{-1} and $\mu = 1.2 \times 10^{-7}$ cm^2 V^{-1} s^{-1}, respectively.

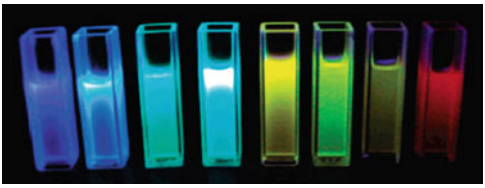

Fig. 19 Luminescence of the THF solutions of TS derivatives (from *left* to *right*): $TSSi_2$, TSSiS, $PyTS_2S_2$, $TSPy_2$, $T_2TS_2S_2$, $2TS_2S_2$, $TS3T_2Et$, TS_3S_2 (for chemical formulas – see Fig. 18). Reproduced with permission of the American Chemical Society from [83]

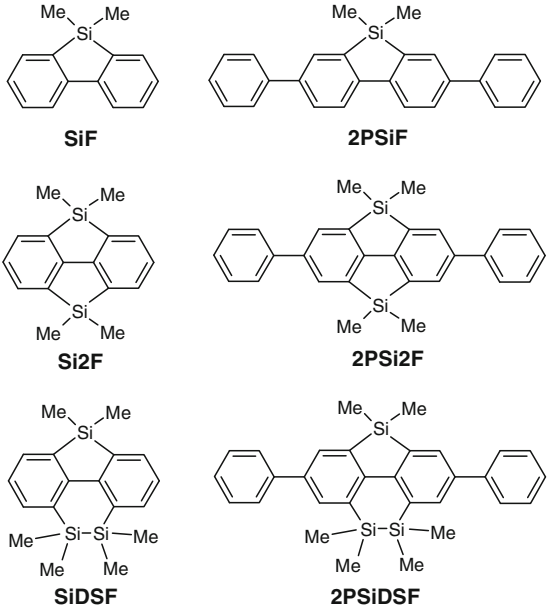

Fig. 20 Silafluorene oligomers with different number of silicon-bridge atoms

Shimizu et al. investigated silicon-bridge effects on photophysical properties of silafluorenes with different bridge structures (Fig. 20) [84]. 4,5-Dimethylsilylene- or 4,5-tetramethyldisilylene-bridged 9-silafluorenes Si2F and SiDSF were prepared by lithiation of $2,2',6,6'$-tetrabromobiphenyls followed by silylation with dichlorodimethylsilane or 1,2-dichloro-1,1,2,2-tetramethyldisilane, respectively. X-ray analysis of the silylene-bridged silafluorene revealed that the molecular framework was perfectly planar and four Si-C(methyl) σ-bonds were completely orthogonal to the plane. Additional silicon bridges connecting the 4,5-positions were found to induce a red shift in the absorption and fluorescence spectra compared to 9-silafluorenes (SiF). Density functional theory (DFT) calculations suggested that an introduction of the silicon bridges to 9-silafluorene increases the energy of the HOMO and LUMO levels simultaneously.

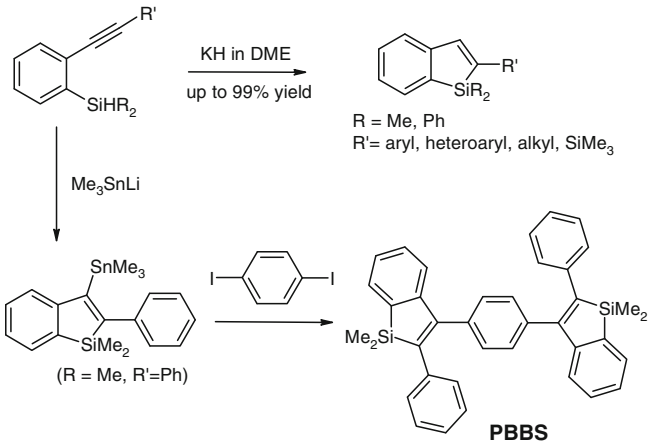

Fig. 21 Functionalized benzosiloles and their derivatives

Benzosilole derivatives, in which phenylene ring replaces a double bond in the silole structure, have also been recognized as prospective building blocks for the synthesis of oligomers with interesting electronic and photonic properties. The group of Nakamura and Tsuji reported a trimethylstannyllithium promoted cyclization of (*o*-alkynylphenyl)silane to a 3-stannylbenzosilole that proceeds via an addition to the triple bond followed by intramolecular cyclization in a cascade fashion. This intermediate can be functionalized with either electrophiles or nucleophiles to 2,3-disubstituted benzosiloles (Fig. 21). Phenylene-bis(benzosilole) PBBS shows an electron mobility up to $\mu = 6 \times 10^{-4}\,\mathrm{cm^2\,V^{-1}\,s^{-1}}$ in an amorphous film, which makes this class of compounds promising for the use in organic light-emitting devices and OPVs [85]. Recent results from the same group showed an intramolecular cyclization of (2-alkynylphenyl)silanes in the presence of potassium hydride to obtain a variety of new 2-substituted benzosiloles in good up to excellent yields (Fig. 21). Some of these compounds showed a high fluorescence quantum yield both in solution and in the solid state [86].

Silicon-bridged biaryls (SBArs) can be synthesized conventionally by dilithiating the corresponding $2,2'$-dihalobiaryls followed by reaction with dichlorosilanes. Recently Shimizu et al. reported on a novel and versatile approach to SBArs which involves Pd-catalyzed intramolecular direct arylation of readily available 2-(arylsilyl)aryl triflates (Fig. 22) [87]. This approach is applicable to the facile synthesis of not only symmetrical and asymmetrical functionalized 9-silafluorenes, but also SBArs containing heteroaromatic rings, such as furan, thiophene, and pyrrole. This synthetic approach was used to synthesize silicon-bridged 2-phenylindole (SBPI), which exhibits highly efficient blue fluorescence in the solution ($\Phi_F = 0.70$) and in the solid state ($\Phi_F = 0.90$–1.00) (Fig. 23).

In summary, silole-based oligomers present an interesting class of organosilicon σ–π conjugated compounds with unique electronic and optical properties. A low lying LUMO level can be further adjusted by appropriate combination with other

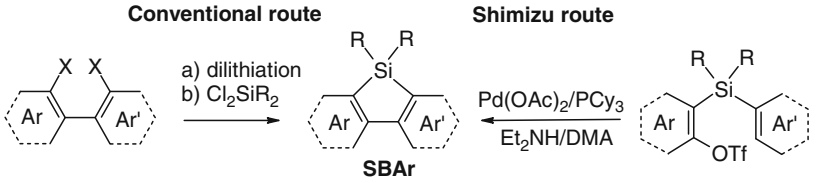

Fig. 22 Two approaches to silicon-bridged biaryls

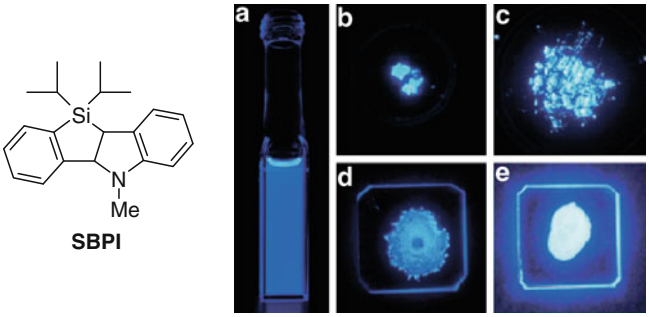

Fig. 23 Silicon-bridged 2-phenylindole (SBPI) and its fluorescence images ($\lambda_{ex} = 365$ nm): (**a**) 1.9×10^{-5} M solution in cyclohexane; (**b**) microcrystal; (**c**) powder; (**d**) thin-film prepared by spin-coating from a toluene solution; (**e**) dispersed in PMMA film (reproduced with permission of John Wiley & Sons, Inc from [87])

π-conjugated (hetero)cycles. In combination with the unique AIE phenomena, this class of compounds yields an extremely high solid state PL efficiency. The highest potential for applications of silole-based oligomers seems to be in OLED structures, especially as blue light emitters.

2.4 Silicon Analogs of Oligo(p-Phenylenevinylene)s

Recently a new class of conjugated organosilicon oligomers has been reported: silicon analogs of oligo(*p*-phenylenevinylenes). Yamaguchi, Xu, and Tamao synthesized a homologous series of bis-silicon-bridged stilbenes [88] via an intramolecular reductive cyclization of bis(*o*-silyl)-diphenylacetylene (Scheme 4). Bis(*o*-silyl)-diphenylacetylenes are reacted with excess lithium naphthalenide to undergo a two-electron reduction at the acetylene moiety to produce a dianion intermediate. This dianion further undergoes a double cyclization in a 5-exo mode to yield bis-silicon-bridged stilbenes. This method can be successfully applied to the synthesis of tetrakis-silicon-bridged bis(styryl)benzenes. The obtained silicon-bridged π-conjugated systems show an intense fluorescence in the visible region which differs significantly from its carbon analog.

This synthesis methodology was expanded to the synthesis of ladder oligo(*p*-phenylenevinylene)s (LOPVs) and related π-electron systems, having annelated

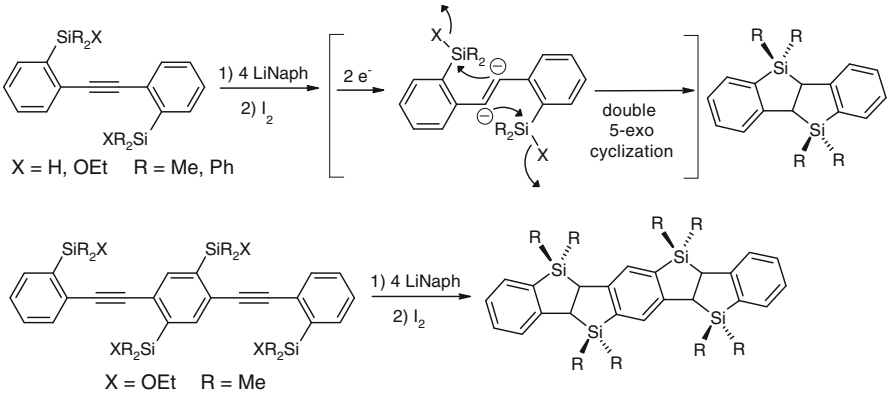

Scheme 4 Synthesis of bis-silicon-bridged stilbenes

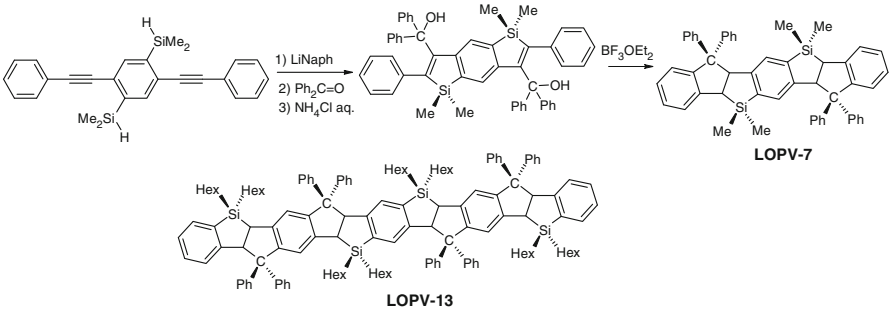

Scheme 5 Synthesis of ladder oligo(*p*-phenylenevinylene)s and the longest molecule obtained by this technique

π-conjugated structures with silicon and carbon bridges [89, 90]. In this case a combination of two cyclization reactions was applied, i.e., an intramolecular reductive cyclization of (*o*-silylphenyl)acetylene derivatives and an Friedel–Crafts-type cyclization (Scheme 5). This allowed the synthesis of a homologous series of ladder molecules up to LOPV-13, a system with 13 fused rings. The crystal structure of LOPV-13 proves a nearly flat π-conjugated framework with a length of ca. 2.9 nm. All obtained ladder π-electron systems show intense fluorescence in the visible region ($\lambda_{max} = 443$–523 nm) with high quantum yields up to $\Phi_F = 0.84$, but relatively small Stokes shifts (18–23 nm).

Disilene (Si = Si) analogs of oligo(*p*-phenylene-vinylene)s were successfully synthesized by use of a 1,1,3,3,5,5,7,7-octaethyl-*s*-hydrindacen-4-yl (Eind) ligand (Fig. 24) [91]. Their X-ray crystal structures and spectroscopic data demonstrate that the π-conjugation effectively extends over the Si-OPV framework. Tetrasiladistyrylbenzene TSDSB exhibits an orange fluorescence even at room temperature both in solution and in the solid state, which is attributable to the effective extension of conjugation and a low tendency to aggregate. TSDSB is the first example of a disilene derivative with fluorescence even at room temperature.

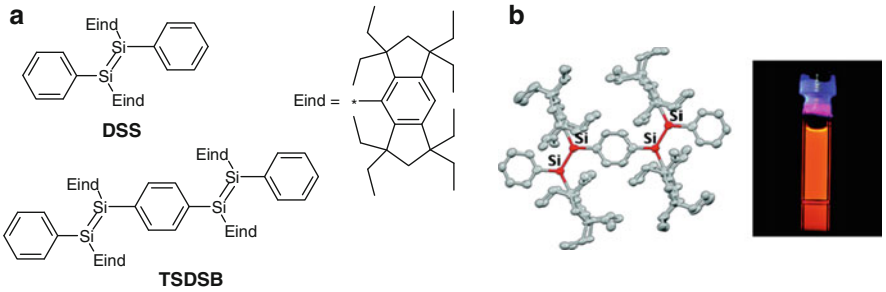

Fig. 24 (**a**) Disilene analogs of the oligo(*p*-phenylenevinylene)s (Si-OPVs): disilastilbene DSS and tetrasiladistyrylbenzene TSDSB. (**b**) Highly planar crystal structure of tetrasiladistyrylbenzene and its fluorescence – reproduced with permission of the American Chemical Society from [91]

Despite the few reports on silicon analogs of oligo(*p*-phenylenevinylenes) it appears that this emerging class of organosilicon materials exhibits promising optical properties for future photonic applications.

3 Branched Conjugated Organosilicon Oligomers

Albeit some of the linear oligomers described in Sect. 2 also have branched molecular shape, all of them have a 1D conjugation backbone that allows them to be considered as linear conjugated oligomers. This section will concentrate on oligomers having several conjugated units connected to three- or four-functional central silicon atom.

One of the first conjugated organosilicon oligomers was spiro-bis-septithiophene Spiro-Si-7T (Fig. 25) [92] This molecule is a branched analog of septithiophene Me_3Si–T7–Me_4SiMe_3 (see Sect. 2.1), in which two oligothiophenes connect via a C-Si isolated bridge and build a 90° torsion angle. This unique structure separates the two perpendicular chromophores and allows oxidation of each of the 7T units sequentially and independently of each other that proceeds via four distinct species: a mono radical cation, a bis-(radical cation), a radical cation/dication, and a bis-(dication). It has been proposed to use these structures in future to build molecular electronic devices for memory, logic, and amplification functions [93, 94], in which the oxidized (doped) and the neutral (nondoped) states of the oligothiophenes may serve as bit states "one" and "zero."

A series of four asymmetrically aryl-substituted 9,9′-spiro-9-silabifluorene (SSF) derivatives, 2,2′-di-*tert*-butyl-7,7′-diphenyl-9,9′-spiro-9-silabifluorene (PSSF), 2,2′-di-*tert*-butyl-7,7′-dipyridin-2-yl-9,9′-spiro-9-silabifluorene (PySSF), 2,2′-di-*tert*-butyl-7,7′-dibiphenyl-4-yl-9,9′-spiro-9-silabifluorene (BPSSF), and 2,2′-di-*tert*-butyl-7,7c-bis(2′,2″-bipyridin-6-yl)-9,9′-spiro-9-silabifluorene (BPySSF) have been reported by Lee et al. [95] (Fig. 26). These molecules were synthesized by the cyclization of the corresponding 2,2′-dilithiobiphenyls with silicon tetrachloride.

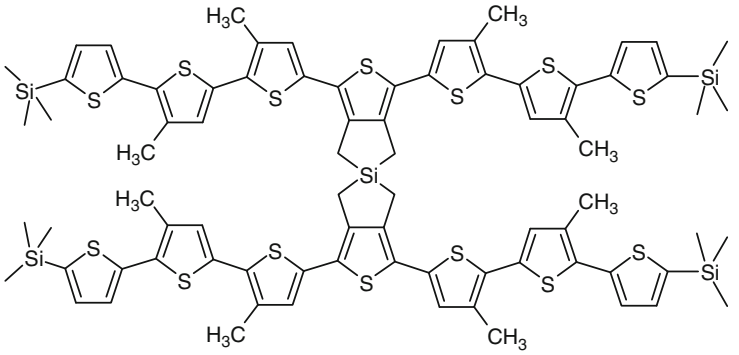

Fig. 25 Spiro-bis-septithiophene Spiro-Si-7T

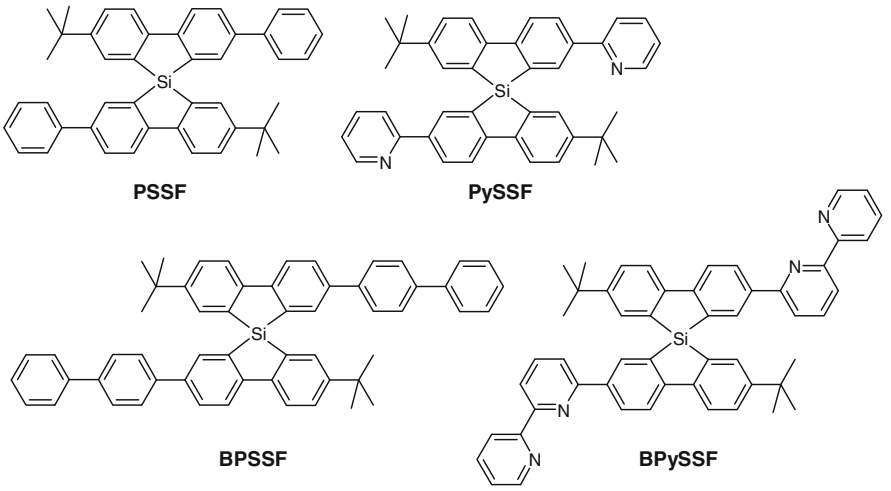

Fig. 26 Spiro-9-silabifluorene derivatives

These spiro-linked siloles form transparent and stable amorphous films with glass transition temperatures above 200°C. The absorption spectrum of each compound shows a significant bathochromic shift relative to the corresponding carbon analog as a result of the effective σ^*–π^* conjugation between the σ^* orbital of the exocyclic Si-C bond and the π^* orbital of the oligoarylene fragment. Solid state films exhibit an intense violet–blue emission with maxima at 398–415 nm and high absolute photoluminescence quantum yields ($\Phi_F = 0.30$–0.55).

As discussed in Sect. 2.1, luminescence efficiency of bi- and terthiophenes can be increased by silylene- and disilylelene substituents. This effect might be enhanced by a further branching of the chromophore to avoid aggregation. Ponomarenko and his group reported a significant increase of the luminescence quantum yield Φ_F in dilute solutions of a series of mono-, di-, tri-, and tetra(5′-hexyl-2,2′-bithiophene)silanes from 0.06 to 0.20 while the absorption and luminescence spectra

only slightly change [96]. Interestingly, tri- and tetra-substituted bithiophenesilanes have almost the same Φ_F (0.19 and 0.20). These oligomers were synthesized in good to excellent yields from the lithium derivative of 5-hexyl-2,2′-bithiophene and the corresponding chlorosilanes similar to the synthesis reported before for a series of bithienylhydridesilanes by Lukevics et al. [97]. Recently a similar route was successfully applied for the synthesis of a series of tetrahedral arylethynyl substituted silanes [98].

An impressive luminescence efficiency and luminescent lifetime was reported by the Ishikawa group for a series of tri-arm star-like bithiophene–disilylene molecules 2T-DSi-stars, in which the synergy of both the branched structure and the disilylene substituents raised the efficiency up to $\Phi_F = 0.49$–0.75 (Fig. 27) [99, 100]. The highest efficiency of $\Phi_F = 0.78$ was reported for bithiophene–silylene star 2T-Si-star. These effects originate from the star-like structure as well as σ–π conjugation

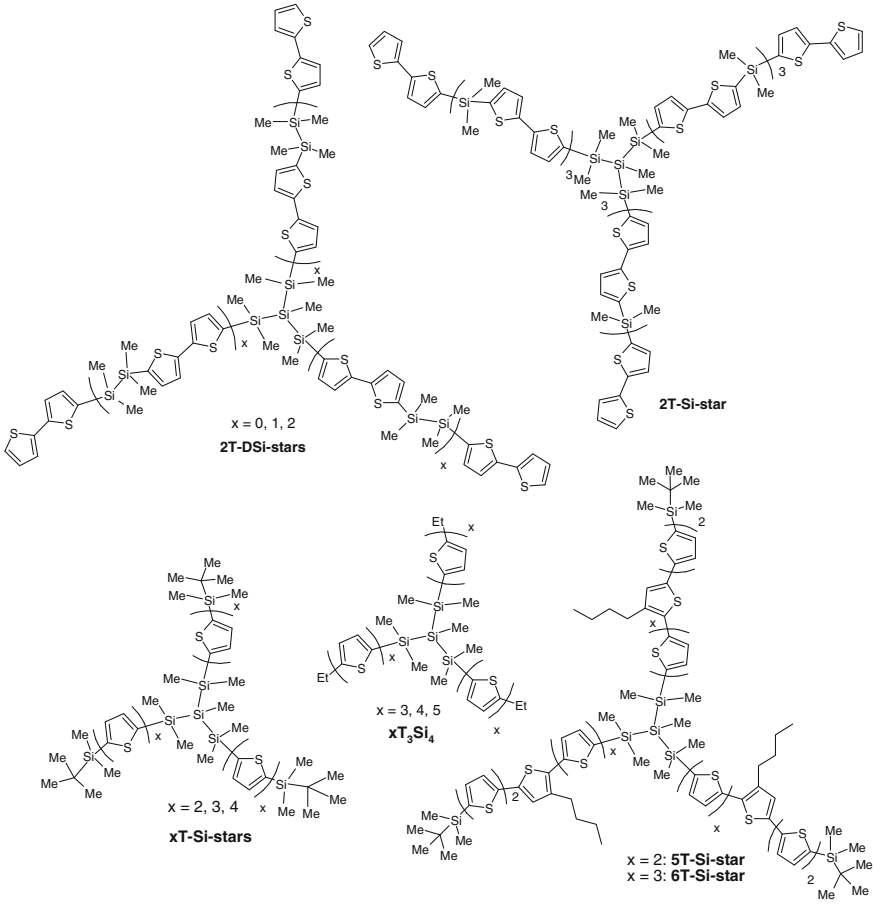

Fig. 27 Tri-substituted oligothiophenesilane nanosized star molecules

between the silicon atoms and bithiophene units by a significant decrease of the nonradiative deactivation rate. Ter-, quater-, quinque-, and sexithiophene-silanylene star molecules also showed increased Φ_F in comparison to their linear analogs, albeit not as dramatic as in the case of the 2T chromophore: (compare $\Phi_F(6T) = 0.36$, Φ_F ($Me_3Si - T6 - Oct_2SiMe_3$) = 0.25, and Φ_F (6T-Si-star)=0.61) [101].

Ohshita et al. has reported on ter-, quater- and quinquethiophenesilane trisubstituted stars xT_3Si_4 (x = 3–5, see Fig. 27) and compared them with linear dimers (Fig. 3) [21]. The quinquethiophenesilane star $5T_3Si_4$ possesses the best semiconducting properties among the oligothiophenesilanes investigated: the OFETs prepared by vacuum sublimation shows a mobility of $6.4 \times 10^{-2}\,cm^2V^{-1}\,s^{-1}$ and on/off ratio of 10^4. It was, however, hardly soluble in organic solvents, and therefore could not be processed to films by spin-coating.

The solubility issue could be solved for tetrasubstituted silanes, possessing tetrahedral symmetry. Lukevicz et al. has reported on the synthesis of a series of radial oligothienylsilanes having four bi-, ter-, or quaterthiophenesilane units attached to a silicon center via a short –$SiMe_2C_2H_4$– spacer [102]. Unfortunately, no optical or semiconducting properties for these materials have been reported. The group of Roncali has described several tetra(terthienyl)silanes (Fig. 28) among which $Si(3T)_4$ was investigated as 3D electro-active π-conjugated material [103] with the expectation that the rigid 3D structure might enhance the light absorption independent

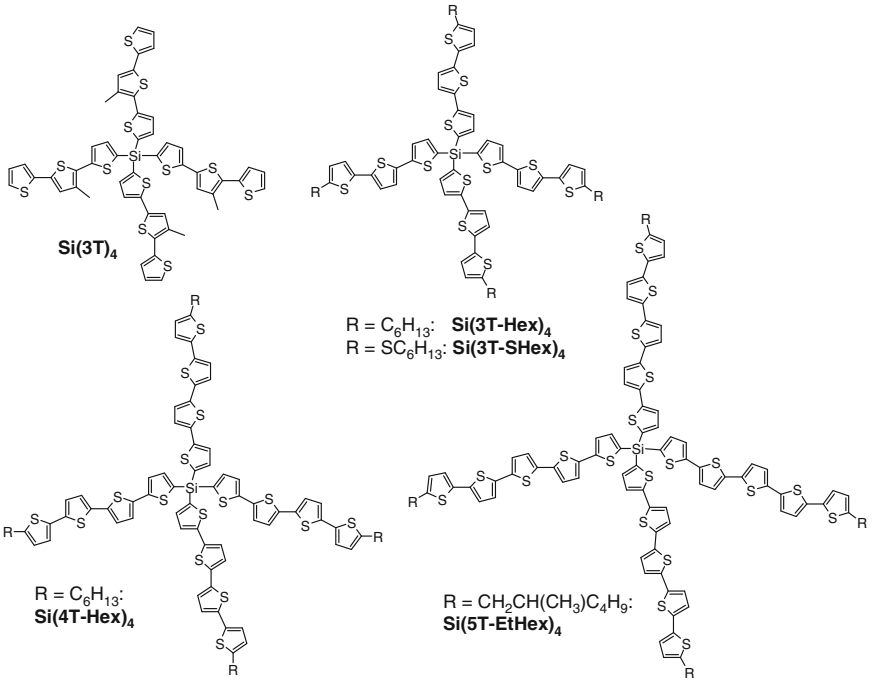

Fig. 28 Tetra(oligothienyl)silanes

of the layer packaging. It is known that linear oligothiophenes have almost perpendicular orientation to the substrate [104] that is useful for OFETs, but prevents their usage in OVPs. Consequently, Si(3T-Hex)$_4$ and Si(3T-SHex)$_4$ were used as donor materials for organic solar cells [105]. Optimal devices using Si(3T-Hex)$_4$ as donor material and PCBM as acceptor material showed an unsatisfactory low PCE of 0.30%; however, this value is five times higher than for a device with the linear oligomer 5-hexyl-2,2′ : 5′,2″-terthiophene Hex-3T. The solar cells efficiency could be improved by increasing the length of the oligothienyl units in corresponding silanes. The group of Ponomarenko recently prepared tetra(quaterthienyl)silane Si(4T-Hex)$_4$ and tetra(quinquethienyl)silane Si(5T-EtHex)$_4$ (Fig. 28) [106]. Heterojunction photovoltaic cells employing composites with C[70]PCBM ([6, 6]-phenyl C71-butyric acid methyl ester) yielded a PCE of 1.0% and 1.35%, respectively. The increasing efficiency in the series of 3D ter-, quater- and quinque thiophenesilanes was attributed to a more effective absorption of the solar light caused by shifting the absorption maxima in the series of oligomers from 390 nm to 414 nm and 437 nm, respectively.

If linear oligothiophenes attach to a silicon branching core via flexible aliphatic spacers, branched structures can be obtained, the ordering of which in layer is determined by the crystallization of the oligothiophene units rather than by the 3D structure of the molecules. Several examples of such materials have been prepared in our group (Fig. 29) [107, 108]. They combine the high crystallinity and semiconducting properties of oligothiophenes with good solubility and solution processability of branched structures – both are useful properties for organic electronics. The terminal groups have a significant influence on the orientation of these molecules along the surface depending on whether they are linear or branched. Molecules with linear end groups G0(Und-4T-Hex)$_4$ orient perpendicular to the surface (Fig. 30), which can be utilized in solution-processed OFETs with the mobility up to $2 \times 10^{-2}\,\mathrm{cm^2\,V^{-1}\,s^{-1}}$ and on/off ratio of 10^5. It is noteworthy that devices made from such materials can be prepared under ambient conditions and their characteristics are stable after storage without any packaging layer for years. Molecules having branched 2-ethylhexyl

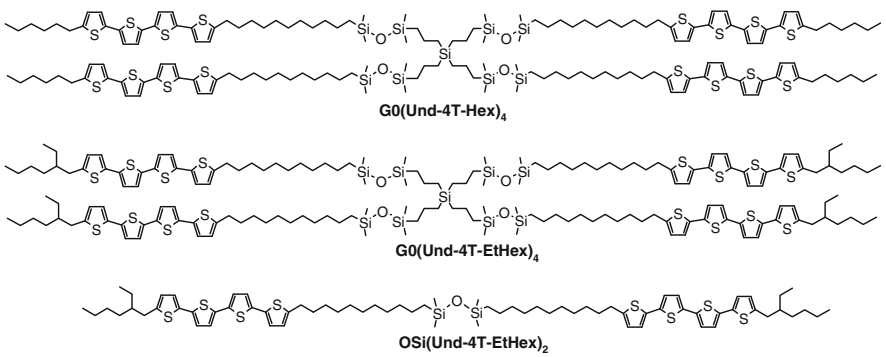

Fig. 29 Quaterthiophene-based flexible multipods bearing two (dimer D1) or four (tetrapods D2-D3) quaterthiophene arms with flexible carbosilane-siloxane cores

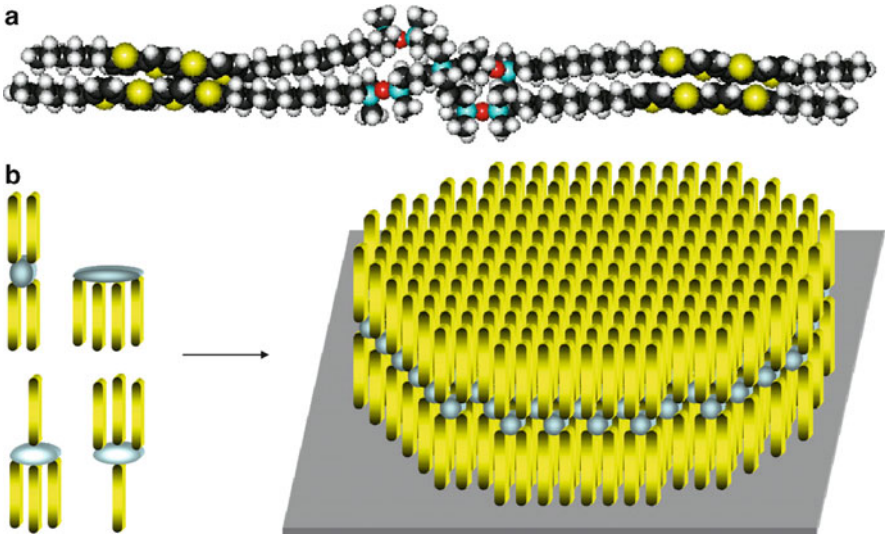

Fig. 30 (**a**) Molecular model of G0(Und-4T-Hex)$_4$ in its extended conformation. (**b**) Schematic representation of different conformations of this molecule as a core with four arms and its self-organization into a monolayer. Reproduced with permission of the American Chemical Society from [107]

end groups G0(Und-4T-EtHex)$_4$ or OSi(Und-4T-EtHex)$_2$ tend to orient parallel to the surface [109], which was used for the creation of photovoltaic cells. The most efficient OPV devices were made from the blend of the dimer OSi(Und-4T-EtHex)$_2$ with fullerene derivative C[70]PCBM, which showed a PCE of 0.9% [110].

Thus, connecting of π-conjugated units to branching silicon center could lead to the following consequences resulting from a decreased tendency to agglomerate: (1) increased luminescence efficiency; (2) improved solubility; (3) changed film morphology. Branching therefore is a versatile concept to modify the properties of conjugated oligomers and provides promising candidates for functional (semiconducting, photo-, or electroluminescent) layers in different organic electronic and photonic devices.

4 Conjugated Organosilicon Dendrimers

As discussed in Sect. 3, the σ-orbitals of silicon overlap with the π-system of the chromophore if the silicon is directly attached by a single bonds to the π system. Despite this σ–π-interaction, silicon does not facilitate conjugation between two π-systems connected by a silicon bridge. Therefore silicon does not extend the π-system which will have consequences for organosilicon dendrimers, in which π-conjugated units are connected either by silicon atoms which build branches in

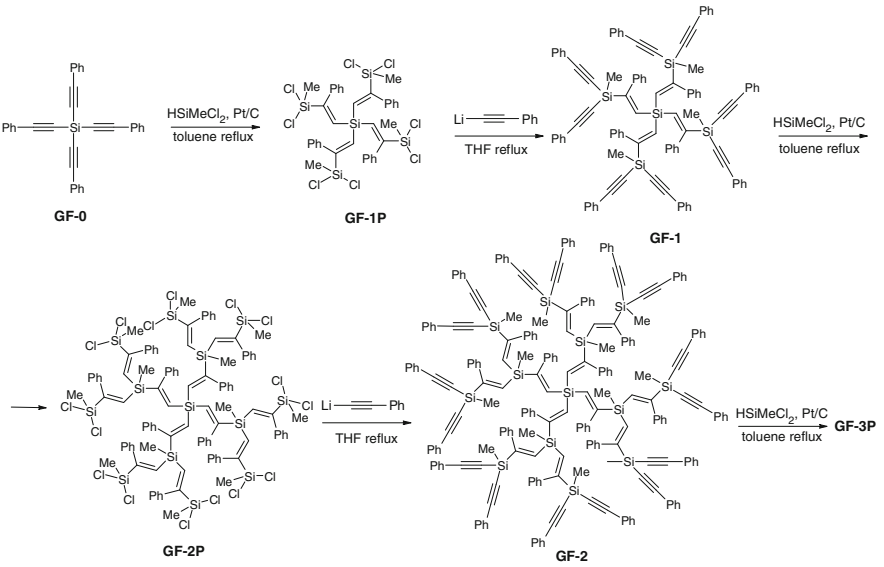

Scheme 6 Synthesis of phenylenevinylene–carbosilane dendrimers

the dendritic structure, or by nonconjugated spacer units. Thiophenes, phenylenes, phenylenevinylenes, and other subunits have been proven to be suitable structures for the construction of chromophores.

The first organosilicon dendrimer containing conjugated units was published by Kim [111]. In an elegant synthetic scheme utilizing a hydrosilylation of the phenylacetylene units of GF-0 with dimethylchlorosilane followed by reaction of terminal chlorosilane groups with lithium phenylacetylide, a series of dendrimers was constructed, which was followed up to the third generation of phenylenevinylene–carbosilane dendrimers with terminal phenyleneacetylene groups (Scheme 6). Unfortunately, few optical properties were reported, among them the absorption maximum and molar extinction coefficient. Independent of the generation the absorption maximum was observed at 287–289 nm. The molar extinction coefficient increased proportionally to the number of alkynyl groups incorporated in the dendrimer.

During recent years, tremendous scientific attention has been devoted towards thiophene-containing dendrimers: (oligo)thiophene groups have been incorporated as core units of the aromatic dendrimers [112, 113] or located at the periphery of organic [114, 115] or organophosphorus [116] dendrimers. Dendritic branches were made from quaterthienyl [117] or 2,3,5-thiophene [118] units. Polythiophene dendrimers have been reported as well [119, 120]. The latter polymers were found to have promising properties in OPV devices [121, 122]. Less attention has been devoted towards oligothiophene-containing organosilicon dendrimers.

Nakayama and Lin have reported on the first organosilicon dendrimer Si_5T_{16}, containing 16 2,5-thienylene rings, connected via tetrasubstituted silicon atoms [123]. Si_5T_{16} was synthesized by the reaction between a tetralithium

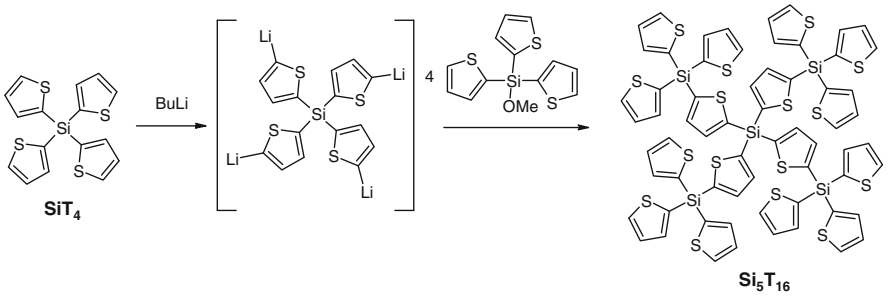

Scheme 7 Synthesis of the first thiophenesilane dendrimer

derivative of tetrakis(2-thienyl)silane with a fourfold molar amount of tris(2-thienyl)methoxysilane with the yield of 19% (Scheme 7). An attempt to access higher generation dendrimers by this synthetic scheme was unsuccessful which may be explained by a low solubility of the polylithium derivatives as well as lithium exchange reactions between products and reagents, both containing active protons in the 5 position of 2-thienyl substituents. Unfortunately neither optical nor electrical properties of this dendrimer have been reported, albeit they would potentially be interesting for organic electronic and photonic applications.

In 2005 Ponomarenko et al. started their work on a series of oligothiophenesilane monodendrons and dendrimers to exploit their optical properties (Fig. 31) [124–128, 130]. The first dendrimer generation G1(2-x) ($x = 1$–4) was synthesized by Kumada and Suzuki coupling reactions of corresponding precursors with moderate to good yields [124, 125]. Bithiophenesilane mono-dendrons of different generations Mn(2–2) ($n = 1$–3) were prepared by reaction of the corresponding chlorosilane with bithienyllithium reagents. This type of reaction was used for a convergent dendrimer synthesis [126] and for further modifications, i.e., to yield carboxyl-containing monodendrons Mn–COOH ($n = 1$–3) [127]. Mn–COOH forms stable and uniform Langmuir monolayers at the air–water interface at a modest surface pressure ($<10\,\mathrm{mN\,m^{-1}}$), which can easily be transferred to a solid substrate. All dendrimers with bithienylsilane core and monothienylsilyl end groups G1(2–1) show luminescent spectrum with a λ_{max} at 385 nm and a quantum yield ($\Phi_F = 0.20$) similar to those obtained for branched tri- and tetrasubstituted bithiophenesilanes [96]. Independent of the generation, all bithiophenesilane dendrimers Gn(2–2) ($n = 1$–3) exhibit violet–blue light emissions with two almost identical emission maxima at 373 and 390 nm and a photoluminescence efficiency of (Φ_F) of 0.30. Bithiophenesilane dendrimers exhibit a significantly (five times) increased luminescence efficiency compared to its constituent luminophores (bithiophenesilanes with $\Phi_F = 0.06$). An explanation may be more favorable energy levels of the 2T chromophores caused by both the inductive effect of the silicon atom and the influence of a local field from the adjacent 2T units, arranged into star-shaped structures within the dendritic molecule [128]. Dendrimers with ter- and quaterthiophenesilane cores G1(3–2) and G1(4–2) as well as "butterfly-like" molecules B1(3–2) and B1(4–2) have shown a so-called "molecular antennae" effect [129, 130]. Energy

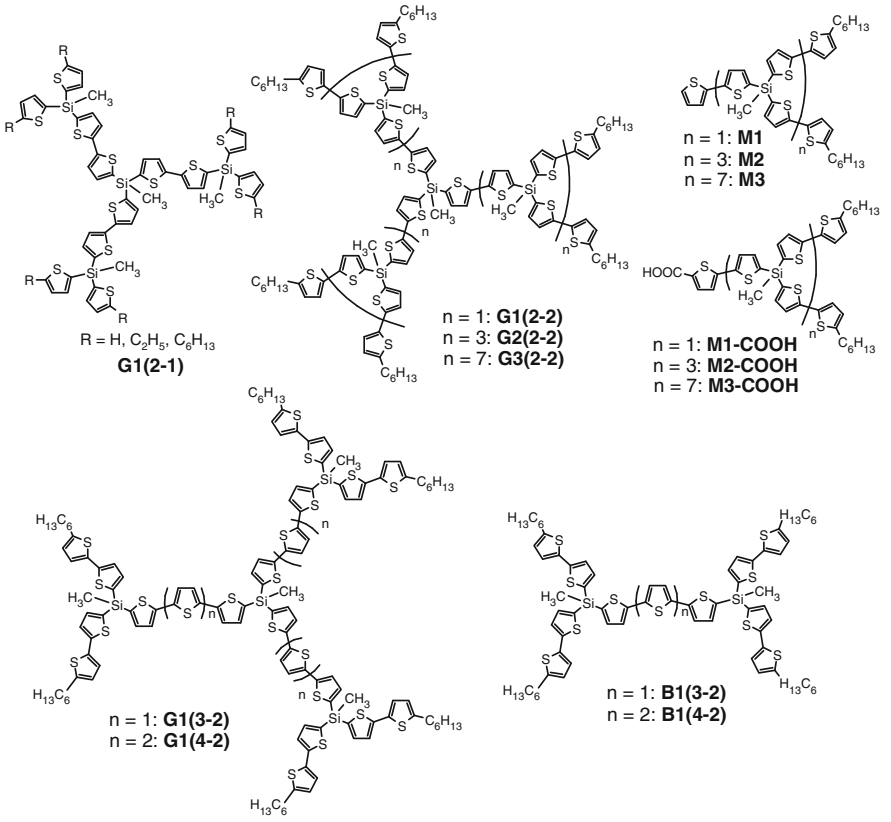

Fig. 31 Oligothiophenesilane monodendrons and dendrimers

captured in the outer segments is efficiently transferred to the inner fragments within the dendritic molecules and have been proposed as promising structures for photo- and electrooptical devices. While this effect has been known since 1994 [131], it took until 2009 to demonstrate G1(3–2) and B1(3–2) as the first organosilicon molecular antennas [129]. Dendrimers G1(3–2) and G1(4–2) emit green light in simple one layer OLED devices [132]. Although their efficiency was rather low, these results indicate that oligothiophenesilane dendrimers possess not only hole but also ET properties. This untypical behavior for oligothiophenes can be explained by a σ–π conjugation between the silicon atoms and the oligothiophene units lowering the dendrimer HOMO level.

More efficient OLEDs have been reported for phosphorescent tris-cyclometalated homoleptic Ir(III) complex $Ir(TPSppy)_3$ (TPSppy = 2 – (4′-(triphenylsilyl)biphenyl-3-yl)pyridine) with a silane-based dendritic substituent (Fig. 32) [133]. This dendrimer has shown high luminescence efficiency both in solution ($\Phi_F = 0.63$) and in film ($\Phi_F = 0.74$). A polymer-based triplet OLED with this Ir(III) doped emitter exhibits a remarkable efficiency of $32.8\,cd\,A^{-1}$, maximal brightness of

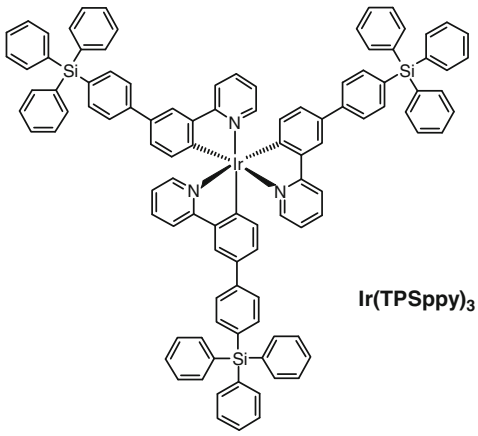

Fig. 32 Phosphorescent tris-cyclometalated homoleptic Ir(III) complex $Ir(TPSppy)_3$ with a silane-based dendritic substituent

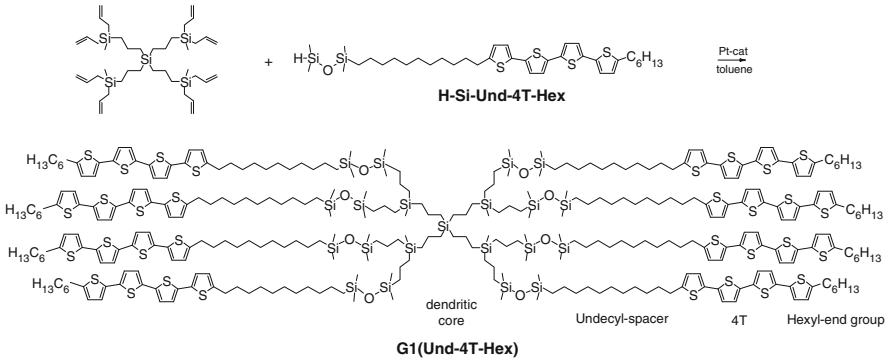

Fig. 33 Synthesis and structural formula of the quaterthiophene-containing carbosilane dendrimer G1(Und-4T-Hex)

$21{,}250\,cd\,m^{-2}$ and maximal power efficiency of $18.7\,lm\,W^{-1}$ at driving voltage of 5–10 V and doped ratio of 5–30%. These values exceed the performance of optimized devices with $Ir(ppy)_3$ (ppy = 2-phenylpyridine) – a similar complex without dendritic phenylenesilane ligands, measured in the same work.

Another type of conjugated organosilicon dendrimers, quaterthiophene-containing carbosilane dendrimers Gn(Und-4T-Hex), have been designed similar to star-shaped oligothiophenes using silicon atoms as branches and additionally flexible aliphatic spacer groups to link the oligothiophene chromophores [107]. They were prepared by a hydrosilylation reaction of polyallylcarbosilane dendrimers of generations 0 (tetraallylsilane), 1, 3, and 5 with a monofunctional quaterthiophene precursor H-Si-Und-4T-Hex [134]. An example showing the synthesis of the first generation dendrimer is shown in Fig. 33. All dendrimers containing the quaterthiophene chromophores and hexyl end groups were soluble in common organic solvents at an elevated temperature of 40–60°C, while at room temperature they formed gels. AFM measurements revealed three typical morphologies:

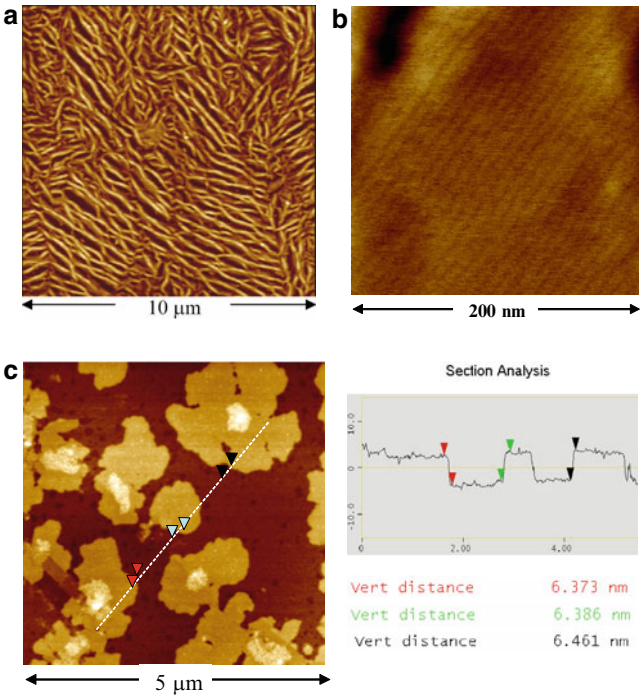

Fig. 34 AFM height images of the dendrimer thick films on graphite substrate: (**a**) G0(Und-4T-Hex) spin-coated from 1 mg ml^{-1} THF solution; (**b**) G1(Und-4T-Hex) from melt; (**c**) G3(Und-4T-Hex) from melt and its cross-section analysis along the line crossing the image [134]

mesowire-like structure, ordered lamellar domains, and smectic-like layered structures, which were common for all these dendrimers (Fig. 34). DSC measurements revealed a high degree of crystallinity, which significantly decreases for dendrimers of higher generations (G3 and G5). A unique feature of these materials is the formation of highly ordered thin films with smectic-like ordering due to π–π-stacking of quaterthiophene groups which might be favorable for OFETs. Indeed, 4T-containing dendrimers up to third generation exhibited field-effect characteristics with a maximum charge carrier mobility of 0.02 cm^2 V^{-1} s^{-1} (for the G0 dendrimer, decreasing with increasing generation), on/off ratios in the order of 10^5–10^6, and threshold voltages close to 0 V.

The few works published on conjugated organosilicon dendrimers indicate that the dendritic structure generally seems to help to yield increased luminescence efficiency, important for OLEDs. Flexibility in the molecular design and good processability from solution are prerequisites for cost efficient OFETs and OLEDs. The current results suggest that the first generation dendrimers already show the optimal effect, and thus the costly synthesis of higher generations will not be necessary.

5 Hyperbranched Conjugated Organosilicon Polymers

Hyperbranched polymers are highly branched macromolecules with 3D dendritic architecture [135]. They may be considered as simplified analogs of dendrimers, which often possess similar properties. In contrast to dendrimers, HB polymers can be produced in a one-pot reaction, leading to highly branched, albeit nonregular molecular structures.

In 1999 Yao and Son reported one of the first examples, an HB poly(2,5-silylthiophene)s HB-SiT-R, prepared by one-pot reaction between 2-bromo-5-(trimethoxysilyl)thiophene TMOS-T-Br and magnesium in good to excellent yields (Scheme 8) [136]. This structure is indeed quite similar to the thiophenesilane dendrimer of Nakayama [123], the main difference being the highly regular and almost defect-free structure of the dendrimer. The intermediate methoxy-substituted HB polymer HB-SiT-OMe was functionalized with Grignard reagents, leading to a series of air- and moisture-stable polymers HB-SiT-R with R being methyl-, vinyl-, 2-thienyl-, and phenyl-groups. The extent of σ–π conjugation in these polymers was examined using optical spectroscopy, which showed (compared to a non-substituted thiophene) a significantly red-shifted π–π* transition (at ~250 vs 230 nm) independent of the group R. This absorption originating from the HB-SiT-R polymer subunit indicates a significant degree of conjugation between the thiophene ring and the silicon atom, but not between the thiophene ring and the attached group R. A weak and broad absorption in the region of 300–320 nm was attributed to a charge transfer from thiophene to silicon, albeit it may also stem from a small fraction of bithiophene–silylene fragments – potential side products from the Grignard reaction of monothienyl reagents [137]. Therefore, the electronic effects of this 3D polymer structure may require more investigations, but at least the effects contributing to the π–π* absorptions appear to be well established. The λ_{max} and extinction coefficients for HB-SiT-R are similar to those obtained for linear polymers.

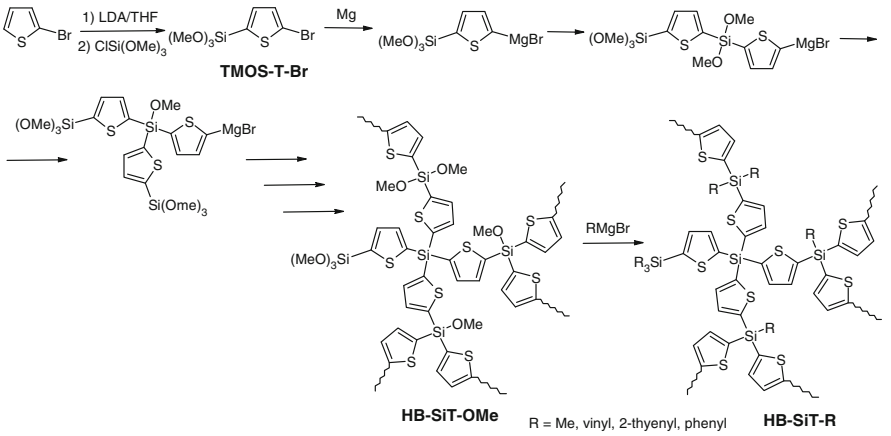

Scheme 8 Reaction sequence, leading to hyperbranched poly(2,5-silylthiophene)s

Two other types of HB organosilicon polymers containing conjugated units were synthesized by hydrosilylation reaction of AB_2- or AB_3-functional monomers [138, 139]. Poly(silylenevinylene) with ethynyl functional groups HB-SVE were prepared by hydrosilylation of AB_2-functional methyldiethynylsilane (MDES) (Scheme 9) [138]. HB poly(carbosilarylene)s HB-SPVs were prepared by hydrosilylation of AB_3-functional arylsilane monomers 1-(dimethylsilyl)-4-(trivinylsilyl)-benzene (DMS-1,4-Ph-TVS), 1-(dimethylsilyl)-3-(trivinylsilyl)-benzene (DMS-1, 3-Ph-TVS), and 1,1,3,3-tetramethyl-1-(4′-(trivinylsilyl)-phenylene-1)-disiloxane (TMDS-1,4-Ph-TVS) (Scheme 10) [139]. The latter type of polymers contains σ–π conjugated disilylene-phenylene units separated by ethylene or disiloxane nonconjugated spacers. Unfortunately, in both cases no optical or electrical characterization of the HB polymers were reported, allowing no insight into their potential in the field of organic photonics and electronics.

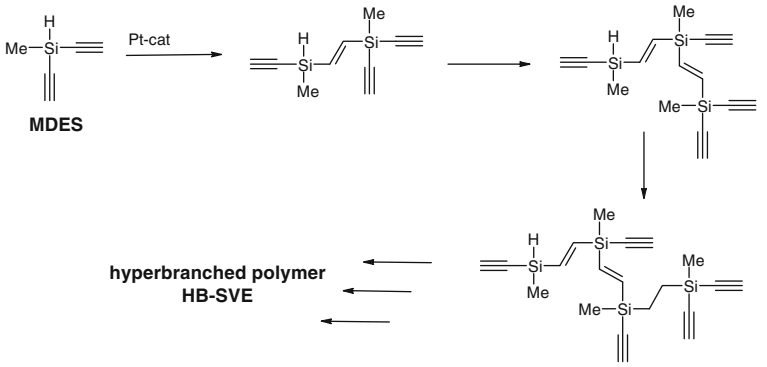

Scheme 9 Synthesis of hyperbranched poly(silylenevinylene) with ethynyl functionalization

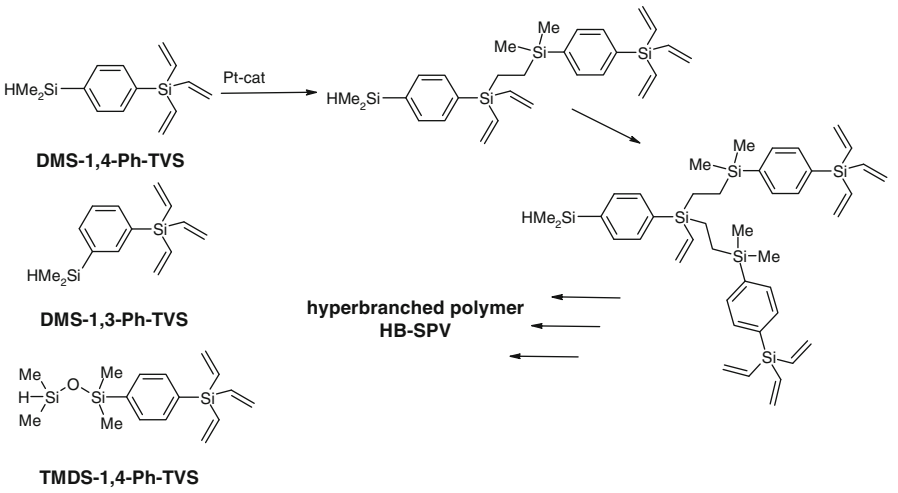

Scheme 10 Arylsilane monomers and an example of hyperbranched poly(carbosilarylene) formation from the first of them

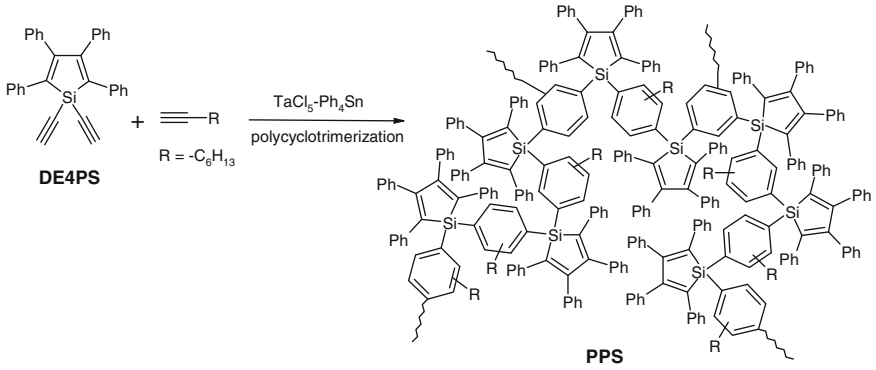

Scheme 11 Synthesis of hyperbranched poly(penylenesilolene)s

Very interesting features were reported by Chen et al. for HB poly(phenylenesilolene)s (PPS) [140]. These HB polymers were prepared in a one-pot synthesis by homo-polycyclotrimerization of 1,1-diethynyl-2,3,4,5-tetraphenylsilole (DE4PS) and its co-polycyclotrimerizations with 1-octyne catalyzed by $TaCl_5 - Ph_4Sn$ in high yields (Scheme 11). The silole units in PPS are interconnected by trisubstituted benzene units, which link the phenyl rings to form 3D structures. This unique molecular structure leads to a number of interesting properties: these polymers are readily processible (completely soluble), thermally stable (T_d up to ~400°C), contain extended conjugated chromophores ($\lambda_{max} \sim 520$ nm), exhibit nonlinear optical activity ($F_L \sim 180\,mJ\,cm^{-2}$), and readily emit light upon excitation at low temperatures (cooling-enhanced emission, CEE). Their molecular weights, measured by GPC relative to a linear polystyrene standard, were measured to be in the range 3,530–5,820 Da (M_w), but this value might significantly underestimate the real molecular weight (the authors suggested the "real" molecular weight may be up to seven times higher) due to the HB and rigid structure of these polymers. All PPS polymers absorb in the visible region, while the monomeric siloles absorb in the UV spectral region ($\lambda_{max} = 378$ nm). The extended conjugation of these HB polymers originates possibly from the synergistic interplay of a σ–π conjugation of the silole rings with the π-orbitals of the chromophore and an electronic interaction of the aromatic rings via the silicon bridges. This extended electronic conjugation results in a nonlinear optical effect, an optical limitation.[2] In this regard the effect of PPSs has been found superior to C_{60}, the best-known optical limiter so far. In contrast to siloles or linear poly(silolylacetylene)s [141], solutions of PPSs are somewhat luminescent ($\Phi_F = 0.01$, this low value is however 10–100 higher than that for low molar weight siloles), but are completely inactive towards AIE. The luminescence of PPS polymers is, however, enhanced at low temperatures. This unique phenomenon of cooling-enhanced emission (CEE) was explained by the restricted intramolecular rotations of the phenyl rings around the axes of the

[2] An optical limitation is an optical transmittance that sharply decreases at high light levels and strongly attenuates the optical power of intense laser pulses.

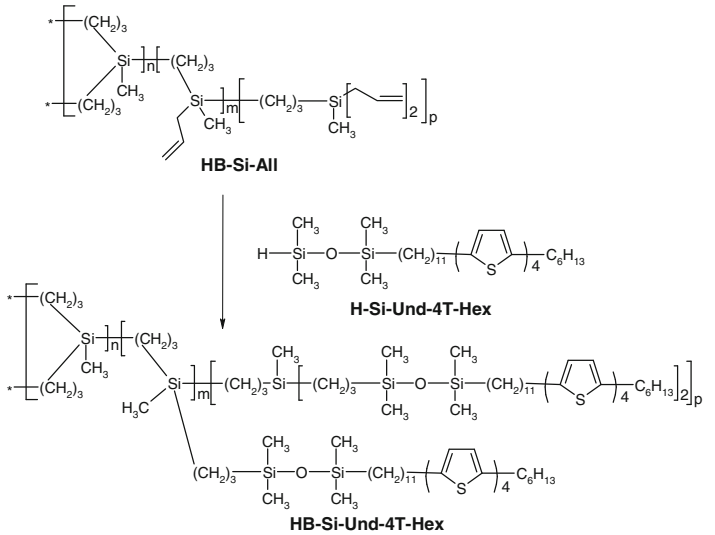

Scheme 12 Synthesis of hyperbranched polycarbosilanes with quaterthiophene end groups

single bonds linked to the silole cores at lowest temperatures. This effect may be regarded as a special type of thermochromism, offering a versatile mean for tuning the photoluminescence of the HB polymers.

A recent example of HB conjugated organosilicon polymers are HB polycarbosilanes with quaterthiophene end substituents prepared by the authors group [142]. They were received from nonconjugated HB polyalyllsilanes HB-Si-All modified with a silane-containing quaterthiophene precursor H-Si-Und-4T-Hex by hydrosilylation similar to the synthesis of carbosilane dendrimers Gn(Und-4T-Hex) [134] (Scheme 12). While dendrimers resemble a single species of defined molecules, HB polymers represent a distribution of molecules with different molecular weights and a large polydispersity. Samples of HB polymers with three different molecular weight distributions were compared to corresponding dendrimers: the initially obtained HB polycarbosilane was recrystallized to remove low molecular weight impurities (HB-1) and two samples with narrow molecular weight distribution were prepared by fractionation of the initial HB-Si-All (HB-2, HB-3). In OFETs all samples showed sufficient hole mobility, good on/off ratio, and good threshold voltage comparable to their dendritic analogs (Table 1). Sample HB-2 with the lowest molar weight and narrowest distribution showed the highest field-effect mobility ($\mu = 10^{-3}\text{cm}^2\text{V}^{-1}\text{s}^{-1}$) comparable to G1(Und-4T-Hex).

To date, the information on HB conjugated organosilicon polymers is rather limited. While dendrimers and especially linear polymers have been extensively studied, many of their HB analogs are waiting for their synthesis. Some HB polymers have been made without performing a detailed analysis of their optical and electrical characteristics. Nevertheless, available data indicate that HB polymers indeed might serve as a more cost efficient alternative to dendrimers in electronic applications. In addition, some HB structures may also induce unique optical

Table 1 Molecular weights characteristics and semiconducting properties of Und-4T-Hex-containing carbosilane dendrimers and hyperbranched polycarbosilanes

Sample	M_n^a	M_w^a	M_w/M_n	Mobility, $cm^2V^{-1}s^{-1}$	On/off ratio	Threshold voltage, V
HB-1	13,600	35,600	2.62	1×10^{-4}	10^4	−2
HB-2	10,100	11,500	1.14	1×10^{-3}	10^5	−1
HB-3	21,700	24,800	1.14	2×10^{-4}	10^5	−3
G0	2,997[b]	–	–	2.0×10^{-2}	10^6	0
G1	6,301[b]	–	–	1.3×10^{-3}	10^6	1
G3	16,279[b]	–	–	4.0×10^{-4}	10^6	−2

[a]Determined by GPC using polystyrene standards
[b]Molar weight of the dendrimers measured by MALDI–TOF (matrix assisted laser desorption ionization–time-of-flight mass spectrometry)

properties (i.e., CEE) different to those of their monomeric, linear, or dendritic analogs. We expect further progress in this field, striving for a comprehensive understanding of conjugated HB molecular structures and their contribution to electronics and photonics. This will result in a manifold of new structures and a detailed insight into electrical and optical properties of these compounds.

6 Linear Conjugated Organosilicon Polymers

Presently described linear conjugated organosilicon polymers can be divided into three large subgroups: (1) conjugated polymers with Si atoms in the side chains, which are directly linked to the conjugated backbone, (2) silanylene-containing polymers having Si atoms, which link the conjugated fragments to form a main chain, and (3) silol-containing polymers, possessing the special "silol"-units being a kind of silicon-containing chromophore.

6.1 Polymers with Silicon Atoms in the Side Chains

The predominant π-conjugated polymers with organosilicon substituents in the side chains are polyacetylenes [143–148], polythiophenevinylenes (PTV) [149], and poly(1,4-phenylene vinylene)s (PPV) [150–175].

Unlike unsubstituted polyacetylene, its silicon derivatives are air stable and highly soluble [143]. Since the discovery of poly[1-(trimethylsilyl)-1-propene] [144], silicon-substituted polyacetylenes are well-known for their extremely high gas permeation properties caused by a large free volume in the polymer films [145, 146]. However, organosilicon substituents, directly attached to a polyacetylene backbone, weaken the interchain interactions, which might cause inferior electrical properties. This can be a reason for the little work reported on the application of this type of polymers in organic electronics and photonics.

Soluble, air stable, and conductive copolymers were prepared by polymerization of $(HC{\equiv}CSiMe_2)X$ (where X = single bond, $–CH_2–$, $–CH_2CH_2–$, $–SiMe_2–$, O) with WCl_6 or $MoCl_5$ catalysts [147]. Although the pristine polymers were not conductive, a conductivity of $10^{-2}\,S\,cm^{-1}$ was obtained by doping with $(NEt_2)_3S^+SiF_2Me_3^-$ (or $NBu_4^+F^-$) and I_2 (or SO_3). A series of 1,2,3,4,5-pentaphenylsilolyl-containing polyacetylenes 5PS-Ac, 5PS-9C-Ac, and 5PS-9C-PAc (Fig. 35) have been prepared by polymerization of the corresponding substituted acetylenes using $NbCl_5$- and WCl_6-Ph_4Sn catalysts [148].The polymers were thermally stable up to 350°C, but practically non-luminescent in good solvents. Nevertheless, some polymers with nonanyloxy spacer between the pentaphenylsilol pendant groups and polyacetylene backbone (5PS-9C-Ac and 5PS-9C-Pac) showed aggregation- or cooling-induced emission. These effects were explained by the restricted intramolecular rotation or twisting of the silole chromophores introduced by aggregation due to incomplete solution (by using poor solvents or at low temperature). A multilayer electroluminescent device using 5PS-9C-PAc as an active layer emitted blue light of 496 nm with a maximum brightness of $1,118\,cd\,m^{-2}$, and showed a current efficiency of $1.45\,cd\,A^{-1}$ with an external quantum yield of 0.55%.

The synthesis of long alkylsilyl-substituted poly(thienylenevinylene) PSiTV (Fig. 36) via heteroaromatic dehydrohalogenation polymerization was reported by Shim et al. [149]. The polymer was determined to have a molecular weight of

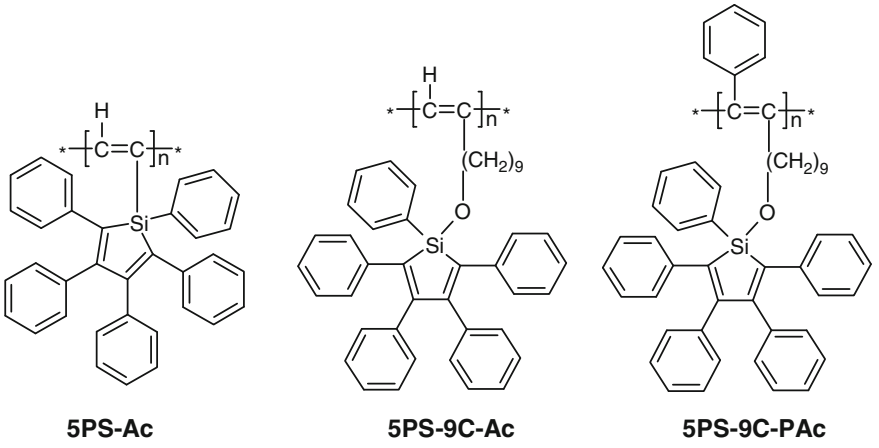

Fig. 35 1,2,3,4,5-Pentaphenylsilolyl-containing polyacetylenes

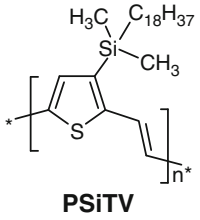

Fig. 36 Silyl-substituted polythiophenevinylene PSiTV

26.4 kDa (M_n, polydispersity of 5.5) and was completely soluble in common organic solvents (e.g., chloroform, THF, xylene), due to the attached dimethyloctadecylsilyl side chains. PSiTV was thermally stable up to 340°C (5% weight loss) and had a T_g of approximately 148°C. The maximum absorption occurs at 563 nm with an onset at 788 nm that corresponds to a promising rather low bandgap of 1.57 eV.

Work in the area of π-conjugated organosilicon substituted polymers has mainly been devoted to the synthesis and investigation of silicon-substituted poly(1,4-phenylenevinylene)s (Si-PPV). The first Si-PPV derivative, poly[2-(3-*epi*-cholestanol)-5-(dimethylthexylsilyl)-1,4-phenylenevinylene] (CS-PPV), was reported by Wudl et al. (Fig. 37) [150].The silicon group in this polymer enlarges the band gap and changes the polymer's absorption peak from 510 nm (orange, reported for the carbon analog bis(3-*epi*-cholestanoxy)PPV) to 450 nm (yellow). In a non-optimized single layer OLED device with Al electrodes CS-PPV doped with an electron transporting molecular dopant, 2-(4-biphenylyl)-5-(4-*tert*-butylphenyl)-1,3,4-oxadiazole (PBD), emitted green light with a power efficiency of 0.3% [151].

The simplest representative of this class of polymers is poly(2-trimethylsilyl-1,4-phenylenevinylene) (TMS-PPV), first reported by Shim et al., which also shows green electroluminescent emission [152] The electrical conductivity of TMS-PPV doped with I_2 was measured to be $2 \times 10^{-2}\,\mathrm{cm}^{-1}$. This is quite different from unsubstituted PPV, which cannot be doped with iodine. Substitution of one

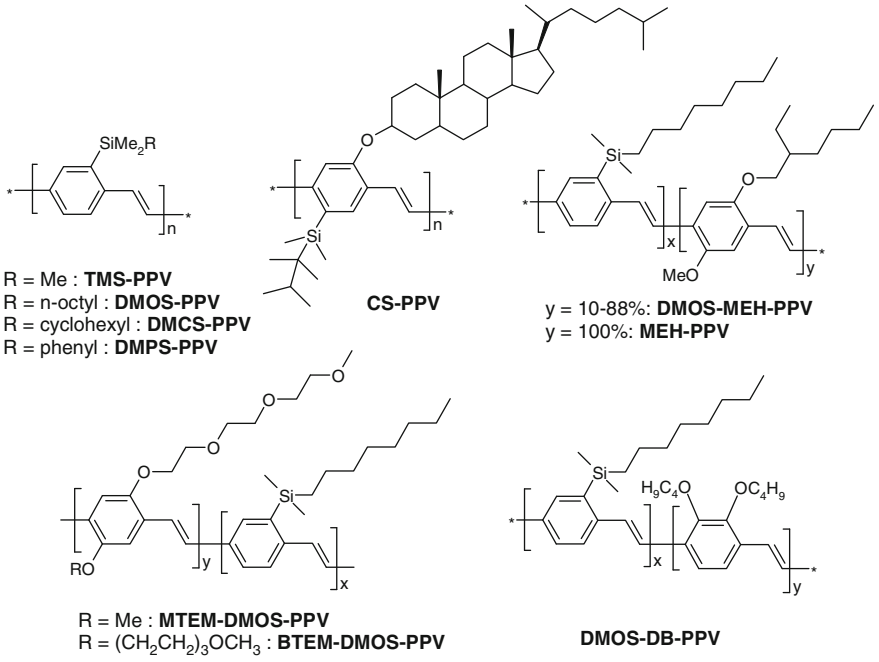

Fig. 37 Silyl-substituted poly(1,4-phenylene vinylene)s (PPV)

methyl group in TMS-PPV by an *n*-octyl group led to poly(2-dimethyloctylsilyl-1,4-phenylenevinylene) DMOS-PPV – another green polymeric emitter [153]. Films of DMOS-PPV were found to be highly fluorescent, with a quantum efficiency exceeding 0.60, an efficiency significantly higher than the value for PPV and MEH-PPV (0.27 and 0.15, respectively) [154]. Single layer electroluminescent devices (layer structure: ITO/DMOS-PPV/Ca or Al) exhibit an emission maximum at 520 nm with an internal quantum efficiency in the range of 0.2–0.3% [155] In double layer devices with an additional PBD electron conducting and hole blocking layer the internal quantum efficiency increased up to 2% [156]. However, as emitter in OLEDs the homopolymer DMOS-PPV has a disadvantage of a high turn-on voltage (15 V). Statistical copolymers of DMOS-MEH-PPV (Fig. 37) have been prepared to overcome this problem, which indeed showed a reduced turn-on voltage in OLED devices (6–7 V), however, accompanied by a decreased PL and EL efficiency with increasing ratio of DMOS to MEH [157]. Further improvements were achieved in DMOS-MTEM-PPV and DMOS-BTEM-PPV copolymers, containing silyl-substituted DMOS-PPV units as well as ion-transporting 2-methoxy-5-(trimethoxyethoxy)-1,4-phenylenevinylidene (MTEM-) or 2,5-bis(trimethoxyethoxy)-1,4-phenylenevinylidene (BTEM-)units. In so-called light-emitting electrochemical cells (LECs) mobile ions move during charge transfer from and into the polymer layer [158]. Both copolymers yielded LECs with low turn-on voltages (down to 2.5 V) and an increased efficiency (up to $0.5\,\mathrm{lm\,W^{-1}}$).

Cyclohexylsilyl- and phenylsilyl-substituted PPV derivatives, poly[2-dimethylcyclohexylsilyl-1,4-phenylene vinylene] (DMCS-PPV) and poly[2-dimethylphenylsilyl-1,4-phenylene vinylene] (DMPS-PPV) (Fig. 37), as well as disubstituted poly[2,5-bis(dimethylcyclohexylsilyl)-1,4-phenylene vinylene] (BDMCS-PPV) and poly[2,5-bis(dimethylphenylsilyl)-1,4-phenylene vinylene] (BDMPS-PPV) (Fig. 38), were synthesized from bromine functionalized precursors and Gilch dehydrohalogenation polyaddition [159]. The disubstituted polymers BDMCS-PPV and BDMPS-PPV yielded insoluble thin films from soluble polymer precursor materials by a thermal conversion mechanism. Monosilylsubstituted DMCS-PPV and DMPS-PPV exhibited good solubility, good film-forming properties, and high molecular weights. These polymers feature a thermal stability which outperforms most other PPV derivatives including alkylsilyl-substituted PPVs, with higher glass transition temperature ($Tg = 125$–$127^{\circ}C$), and remarkably high PL efficiencies both in solution ($\Phi_F = 0.86$–0.88) and as film ($\Phi_F = 0.82$–0.83). Simple single layer OLEDs fabricated from DMCS-PPV and DMPS-PPV (layer structure: ITO/polymer/Al) showed EL maxima at 510 and 515 nm, respectively, with an external EL quantum efficiency up to 0.03%. An additional poly(vinylcarbazole) (PVK) HTL increased the EL quantum efficiencies up to a maximum of 0.08%.

Silyldisubstituted PPV [poly(2,5-bis(trimethylsilyl)-1,4-phenylenevinylene)] (BTMS-PPV, Fig. 38) was prepared via two different precursor polymers, a water-soluble sulfonium and an organic soluble thiophenoxy precursor polymer [160]. In a single layer OLED device fabricated with BTMS-PPV (from the thiophenoxy precursor) as emitter showed a emission peak at about 545 nm, although with a turn-on voltage of 20 V and an external quantum efficiency of

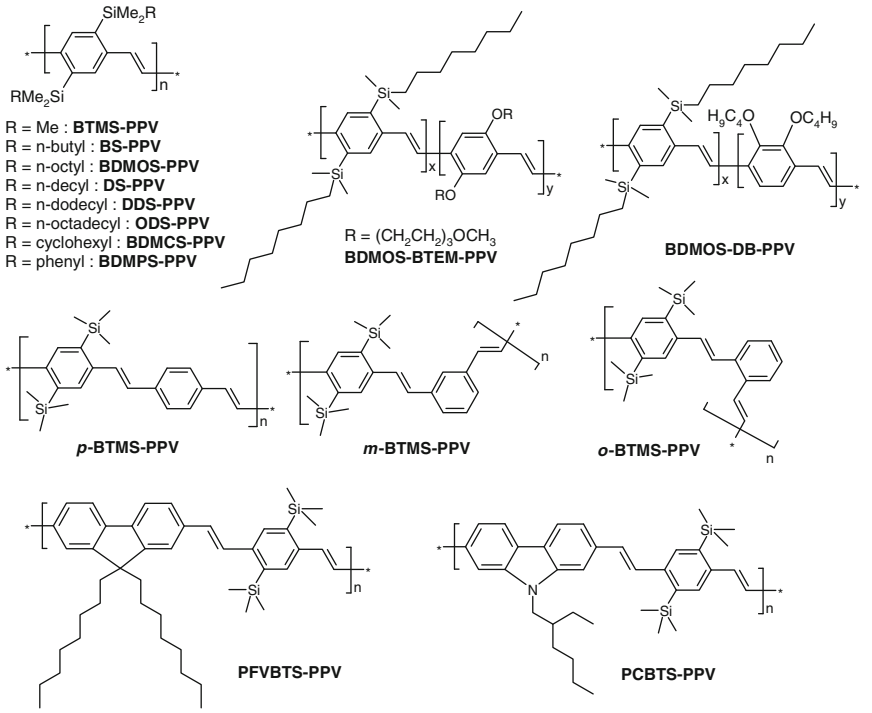

Fig. 38 Silyl-disubstituted poly(1,4-phenylene vinylene)s (PPV)

$6.0 \times 10^{-4}\%$ in air. Silyl disubstituted PPV with longer alkylsilyl groups – poly (2,5-bis (dimethylbutylsilyl)-1,4-phenylenevinylene) BS-PPV [161, 162], poly(2,5-bis(dimethyloctyl-silyl)-1,4-phenylenevinylene) BDMOS-PPV [163], poly(2,5-bis(dimethyldecylsilyl)-1,4-phenylenevinylene DS-PPV [162], poly(2,5-bis (dimethyldodecylsilyl)-1,4-phenylene-vinylene DDS-PPV [162], and poly(2,5-bis(dimethyloctadecylsilyl)-1,4-phenylenevinylene ODS-PPV [162, 164], as well as unsymmetrically disilylsubstituted PPVs - were also reported [165]. Disubstituted BDMOS-PPV were found to have similar properties as their monosubstituted analog DMOS-PPV, both emitting light in the green region. However, BDMOS-PPV is thermotropic liquid crystalline between 160 and 180°C and emits polarized light from the film. Apparently the polymer is both hole and electron conducting, since a single layer device emits light at positive as well as negative bias. The statistical copolymer poly[2,5-bis(dimethyloctylsilyl)-1,4-phenylenevinylene)]-*co*-[2,5-bis(trimethoxyethoxy)-1,4-phenylenevilylene] BDMOS-BTEM-PPV exhibits an optical absorption and luminescence, in between the two homopolymers [166]. Both polymers were tested in OLED and LEC devices. Statistical copolymers of BDMOS units with 2,3-bis(dibutoxy)-1,4-phenylenevilylene units (BDMOS-DB-PPV) showed an EL efficiency up to $0.72\,\mathrm{cd\,A^{-1}}$ with a maximum luminance of $1,384\,\mathrm{cd\,m^{-2}}$ at 12 V and a turn-on voltage of 4.0 V, which was superior to its monosilylsubstituted analog, the DMOS-DB-PPV copolymer [167, 168].

Tuning the color of silyl-disubstituted PPVs is possible by introduction of *o*-, *m*-, or *p*-phenylenevinylene units into the copolymers having different effective conjugation lengths. Shim et al. reported on synthesis of poly[$o(m,p)$-phenylenevinylene-*alt*-2,5-bis(trimethylsilyl)-*p*-phenylenevinylene], $o(m,p)$-PBTMS-PPV (Fig. 38) by the Wittig condensation polymerization of diphosphonium salts with dialdehyde monomers such as terephthaldicarboxaldehyde, isophthalaldehyde, and phthalicdicarboxaldehyde [169, 170]. Their photoluminescence spectra have peaks at 485, 470, and 440 nm for *p*-PBTMS-PPV, *o*-PBTMS-PPV, and *m*-PBTMS-PPV, respectively. The electroluminescence spectra of *o*-PBTMS-PPV and *p*-PBTMS-PPV exhibited EL emission at 470 and 490 nm, respectively, with a threshold voltage of 8–9 V. The emission wavelength of *o*-PBTMSPPV corresponds to a pure blue light which obviously is a consequence of the reduced π-conjugation length effected by the ortho-linkage and trimethylsilyl substituent. It is noteworthy that blue EL emission from PPV derivatives is quite exceptional.

Another approach to tune the emission color of PPV derivatives was attempted by introduction of fluorene or carbazole units into the PPV backbone. Thus, poly[*N*-ethylhexyl-3,6-carbazolevinylene-*alt*-2,5-bis-(trimethylsilyl)-*p*-phenylenevinylene] (PCBTS-PPV) and poly[9,9-*n*-dihexyl-2,7-fluorenediylvinylene-*alt*-2,5-bis(trimethylsilyl)-*p*-phenylenevinylene] (PFBTS-PPV) have been synthesized by a Wittig polycondensation reaction [171]. These resulting polymers have shown a photoluminescence with maximum peaks at 480 and 495 nm corresponding to blue and greenish-blue emissions, respectively. The shift to shorter wavelengths compared to other PPV-based copolymers seems to be caused by the electron-donating effect of the silyl group. In films, PFBTS-PPV and PCBTS-PPV showed remarkably high PL efficiencies ($\Phi_F = 0.64$ and 0.81, respectively). As single layer OLEDs (layer structure: ITO/polymer/Al) the polymers emit blue and greenish-blue light with emission maxima of 480 nm (PCBTS-PPV) and 500 nm (PFBTS-PPV). Compared to MEH-PPV the relative EL quantum efficiencies of PCBTS-PPV and PFBTS-PPV were found to be 13 and 32 times higher.

A series of PPV derivatives containing a dimethyldodecylsilylphenyl unit as a pendant group was reported by the Jin group (Fig. 39) [172–174]. All polymers were completely soluble in common organic solvents, had high thermal stability (up to 400°C), and were used as emitting layer in OLEDs. Poly[2-(4-dimethyldodecylsilylphenyl)-1,4-phenylenevinylene] (*p*-SiPhPPV), synthesized via

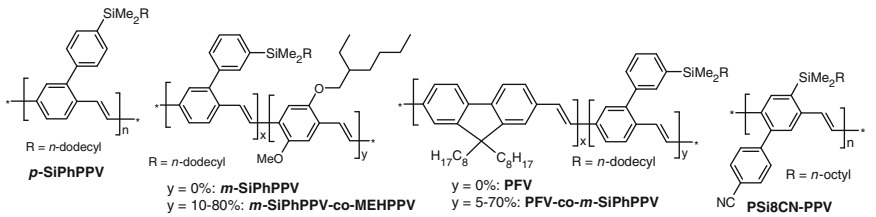

Fig. 39 Alkylsilylphenyl-containing PPV homo- and co-polymers used in OLEDs

Gilch polymerization, had a very high molecular weight of 300 kDa (M_n, polydispersity of about 3). In a single layer OLED device it showed a strong green emission at 524 nm with a maximum brightness of 5,900 cd m^{-2} (at 17 V) [172]. Asymmetric homo- and co-polymers: poly[2-(3′-dimethyldodecylsilylphenyl)-1,4-phenylene vinylene] (*m*-SiPhPPV) and poly[2-(3′-dimethyldodecylsilylphenyl)-1,4-phenylene vinylene-*co*-2-methoxy-5-(2′-ethylhexyloxy)-1,4-phenylene vinylene] (*m*-SiPhPPV-*co*-MEHPPV) were prepared similarly [173]. These polymers also had high molecular weights with narrow weight distributions. The copolymers showed better optical and EL properties than those of the homopolymers *m*-SiPhPPV and MEH-PPV. While devices made from the homopolymer *m*-SiPhPPV need a rather high turn-on voltage (14 V), the replacement of just 10% of the monomeric units by MEHPPV units in the copolymer reduced the turn-on voltage to 5.5 V, while 25% reduced to 2.3 V. Single layer light-emitting devices fabricated from *m*-SiPhPPV-*co*-MEHPPV emitted orange–red light ($\lambda_{max} = 588 - 595$ nm) with maximum brightness and an external luminance efficiency up to 19,180 cd m^{-2} or 2.9 lm W^{-1}. A series of similar copolymers, poly[9,9-di-*n*-octylfluorenyl-2,7-vinylene]-*co*-(2-(3-dimethyldodecylsilyl-phenyl)-1,4-phenylene vinylene)] (PFV- *co*-*m*-SiPhPV), emitted green light with turn-on voltages in the range of 4.5–6.0 V, maximum brightness up to 9,691 cd m^{-2} at 16 V, and a luminance efficiency up to 3.27 cd A^{-1} [174]. Thin films of PFV, *m*-SiPhPV, and PFV-*co*-*m*-SiPhPV were found to exhibit photoluminescence quantum yields between 21 and 42%, exceeding those of MEH-PPV.

Poly(*p*-phenylenevinylene) derivatives with an electron-withdrawing cyanophenyl group on the polymer backbone, poly[2-dimethyloctylsilyl-5-(4′-cyanophenyl)-1,4-phenylenevinylene] (PSi8CN-PPV, Fig. 39), were synthesized via the Gilch polymerization [175]. They showed very high glass transition temperatures (above 180°C). The presence of the electron-withdrawing cyanophenyl group lowered the HOMO and LUMO energy levels of PSi8CN-PPV relative to common PPV derivatives. OLEDs (layer structure: ITO/PEDOT/PSi8CN-PPV/LiF/Al) emitted light with a maximum at 513 nm, corresponding to green light with a CIE coordinate of (0.330, 0.599) close to standard green (0.30, 0.60), a maximum external quantum efficiency of 0.67%, and a maximum brightness of 2,900 cd m^{-2}.

The optical properties of silicon-substituted PPV have been summarized in Table 2. As can be seen from these data, these materials often outperform their carbon analogs (PPV, MEH-PPV, PFV), especially with photoluminescence quantum efficiency which reaches 83% in films. Their absorption and emission spectra as well as HOMO–LUMO levels can be tuned by appropriate substitution or copolymerization using a range of comonomers, leading to highly efficient green, blue, or orange–red emitters. The high solubility of such polymers is apparently caused by the twisting of the silicon-containing phenyl ring away from the plane of the conjugated PPV backbone and proves silicon side groups as a valid concept to introduce wet processability into classes of polymers with promising optical and electrical properties.

Table 2 Optical properties of PPV and its silyl-substituted derivatives

Polymer	λ_{max} (UV, nm)		λ_{max} (PL, nm)[b]		PL efficiency (Φ)		λ_{max}	E_g	HOMO	LUMO	
	Solution[a]	Film	Solution[a]	Film	Solution[a]	Film	(EL, nm)	(eV, (UV/nm))[c]	(eV)	(eV)	Reference
PPV	–	426	–	–	–	0.27		2.5	−5.0/−5.1	−2.5	[152, 154, 161]
MEH-PPV	–	510	–	592	0.14	0.15	590	2.1	−4.94	−2.82	[154, 159, 161]
						0.18					
									−5.1	−3.00	[173]
									−5.0	−2.73	[175]
TMS-PPV		420	–	510 (550, 590)	–	–	–	2.43 (510)	–	–	[152]
DMOS-PPV	420	414/420	–	520 (563)	–	0.60	520	2.48 (500)	−5.7	–	[153, 155]
CS-PPV	–	450	–	515 (550)	–	–	530	–	–	–	[150, 151]
BDMOS-PPV	–	436	–	513	–	0.60	545	2.38 (520)	–	–	[160]
ODS-PPV	436	447	494 (527)	510 (526)	–	–	–	2.42 (513)	−5.66	−2.54	[164]
	435	445		510 (536)	0.89			2.43 (510)	−6.52	−2.62	[162]
BS-PPV	434	434	494 (526)	512 (543)	0.72	–	–	2.45 (506)	−5.59	−2.56	[161]
					0.87				−5.54	−2.60	[162]
DS-PPV	435	439	501 (535)	520 (548)	0.86	–	–	2.42 (512)	−5.52	−2.62	[162]
DDS-PPV	436	448	494 (523)	511 (540)	0.87	–	–	2.43 (510)	−5.56	−2.58	[162]
BDMCS-PPV	–	413	–	519 (555)	–	0.53	518 (542)	–	–	–	[159]
BDMPS-PPV	–	370	–	525 (560)	–	0.56	525 (556)	–	–	–	[159]
DMCS-PPV	414	420	483 (515)	510 (545)	0.88	0.82	510	–	−5.64	−2.58	[159]
DMPS-PPV	418	422	485 (517)	513 (547)	0.86	0.83	515	–	−5.55	−2.64	[159]
o-PBTMS-PPV	–	340	–	470	–	–	470	–	–	–	[169, 170]
m-PBTMS-PPV	–	330	–	440	–	–	–	–	–	–	[169, 170]
p-PBTMS-PPV	–	380	–	485	–	–	490	–	–	–	[169, 170]
PCBTS-PPV	–	355	-	480	–	0.64	480	–	–	–	[171]
PFBTS-PPV	–	385	–	495	–	0.81	500	–	–	–	[171]

(continued)

Table 2 (continued)

Polymer	λ_{max} (UV, nm)		λ_{max} (PL, nm)[b]		PL efficiency (Φ)		λ_{max}	E_g	HOMO	LUMO	
	Solution[a]	Film	Solution[a]	Film	Solution[a]	Film	(EL,nm)	(eV, (UV/nm))[c]	(eV)	(eV)	Reference
p-SiPhPPV	427	427	486	524	–	–	524	2.44	−5.43	−2.99	[172]
m-SiPhPPV	–	435	–	525	–	0.35	528	2.38	−5.30	−2.99	[173]
		433		518			525 (562)		−5.18	−2.80	[174]
m-SiPhPPV-*co*-MEH-PPV (3:1)	–	464	–	594	–	0.21	595		−5.21	−3.15	[173]
PFV-*co*-*m*-SiPhPV (1:1)	–	419	–	518	–	0.42	525 (562)	2.39	−5.15	−2.76	[174]
PFV	–	409	–	468, 500	–	0.29	471 (503, 534)	2.63	−5.26	−2.63	[174]
PSi8CNPV	427	434	496 (527)	513 (547)	0.62	–	513	2.47 (501)	−5.72	−2.75	[175]

Notes: UV – absorption, PL – photoluminescence, E_g – optical band gap

[a]Measured in chloroform solutions

[b]Values in parentheses represent shoulder peaks

[c]Determined from the absorption edge (value in parentheses) of the UV-vis spectrum

6.2 Silanylene-Containing Polymers

There is increasing interest in the polymers composed from alternating organosilicon and π-electron units in the backbone due to their unique electronic structure [176, 177]. Typical examples of silanylene-containing polymers are presented in Fig. 40. The main synthetic pathways to such polymers include: (1) Wurtz-type coupling of bis(chlorosilyl) compounds [178, 179], (2) polycondensation of dichlorosilanes with organodilithium derivatives [180, 181], and (3) transition metal-catalyzed polycondensation of magnesium- [182, 183], zinc- [184], or tin-derivatives [185] of diarylsilanes. The first two routes lead to polymers with one to three linked conjugated arylene units within the polymeric chain. The third route allows preparation of polymers with longer chromophores, which show promising properties in organic electronic devices.

A series of mono- and disilylene copolymers with di-, ter-, or quaterphenylene was reported by Ishikawa and his group (MS2P, DSmP, and MS2P3 in Fig. 40) [182] from which the disilanylene-substituted polymers DSmP were found to be photoactive. Thin polymer films degraded during irradiation in air by scission of the Si–Si bonds and degradation products including silanol and siloxy units were formed. The photoactivities of the disilanylene-substituted polymers in solution decrease with increasing extension of the π-electron system. Cyclic voltammogram (CV) measurements proved that the Si–Si orbital plays an important role in the first oxidation step of disilanylene–oligophenylene polymer films [186]. Monosilylene-copolymers MS2P and MS2P3 were found to be inert toward UV irradiation.

Poly[(1,2-tetraethyldisilanylene)-9,10-diethynylanthracene] (DSDEA) was evaluated as hole-transport material in OLEDs with Alq_3 as an electron transporting emitter layer [187]. These devices exhibited a maximum $\eta_{EL} = 0.2\%$. Although this is approximately a magnitude higher than a single layer of Alq_3 in absence of hole-transport material, it is very much below the state of the art, triplet emitter

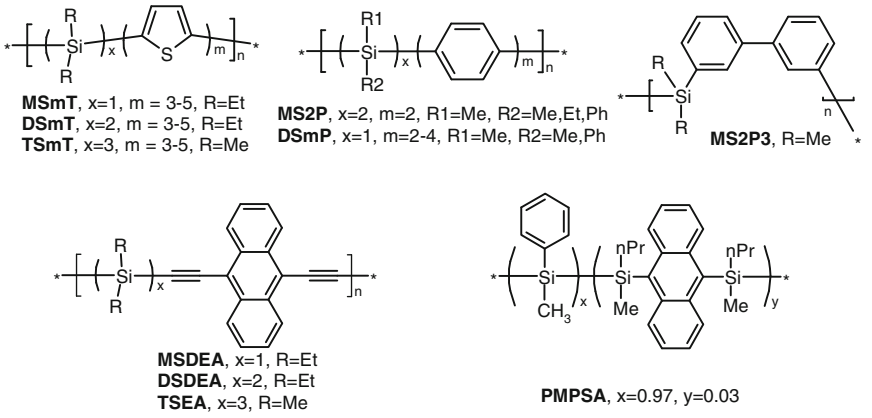

Fig. 40 Typical examples of silanylene-containing polymers

OLEDs reaching an external quantum yield up to 20% and more [188]. The low η_{EL} values of the organosilicon-based devices have been attributed to the poor electron-blocking properties of the organosilicon polymers which allows electrons to migrate from the emitter into the hole-transport layer and combine without light emission. Subsequently a series of similar mono-, di-, and trisilanylene copolymers composed of alternating 9,10-diethynylanthracene and organosilicon units were prepared by coupling reactions of 9,10-di(lithioethynyl)anthracene with dichloromono-, di-, and trisilanes, $Cl(SiR_2)_mCl(m = 1–3)$ by the same group [189] and evaluated in double-layer-type OLEDs employing these polymers as hole-transport materials in combination with Alq_3 as electron transporting-emitter. Increasing the number of silicon atoms in the polymer unit from $m = 1$ to 3 leads to an increased turn-on voltage and decreases the maximum current density of the devices. The highest luminance of $1,300\,cd\,m^{-2}$ was measured for the silanylene-diethynylanthracene polymer MSDEA (Fig. 40).

A poly(methylphenylsilane) containing 3% anthracene units in the polymer backbone (PMPSA) was synthesized by a Wurtz-type coupling reaction of 9,10-bis(methylpropylchlorosilyl)anthracene and methylphenyldichlorosilane [190]. This polymer exhibited light blue photoluminescence with 87% quantum efficiency with a strong photoluminescence emission at 500 nm originating from the anthracene units, and a weak one at 350 nm from the polysilane chain. Intramolecular energy transfer from the polysilane σ^* orbital to the anthracene π^* orbital enables the emission at 500 nm not only by π–π^* excitation of the anthracene unit at 420 nm, but also by σ–σ^* excitation of the polysilane fragments at 250–350 nm.

Poly(silylene)oligothiophenes MSmT were first reported by Corriou and coworkers [180]. Copolymers with smaller oligothienyl blocks ($m = 1 - 3$) were prepared by a coupling reaction of corresponding dilithioderivatives of oligothiophenes and dichlorosilanes in 51–80% yield. Copolymers with longer oligothienyl blocks ($m = 3 - 5$) were synthesized by Pd-catalyzed coupling of zinc derivatives of dithienylsilanes with corresponding aryldibromides in 66–95% yield. Two series of copolymers were obtained with quite low molecular weights (M_w between 1,930 and 5,940). Upon doping with $NOBF_4$ polymer films showed a maximum conductivity of 10^{-2} to $10^{-1}\,S\,cm^{-1}$.

Ishikawa and his group prepared a series of copolymers with alternating mono-, di-, or trisilanylene units and 2,5-oligothienylene groups $[(SiR_2)_xT_m]_n$ with R = Me, Et, $x = 1 - 3$, $m = 2 - 5$ by a $NiCl_2$(dppe)-catalyzed Grignard coupling ($NiCl_2$(dppe) – 1,2-*bis*(diphenylphosphino)ethane nickel(II) chloride) [183, 191]. DSmT copolymers were readily obtained in 75–97% yield and a moderate molecular weight of 17–53 kDa (M_w, polydispersity of 2.1–4.8) [183]. Other copolymers were obtained with similar properties. Irradiation of the DSmT copolymers with UV light resulted in cleavage of the silicon–silicon bonds, but with an increasing number of thienyl units the sensibility towards UV irradiation decreased. With an increasing number of thienyl units the UV absorption and emission maxima shifts to lower energies, and is little affected by the length of the silicon chain. Doping the polymers by exposition of films to $FeCl_3$ vapor, moderate conductivities of $1.3 \times 10^{-4} - 2.3 \times 10^{-1}\,S\,cm^{-1}$ were observed. In general the conductivities tended

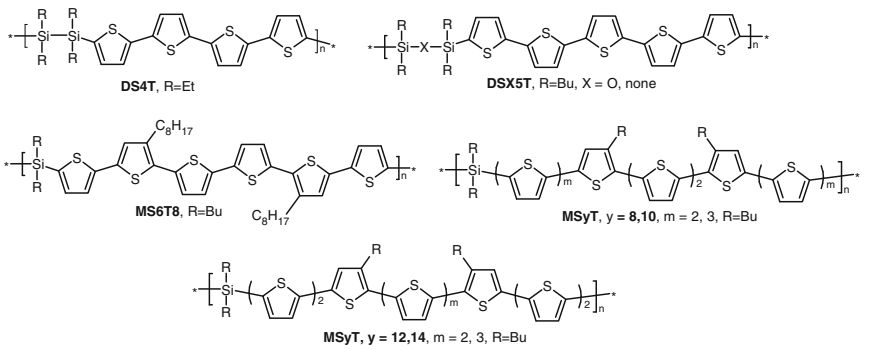

Fig. 41 Chemical structures of copolymers of silylene and 2,5-oligothienylenes used in EL and OFET devices

to increase with the number of thienyl units, and decreased with the length of the silicon chain. Conductive films made by electrochemical doping showed similar results and tendencies [192].

In 1993 the evaluation of poly[(silylene)- and (disilanylene)oligothienylenes] in an OLED was started by Hadziioannou and coworkers [193]. MS6T8 used as emitter (Fig. 41) in a simple device with ITO as the hole- and electron-injecting electrodes emits orange–red light ($\lambda_{max} = 612$ nm). More sophisticated double-layer-type OLEDs were tested using MSmT ($m = 3$–5) and DS4T copolymers as the hole-transporting materials in combination with the emitter Alq_3 [191]. Both, a decreasing number of thienyl units and a decreasing length of the silicon chain increased the turn-on voltage and reduced the maximum current density of the device. The highest luminance of 2,000 cd m^{-2} at 12 V and the lowest threshold voltage at 5 V was obtained from a device based on the DS4T copolymer.

DS5T and its disiloxyl analog DSO5T (Fig. 41) with reasonable molecular weights of 76–94 kDa (M_w with a polydispersity of 2.5–3.8) were used as hole-transport materials in combination with Alq_3 as emitter in a double-layer OLED setup [194]. The OLEDs showed the expected green light from Alq_3 emission after reaching the turn-on voltage. DS5T exhibited a slightly lower turn-on voltage compared to DSO5T, while a similar maximum luminance of 4,000 cd m^{-2} was obtained for both polymers.

Ohshita, Kunai, and coworkers synthesized monosilanylene-oligothienylene alternating polymers **MSyT** with increasing conjugation length of the oligothiophene chromophore (T = 2,5-thienylene or 3-butyl-2,5-thienylene, $y = 8$, 10, 12, and 14, R = Bu, see Fig. 41) and tested these polymer in OLEDs and OFETs [185]. The polymers were obtained by Stille coupling reactions with a molecular weight of 7.3–14.2 kDa (M_w, polydispersity of 1.3–1.7). The onset voltages for the OLED (layer structure: ITO/**MSyT**/Alq_3/Mg:Ag) decreased with increasing conjugation in the chromophore with a maximum luminance of 900 cd m^{-2} for $y = 12$ before higher voltage introduce irreversible damages. The external quantum efficiencies of the devices with MSyT were about 0.1–0.2% at the maximum luminance.

Field-effect charge carrier mobilities in **MSyT** films were determined to be $(3.4–6.9)\times10^{-5}\,cm^2\,V^{-1}\,s^{-1}$, slightly increasing with the length of the oligothiophene unit from $y = 8$ to 12, and almost not affected by the length of the silicon atom chain.

Extensive electrochemical studies of mono- [195] and disilanylene [196–198] copolymers with oligothienylenes proved the sensitivity of the Si–Si bond towards electrochemical oxidation. In the CV of films made from MSmT ($m = 4,5$) two couples of redox peaks were found at a potential in the range of 0–1.2 V. Combined with doping level and in situ spectroelectrochemical measurements the results suggest a mechanism in which in a first step the polymer repeating unit is oxidized to the radical cation followed by the oxidation to the dication. From in situ UV-vis-NIR measurement it was concluded that the radical cation forms π-dimers via a coupling reaction [195]. Poly[(tetraethyldisilanylene)oligo(2,5-thienylene)] derivatives (DSmT; $m = 3–5$) have been successfully doped by electrochemical oxidation. Band-gap energies of 2.52, 2.65, 2.82, and 3.27 eV were measured for DS5T, DS4T, DS3T, and DS2T respectively. Doped films of DS5T, DS4T, and DS3T exhibited electrical conductivities in the order of 10^{-3} to $10^{-4}\,S\,cm^{-1}$ with BF_4^- as counter ion while the work functions increased from 5.1 to ca. 5.5 eV during doping [196]. The instability of Si–Si bonds towards electrochemical oxidation in DSmT ($m = 3–5$) was demonstrated by its cleavage at an electrochemical potential as low as 0.5 V (vs Ag/Ag+), resulting in the dissolution of oligothiophene-like species. The decomposition products were oxidized to form a new polymer film on the surface of an original DSmT film and the new composite polymer film is subsequently doped [197].

Sotzing et al. exploited the electrochemical instability of the copolymers containing silylene and thiophene in an ingenious way [199, 200]. They prepared a series of copolymers of 3,4-ethylenedioxythiophenes and their derivatives with dialkylsilylene units, processed films from solution, and converted the films electrochemically to yield an insoluble highly conductive film of poly(3,4-ethylenedioxythiophene) PEDOT (Scheme 13). The precursor polyarylsilanes, PSEDT, were prepared via step-growth polymerization of dialkyldichlorosilane and dilithiated EDOT derivatives with a molecular weight of 51 and 85 kDa (M_w and polydispersities of 2.1 and 1.7) for PSEDT(a) and PSEDT(c), respectively. Thin films of precursor polymers PSEDT were converted into the conjugated polymer PSEDTx via solid state electrodesilylation under conditions in which polymers PSEDT did not dissolve. Albeit the conversion is not quantitative and residual silylene groups remain in the polymer PSEDTx, the conductivity of PSEDTx(a) was determined to be $20\,S\,cm^{-1}$ which is in accordance with the conductivity of conventionally electrodeposited PEDOT ($16\,S\,cm^{-1}$).

Ohshita et al. synthesized a series of alternating copolymers of 2,6-diaryldithienosilole and organosilicon units [201, 202]. These polymers were obtained in 33–71% yield by nickel-catalyzed coupling of 2,6-dibromodithienosilole with di-Grignard reagents prepared from the corresponding bis(bromoaryl)disilanes or monosilane (Scheme 14) resulting polymer with limited molecular weights of 9.4–15.9 kDa (M_w, polydispersity 1.4–2.6). With units of four conjugated aryl rings

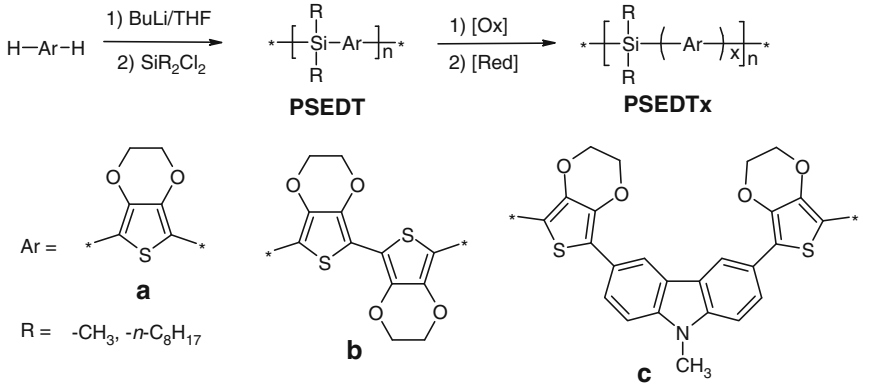

Scheme 13 Schematic representation of synthesis of soluble 3,4-ethylenedioxythiophene containing poly(arylsilane) PSEDT and its electrochemical conversion into highly conducting conjugated polymer PSEDTx

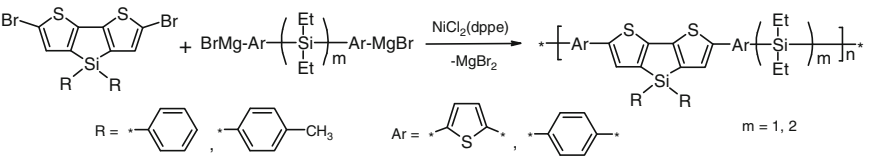

Scheme 14 Synthesis of alternating copolymers of 2,6-diaryldithienosilole and organosilicon units

separated by mono- or disilyl bridges, these polymers strongly absorb light in the UV-vis region and exhibit emission bands at 422–444 and 482–541 nm, respectively. The emission of the Si-bridged polymers is remarkably red-shifted in comparison to the corresponding di- and monosilanylene-quaterthienylene polymers DS4T and MS4T (Fig. 40), indicating the existence of expanded π-conjugation due to the silole ring. Their CV display first oxidation peaks at 0.95–1.00 V vs. SCE (saturated calomel electrode). Upon doping films with $FeCl_3$ vapor, they became conducting with a low conductivity of 3.3×10^{-5} to 8.7×10^{-3} S cm^{-1}. Although copolymers containing disilylene units showed an order of magnitude higher conductivity, their hole-transporting properties appeared to be lower than polymers containing monosilylene units which was evidenced by a study of hole-transport material in OLEDs. Introduction of the silole ring in the copolymer structure introduced some electron transporting properties to the polymers, which were higher compared to MS4T or PVK, but significantly lower compared to typical electron transporting material, such as Alq_3.

Silanylene-containing polymers have shown some (semi)conductive and luminescence properties, which, however, were often well below the values reported for other classes of conjugated polymers. In our view, the most interesting feature of such polymers is redox- and UV-light instability of silanylene and especially disilanylene units, which might be utilized in patterning of the functional electronic layers, necessary to produce complex organic electronics circuits, or for preparation of (insoluble) conductive polymer films from soluble silanylene precursors.

6.3 Silol-Containing Polymers

The incorporation of silole unit opens a wide field of research to modify the electronic structure of known carbon-based polymeric chromophores. Chromophores like the carbon analog of TS and 2,7-fluorene have been successfully used as emitters in OLEDs and semiconductors in OTFT and have been combined with additional structural units to adjust electronic properties. Replacement of the bridging carbon atom in such structural units by silicon has a strong impact on the electronic properties: interaction between the silicon σ-orbitals and the π-system of the carbon chromophore will lift the HOMO and lower the LUMO energy and therefore will decrease the band gap. Silicon modified chromophores may be combined with their carbon analogs and other successfully used structural units like thiophene, bithiophene and phenylene to adjust further the energy levels of HOMO and LUMO. Incorporation of benzothiadiazole (BT) and other structural units with nonbonding electrons will introduce new energy levels to form donor–acceptor type polymers with even smaller band gaps (Fig. 42).

The TS-based homopolymer, poly(4,4-di-*n*-hexyldithienosilole) (TS6) as well as its copolymers with mono- and bithiophene subunits, poly(4,4-di-*n*-hexyldithienosilole-*alt*-(bi)thiophene) (TS6T1,TS6T2), were almost simultaneously reported by Facchetti and Marks [203, 204] and Ohshita [205] (Fig. 43). Facchetti and Marks examined in detail the consequences of introducing TS and BS structures into a thiophene polymer backbone by comparison of the new BS-based homopolymer, poly(9,9-di-*n*-octyldibenzosilole) (BS8) and copolymers with mono- and bithiophene subunits, poly(9,9-di-*n*-octyldibenzosilole-*alt*-(bi)thiophene) (BS8T1, BS8T2), with their carbon analogs F8T1 and F8T2. Thiophene-based copolymers were prepared by Stille coupling, while for phenylene-based copolymers Suzuki coupling reactions proved to be suitable. The molecular weight of thiophene-based copolymers was around 35 kDa (M_w, polydispersity 2.9–3.7) and around 120 kDa

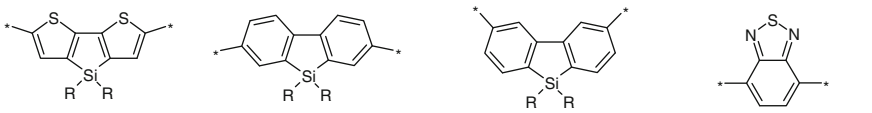

Fig. 42 General structural units often used in silole-containing copolymers design

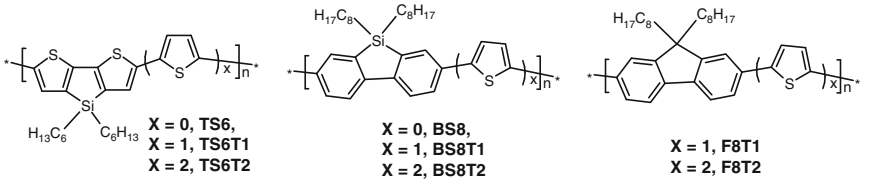

Fig. 43 Dithienosilole- and dibenzosilole-based homopolymers, their mono- and bithiophene copolymers and carbon analogs

for phenylene-based copolymers. Charge carrier mobilities turned out to be higher for thiophene-based copolymers with a maximum of $0.08\,cm^2\,V^{-1}\,s^{-1}$ for copolymer TS6T2 and a quite acceptable on/off ratio of 10^4–10^6 (unaligned films under ambient conditions). Non-encapsulated OTFTs were proven to be highly stable in air, obviously due the absence of alkyl side groups on the thiophene ring in contrast to regioregular poly(3-hexylthiophene) (P3HT). All silole-containing copolymers studied are apparently of excellent thermal stability, no significant weight loss being measured below 400°C by TGA. The absorption maxima values of BS-based copolymers were red-shifted by 40–50 nm vs fluorene-based analogs F8T1 and F8T2, demonstrating Si σ^*-orbital overlap with the π-conjugated chromophore.

Ohshita and his coworkers synthesized poly(dithienosilole-2,6-diyl)s with a molecular weight of 2.7–13.2 kDa (M_w, polydispersity 1.1–1.8 after precipitation) using palladium-catalyzed oxidative homocoupling of 2,6-bis(tributylstannyl) dithienosiloles with $CuCl_2$ (Scheme 15a) [205]. Compared to the corresponding silole-free polythiophenes, the absorption peak of these polymers is red-shifted by about 100 nm. Alternating copolymers with molecular weights of 5.3–12.8 kDa (M_w, polydispersity 1.3–1.7 after precipitation) were prepared by palladium-catalyzed cross-coupling reactions using 2,6-dibromodithienosiloles and distannylthiophene or bithiophene as starting materials (Scheme 15b, c).

The polymers were studied in OLEDs as emitters and as hole-transport materials in combination with the electron conducting emitter Alq_3. Used as emitter in a single layer device they emit red light while in combination with Alq_3 they act as

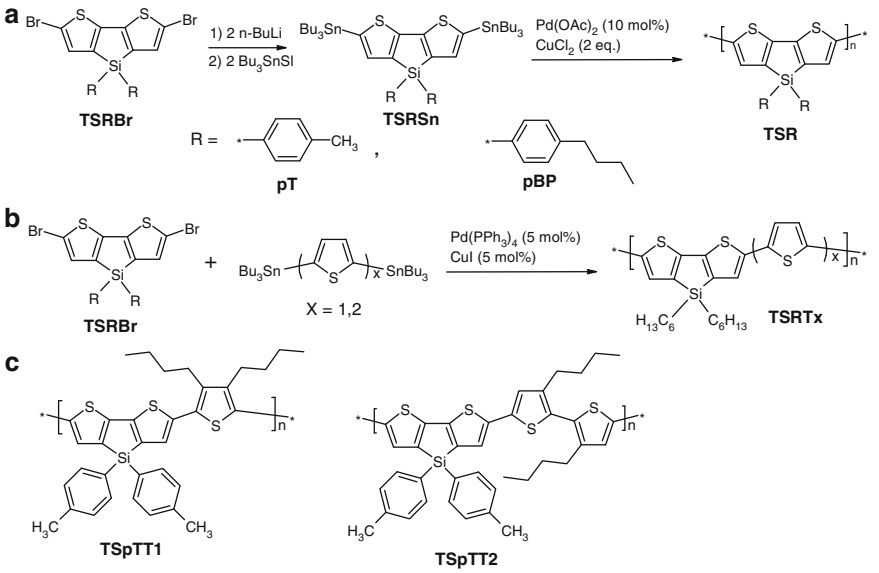

Scheme 15 (**a**) Synthesis of poly(dithienosilole-2,6-diyl)s by oxidative homocoupling, (**b**) synthesis of alternate dithienosilol copolymers by Stille cross-coupling reactions, and (**c**) structures of the most soluble copolymers

hole-transport material with a maximum luminance of 500 cd m^{-2} at 13 V (obtained for copolymer TSpTT2). In this class of polymers, solely TSpBP was found to work as semiconductor in OTFT with a low mobility of 10^{-7} cm^2 s^{-1}.

In 2005 Holmes et al. prepared poly(9,9-dihexyl-2,7-dibenzosilole) BS6 by Suzuki copolymerization of dibromo and bis(boronate) 2,7-disubstituted BS monomers. The monomers were synthesized by the selective *trans*-lithiation of 4,4′-dibromo-2,2′-diiodobiphenyl followed by silylation with dichlorodihexylsilane [206]. BS6 was obtained in 93% yield with molecular weight of 220 kDa (M_w) and broad polydispersity (approximately 7). The polymer revealed similar optical properties in thin films as the corresponding polyfluorene (PF) with an absorption maximum at 390 nm and a luminescence maximum at 425 nm and an optical band gap of 2.93 eV (PL efficiency 0.62). Preliminary studies with single layer light-emitting OLEDs confirmed the emission maxima at 431 and 451 nm and a similar efficiency as PF8. Films of polymer BS6 exhibit a glass temperature of 149°C and are apparently resistant to thermal stress: annealing at 250°C for 16 h in air with ambient light did not change its photoluminescence spectrum significantly (Fig. 44). This is in clear contrast to its carbon analog PF8, the photoluminescence spectrum of which degraded completely after 4 h at a temperature of 200°C.

Two random copolymers based on poly(di-*n*-hexylfluorene-*co*-4,4-diphenyldithienosilole) (PF-TS) were synthesized by Jen and coauthors by Suzuki coupling reaction (Scheme 16) [207]. The molecular weight of the polymers obtained reached 146 kDa (M_w, polydispersity 2.8) for PF9-TS, and 76 kDa (M_w, polydispersity 2.2) for PF19-TS. Both copolymers were thermally stable to thermal decomposition temperature up to 400°C. PF9-TS exhibit a slightly higher T_g of 100°C than PF19-TS (95°C), likely due to the higher content of rigid diphenyldithienosilole units in PF9-TS.

Apparently even the presence of a small fraction of electron-deficient TS moiety in the copolymers increases their electron affinity significantly. Subsequently they facilitate charge recombination by acting as charge-trapping sites for both holes and electrons. By exploiting a Förster energy transfer from the higher energy fluorene segments to the lower-energy TS-containing segments it is possible to tune the color of emitted light to longer wavelengths. In an OLED emitting

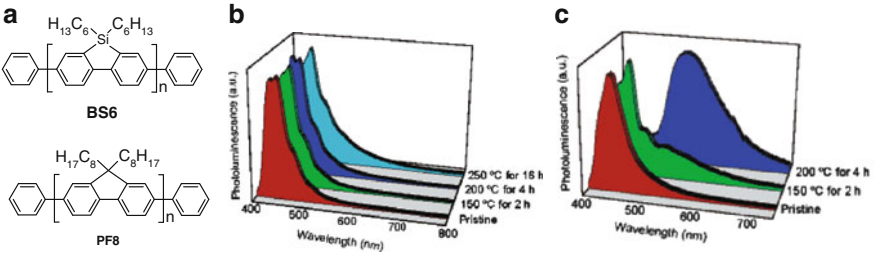

Fig. 44 (**a**) Structures of poly(9,9-dihexyl-2,7-dibenzosilole) BS6 and poly(9,9-dihexyl-2,7-fluorene). PL spectra of BS6 (**b**) and PF8 (**c**) films after annealing at different temperatures. Reproduced with permission of the American Chemical Society from [206]

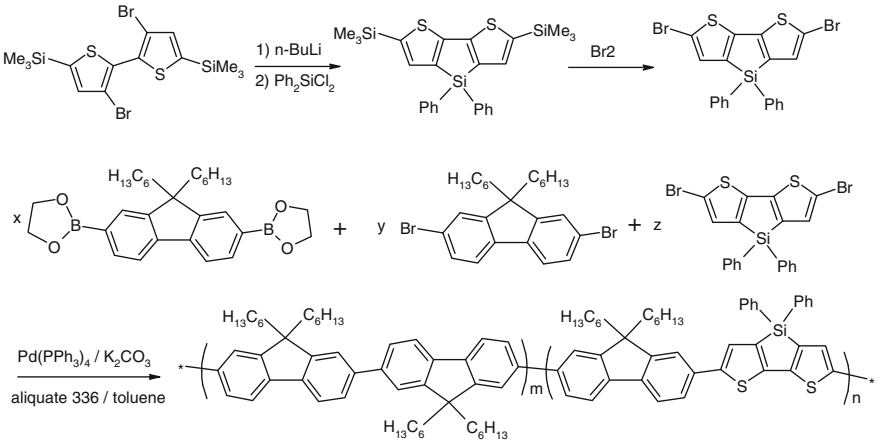

Scheme 16 Synthetic scheme for 4,4-diphenyldithienosilole monomer and silole-containing copolymers by Jen and coauthors [207]

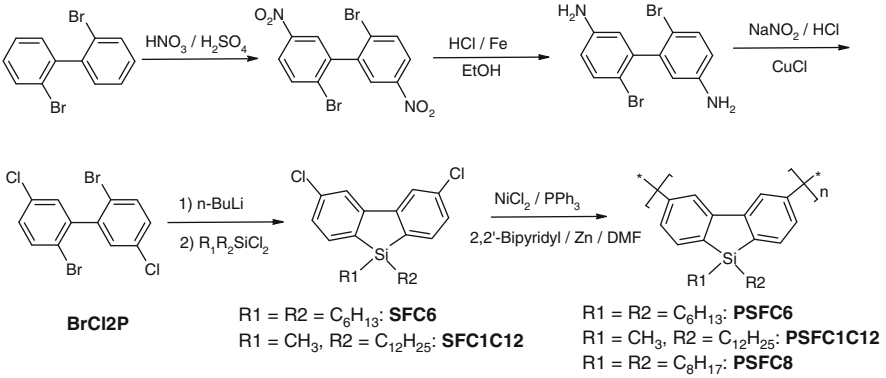

Scheme 17 Synthesis route of poly(3,6-silafluorene)s (PSF)

green light the low turn-on voltage of 4.6 V together with a maximum brightness of more than 25,900 cd m^{-2}, and a maximum external quantum efficiency of 1.64% was attributed to improved charge injection and recombination when PF9-TS was used as emitter in combination with in situ polymerized hole-transport material bis-tetraphenylenebiphenyldiamine-perfluorocyclobutane (BTPD-PFCB).

Cao et al. synthesized poly(9,9′-alkyl-3,6-silafluorenes as an ultraviolet-emitting polymers with a wide band gap of 4.0 eV [208]. Since the silole ring in the silafluorene undergoes a ring-opening reaction during bromination with standard bromination reagents and during oxidative polymerization, e.g., with $FeCl_3$, the authors had to design a new synthetic route (Scheme 17). The starting monomers, 3,6-dichloro-9,9′-alkylsilafluorenes (SFC6 and SFC1C12), were synthesized from 2,2′-dibromobiphenyl via 2,2′-dibromo-5,5′-dichlorobiphenyl (BrCl2P) following

the procedure shown in Scheme 17. Nickel-catalyzed Yamamoto coupling reaction of the resulting 3,6-dichloro-9,9′-alkylsilafluorene in the presence of triphenylphosphine, zinc, 2,2′-bipyridine, and $NiCl_2$ resulted in the desired polymer with a molecular weight of around 10 kDa (M_n, polydispersity of around 1.6). Poly(3,6-silafluorene) reveals an excellent thermal stability with a decomposition temperature of 442°C for PSFC6 and 425°C for PSFC1C12, even higher than poly(2,7-fluorene) (385°C) [209] and a stability towards oxygen and light similar to PFs. Replacement of carbon in position 9 of PF by silicon obviously has little impact on rigidity of the polymer chain.

The optical properties of polymers PSFC6 and PSFC1C12 were found to be similar, both exhibiting an absorption peak at 250–300 nm and an absorption edge of around 310 nm in solid films and solutions. All absorptions are significantly blue-shifted compared to poly(9,9-dialkyl-2,7-fluorene)s [210] and poly(9,9-dialkyl-2,7-silafluorene with an absorption maximum of 380 nm and absorption onset at 420 nm [206]. A reduced conjugation of the 3,6-linkage compared to 2,7-linkage in silafluorenes may account for the change in optical properties. Poly(3,6-silafluorenes) PSFC6 and PSFC1C12 show a maximal photoemission at 355 and 360 nm, in solution and as solids, with a luminescence quantum efficiency of 0.25 and 0.30. Unlike most other conjugated polymers, the PL emission of polysilafluorene in the solid state shows almost no red shift compared to spectra in solution.

Almost simultaneously to Cao et al., Holmes et al. described the preparation of the 3,6-disubstituted dibenzosilole monomers 4, 5, and 10 by two alternative routes (Scheme 18) [211]. The first method employs selective transmetalation of 2,2′-diiodo-5,5′-dibromobiphenyl (**3**) followed by silacyclization (as used for the corresponding 2,7-dibenzosilole) [206], while the second exploits the displacement of methyl groups from a dibenzosilole **8**. The latter route demonstrates the versatility of the alkyl-displacement on silicon reaction to introduce solubilising substituents to the bridging silicon, keeping in mind the limited commercial availability of disubstituted dichlorosilanes.

Suzuki copolymerization of monomers **4** and **5a** with phenyl group end-capping yielded poly(9,9-dioctyl-3,6-dibenzosilole) (PSFC8) in 93% yield with similar molecular weight as obtained by Cao et al. (M_n 11 kDa, polydispersity 2.1). The polymer has a sufficiently high triplet energy (2.55 eV), higher than that of

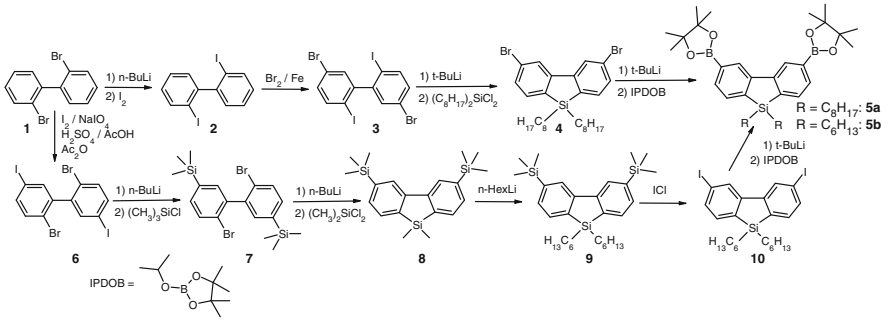

Scheme 18 Synthesis of 3,6-disubstituted dibenzosilole monomers

commonly used PFs (2.1 eV) [212] and comparable with that of polycarbazoles (2.6 eV) [213], to act as a host for green electrophosphorescent emitters. From CV measurements the LUMO energy of PSFC8 was determined as −2.15 eV (cf. PVK at −2.0 eV), indicating a withdrawal of electrons from the phenyl rings by σ^*–π^* conjugation, which is often observed in molecular and polymeric siloles [58, 214]. The HOMO level calculated from the optical band gap (3.5 eV) was estimated to be −5.65 eV (cf. PVK at −5.8 eV) [215]. A lower HOMO energy of polymer PSFC8 compared to PVK is expected to result in a lower hole-injection barrier at the PEDOT:PSS interface. The HOMO and LUMO energies of PSFC8 facilitate both electron and hole injection in OLEDs. In a triplet layer structure a complete energy transfer occurred from the polymer to the triplet dopant f*ac*-tris[2-(2-pyridyl-κN)-5-methylphenyl]iridium(III) ($Ir(mppy)_3$) (**12**) with a triplet energy of 2.4 eV and resulted in a at a low device turn-on voltage.

Another series of copolymers (PSiFF) based on 3,6-silafluorene and 2,7-fluorene were synthesized by Cao and coauthors via the Suzuki reaction (Fig. 45a) [216]. The content of the 3,6-silafluorene subunits was between 5 and 50 mol%. The molecular weights ranged from 19 to 39 kDa (M_n, polydispersity 1.4–2.5). All copolymers exhibited good thermal stability with degradation temperatures of 395–418°C.

Both in solution and as film, poly(3,6-silafluorene-*co*-2,7-fluorene) showed only a single absorption peak which shifts to shorter wavelengths with increasing 3,6-silafluorene content in the copolymers (381 nm for the PFO homopolymer, 283 nm for the PSiF homopolymer). Parallel to the absorption spectra, the PL spectra of the PSiFF copolymers in solution and as films significantly shift to the blue with increasing 3,6-silafluorene content in the copolymers (431 nm for the PFO homopolymer to 420, 416, and 400 nm for copolymers). Absolute PL efficiencies of copolymer films start with 0.67 for the poly(9,9-dihexyl)fluorine homopolymer,

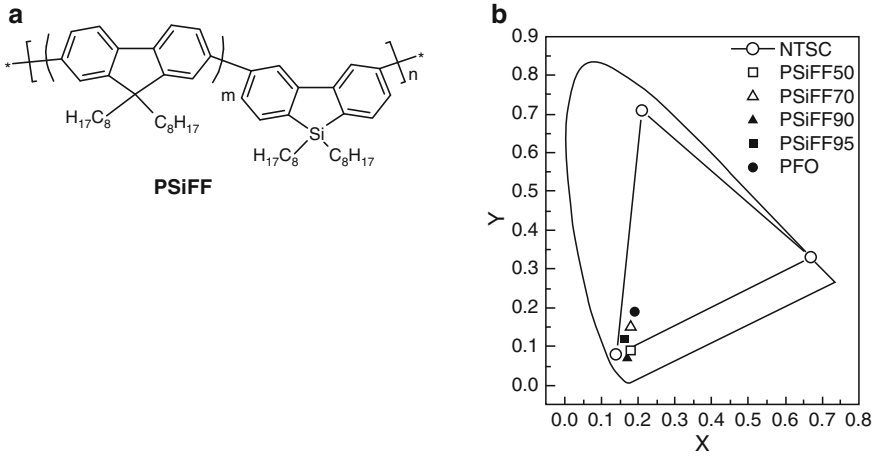

Fig. 45 (**a**) Chemical structure of 3,6-silafluorene and 2,7-fluorene copolymers PSiFF. (**b**) CIE coordinates of the devices fabricated from the PSiFF copolymers. Reproduced by permission of The Royal Society of Chemistry [216]

reach a maximum at the copolymer containing 10% of 3,6-silafluorene units (PSiFF90) (0.84), and then drop quickly with increasing 3,6-silafluorene content to 0.38 (alternating copolymer with 50% of 3,6-silafluorene units) and 0.14 for the poly(3,6-(9,9-dihexyl)silafluorene) homopolymer.

The incorporation of 3,6-silafluorene units into PF suppresses long-wavelength emission, and significantly improves the color purity in OLEDs. Fluorene and 3,6-silafluorene contribute to the conjugation of the chromophore and the emission is remarkably blue-shifted with increasing 3,6-silafluorene content. In OLEDs (layer structure: ITO/PEDOT:PSS/PVK/polymer/Ba/Al) PSiFF90 reached η_{EL} of 3.34% and a luminous efficiency of $2.02\,cd\,A^{-1}$ at a brightness of $326\,cd\,m^{-2}$. The CIE coordinates of (0.16, 0.07) almost match the NTSC specification for blue color (0.14, 0.08) (Fig. 45b). Moreover, the incorporation of 3,6-silafluorene into the PF main chain significantly improved the spectral stability during annealing. Poly(3,6-silafluorene-*co*-2,7-fluorene) therefore might be a promising blue emitter with good color purity.

A copolymer derivative P36–27SiF90, containing 10% of 3,6-silafluorene and 90% of 2,7-silafluorene units, was accessed via Suzuki polycondensation (Fig. 46a) [217] and obtained with a molecular weight of 47 kDa (M_n, polydispersity 2.5). OLEDs with P36–27SiF90 as emitter (layer structure ITO/PEDOT:PSS/PVK/polymer/Ba/Al) reached $\eta_{EL} = 1.95\%$, a luminous efficiency of $1.69\,cd\,A^{-1}$, and a maximal brightness of $6{,}000\,cd\,m^{-2}$. As in poly(3,6-silafluorene-*co*-2,7-fluorene) polymers, the silafluorene subunit successfully suppresses undesired long-wavelength green emission and produces a dominating emission at 500–600 nm (Fig. 46b, c). The total absence of vulnerable C-9 carbon in the main chain, which is easily oxidized by photo- and/or electro-oxidation, enhanced the oxidative stability ever further.

A series of soluble conjugated random and alternating copolymers (PFO-TST) derived from 9,9-dioctylfluorene (FO) and 1,1-dimethyl-3,4-diphenyl-2,5-bis(2′-thienyl)silole (TST) (Fig. 47a) were synthesized by Cao and his group [218] using palladium(0)-catalyzed Suzuki coupling. Random copolymers exhibited a PFO-segment-dominated UV absorption peak at 385 nm and absorption at 490 nm originating from the narrow band gap TST-segment. In contrast to the random copolymer, the alternating copolymer exhibited a broad absorption band which obviously results from the mixed configuration dominated by the TST segment. In films with a low

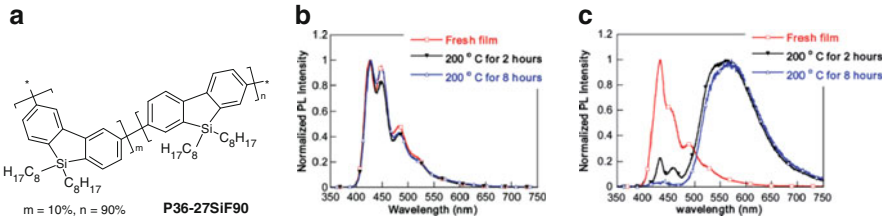

Fig. 46 Copolymer of 3,6-silafluorene and 2,7-silafluorene P36–27SiF90 (**a**). PL spectra of (**b**) P36–27SiF90 and (**c**) PFO in films with thermal annealing in air after different time at 200°C. Reproduced with permission of John Wiley and Sons Inc. from [217]

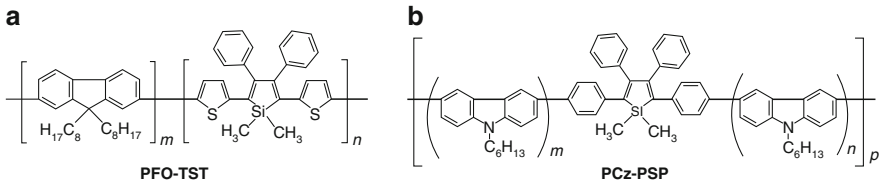

Fig. 47 Structural formulas of (**a**) 9,9-dioctylfluorene (FO) and 1,1-dimethyl-3,4-diphenyl-2,5-bis(2′-thienyl)silole (TST) copolymers PFO-TST [218] and (**b**) *N*-hexyl-3,6-carbazole (Cz) and 1,1-dimethyl-2,3,4,5-tetraphenylsilole (PSP) copolymers PCz-PSP [219]

TST content the excitation energy completely transferred from the PFO to the TST segment. In OLEDs (layer structure ITO/PEDOT/PVK/copolymer/Ba/Al) the emitted light from the copolymers was found to be red-shifted. In bulk-heterojunction photovoltaic cells the PFO-TST alternating copolymer proved their suitability as electron donor when combined with PCBM as electron acceptor to yield an energy conversion efficiency of 2.01%. In OTFT the field-effect hole mobility of the same copolymer was moderate ($4.5 \times 10^{-5}\,\mathrm{cm^2\,V^{-1}\,s^{-1}}$).

Chen and coauthors incorporated *N*-hexyl-3,6-carbazole (Cz) and 1,1-dimethyl-2,3,4,5-tetraphenylsilole (PSP) to yield random and alternating copolymers (PCz-PSP) (Fig. 47b) by Suzuki coupling reactions [219]. The molecular weights were around 11–17 kDa (M_w, polydispersity between 1.3 and 1.7). The HOMO levels of the copolymers were found to be between −5.15 and −5.34 eV. Single layer OLEDs (layer structure ITO/copolymer/Ba/Al) using a copolymer with a content of 20% PSP segments exhibited a maximum η_{EL} of 0.77%. In OTFT, hole mobilities of the copolymers used as semiconductor decreased with the content of PSP segments with a maximum mobility of $9.3 \times 10^{-6}\,\mathrm{cm^2\,V^{-1}\,s^{-1}}$.

In a search for highly efficient red and green emitters, the Cao group synthesized via Suzuki coupling a series of 2,7-silafluorene copolymers with electron rich comonomers like 4,7-di(4-hexyl-2-thienyl)-2,1,3-benzothiadiazole (DHTBT) and 2,1,3-benzothiadiazole (BT) which narrow the bandgap of PSiF-DHTBT10 and PSiF-BT10 copolymers with a 10% molar ratio (Scheme 19) [220]. The molecular weights were determined to be 40 and 17 kDa (M_n, polydispersity 2.8 and 2.5) Both copolymers exhibited good thermal stability with degradation temperatures above 400°C and glass transition temperatures of 72–93°C. Compared to their PF analogs, PSiF-DHTBT10 and PSiF-BT10 show a higher PL emission. OLEDs (layer structure ITO/PEDOT:PSS/PVK/polymer/Ba/Al) with these polymers as emitters showed a maximum η_{EL} of 2.89% (PSiF-DHTBT10) and 3.81% (PSiF-BT10) as well as current efficiency of $2.0\,\mathrm{cd\,A^{-1}}$ (PSiF-DHTBT10) and $10.6\,\mathrm{cd\,A^{-1}}$ (PSiF-BT10). The CIE coordinates of both polymers ((0.67, 0.33) and (0.38, 0.57), respectively) are quite promising for future practical use, since they are close to pure red and green colors.

Fluoro-substituted silole-containing polymers were recently prepared by Suzuki polycondensation reaction using 2,5-dihydroxyboryl-1,1-dimethyl-3,4-bis(3-fluorophenyl)-silole or 1,3-dibromo-5-fluoro-benzene as fluoro-containing monomers and 2,7-dibromo-9,9-dioctyl-fluorene or 2,5-dihydroxyboryl-1,1-dimethyl-3,4-bis(phenyl)-silole as co-monomers [221]. With a polymerization

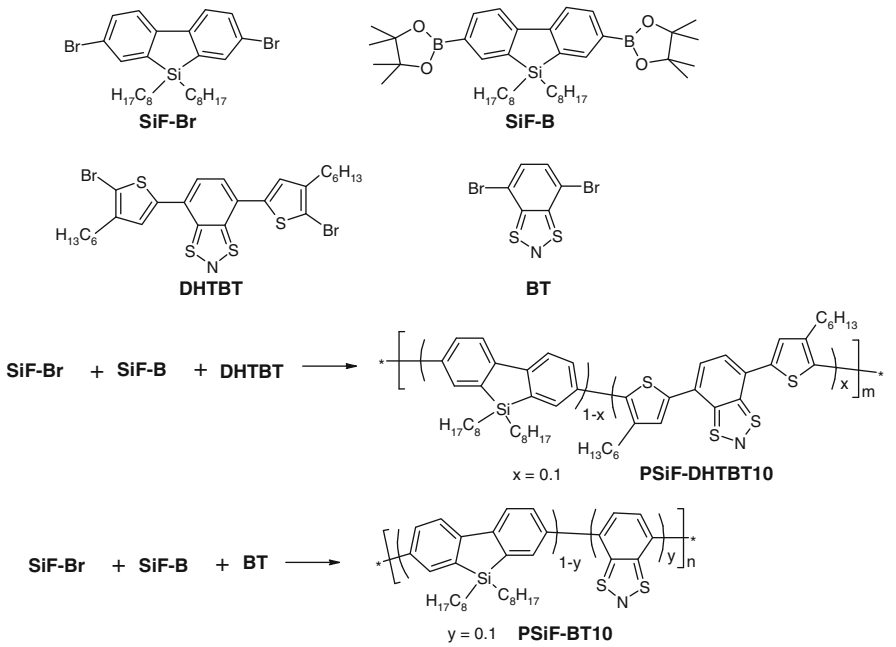

Scheme 19 Synthesis routes to PSiF-DHTBT10 and PSiF-BT10 copolymers

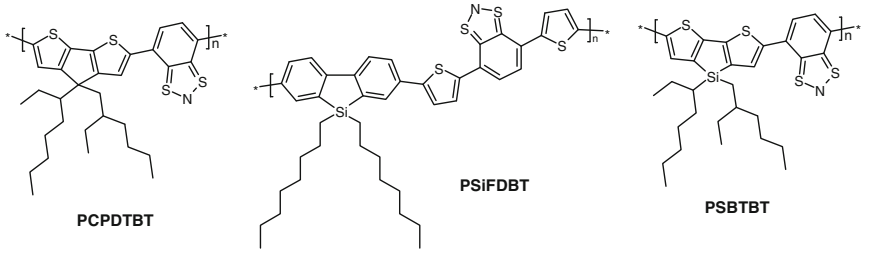

Fig. 48 Structures of PCPDTBT, PSiFDBT, and PSBTBT copolymers

degree ranging between 4 and 8, more or less oligomers were obtained with a weak green PL in the solid state. Cyclic voltammetry, visible absorption spectroscopy, and DFT calculations showed that the fluoro substituents withdraw electrons sufficiently to lower both the HOMO and the LUMO orbital in the oligomer.

The combination of 2,7-silafluorene (SiF) with the electron rich 4,7-di(2-thienyl)-2,1,3-benzothiadiazole (DBT) allowed preparation of an alternating copolymer PSiFDBT with a molecular weight of 79 kDa (M_n, polydispersity 4.2) (Fig. 48) [222]. Besides an excellent thermal stability (up to 430°C) PSiFDBT compared to its carbon analog PFDTBT exhibited a slightly lower optical band gap (1.82 vs 1.92 eV), and an approximately 20 nm red-shifted absorption peak. The shift to longer wavelengths allows absorption of longer wave lengths from solar radiation, and indeed, bulk junction solar sells with PCBM as the electron

acceptor yielded a remarkable PCE up to 5.4% with an open-circuit voltage (V_{oc}) of 0.90 V, a short-circuit current (I_{sc}) of 9.5 mA cm^{-2}, and a fill factor (FF) of 50.7%. In contrast to poly-3-hexylthiophene (P3HT), the commonly used electron acceptor for OPV, the high efficiency was reached without post annealing or addition of additives to control the film morphology. A broad spectrum of absorption, a sufficient hole mobility, and low HOMO are clues to reach a high performance as OPV material. Field-effect transistors fabricated from PSiF-DBT showed a hole mobility of $\sim 1 \times 10^{-3}$ cm^2 V^{-1} s^{-1}, which is nearly ten times higher than that of PFO-DBT ($\sim 3 \times 10^{-4}$ cm^2 V^{-1} s^{-1}). The HOMO level of PSiF-DBT was estimated to be −5.39 eV.

The introduction of 4,7-bis(2-thienyl)-2,1,3-benzothiadiazole units into dithieno [3,2-*b*:2′,3′-*d*]silole backbone as alternating copolymers will also reduce the band gap and increase the interchain interaction which in comparison to the nonmodified silole improve the energy conversion efficiency in the bulk-heterojunction organic solar cells by a factor of three [223]. Copolymers based on dithieno[3,2-*b*:2′,3′-*d*]silole and 2,1,3-benzothiadiazole were also efficient as active layer of OPV [224, 225]. Poly[(4,4′-bis(2-ethylhexyl)dithieno[3,2-*b*:2′,3′-*d*]silole)-2,6-diyl-*alt*-(2,1,3-benzothiadiazole)-4,7-diyl] (PSBTBT) with branched 2-ethylhexyl silicon substituents was of specific interest for wet processing due to its high solubility (Fig. 48). Scheme 20 depicts its synthesis from dichlorobis(2-ethylhexyl)silane **12**, which is synthesized by a two-step reaction route from tetrachlorosilane with a total yield of 40–45% (∼65% for the first step and ∼70% for the second step) and the substituted bithiophene **13** to yield 4,4′-dialkyldithieno[3,2-*b*:2′,3′-*d*]silole **14** in 70% yield [226]. The polymer PSBTBT was prepared by a Stille coupling reaction from the monomer **16**, which was synthesized from **14** by commonly used methods. The molecular weight of the polymer was found to be 18 kDa (M_n, polydispersity 1.2). The polymer is stable up to 250°C in air. The HOMO and LUMO levels of PSBTBT were determined at −5.05 and −3.27 eV with an optical band gap of 1.45 eV, similar to its carbon analog PCPDTBT (Fig. 48). In OTFT the

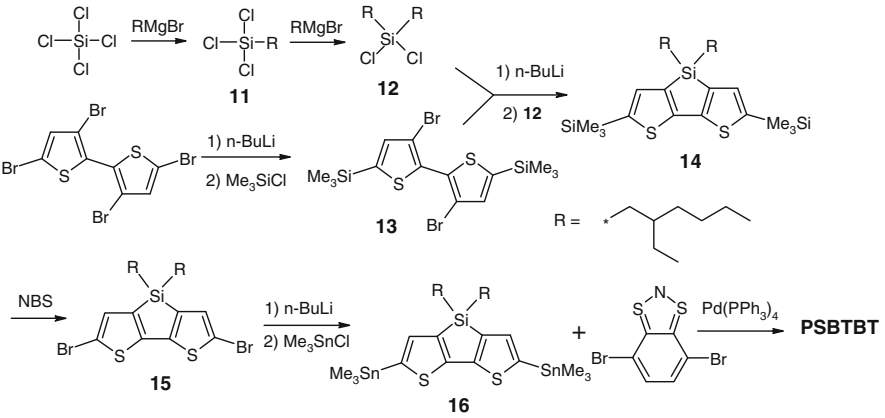

Scheme 20 Synthesis route of the polymer PSBTBT

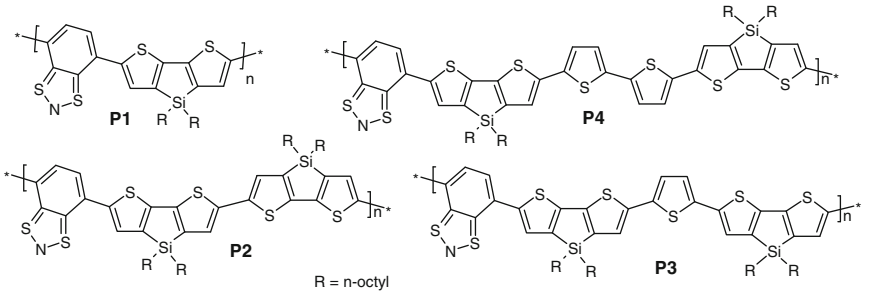

Fig. 49 Structures of DTS-BT copolymers P1, P2, P3, and P4 [228]

hole mobility value of $3 \times 10^{-3}\,cm^2\,V^{-1}\,s^{-1}$ was found to be three times higher than that for PCPDTBT [227]. These characteristics indicate its suitability as active material for OPV, and indeed bulk junction solar cells (layer structure: ITO/PEDOT-PSS/PSBTBT:PCBM/Ca/Al) exhibited a PCE of 4.7% (average of 100 devices, maximum: 5.1% with V_{oc} 0.68 V, J_{sc} 12.7 mA cm^{-2}, and FF 55%).

Recently Müllen and Reynolds described another successful combination of silole and benzothiazole donor–acceptor copolymers: the copolymer of dithieno[3,2-*b*:2′,3′-*d*]silole (DTS) and 2,1,3-benzothiadiazole (BT) (Fig. 49) [228]. In a series of DTS-BT copolymers (P1, P2, P3, and P4) two polymers (P2, P3) were found with unusually broad homogeneous spectral absorptions (in the range of 400–800 nm). Stille coupling reactions were used to obtain the unsymmetrical copolymers P1, P3, and P4, while the symmetrical P2 was polymerized by oxidative coupling with $FeCl_3$ followed by reduction with hydrazine. All polymers exhibited moderate molecular weights 10–20 kDa (M_n) and large polydispersities (3.2–3.8). Hole mobilities in bottom-contact OFETs increased from $10^{-6}\,cm^2\,V^{-1}\,s^{-1}$ for polymer P1 to $10^{-2}\,cm^2\,V^{-1}\,s^{-1}$ for polymer P4 which may be explained by an increasing trend to crystallize due to additional, unsubstituted thienyl monomer units. The unsubstituted bithiophene group in P4 creates effective hopping sites for the charge carriers, reduces the concentration of solubilizing groups, and enhances the backbone planarity. As required for solar cell applications, P4 absorbs light homogeneously across the entire visible spectrum.

In summary, a manifold of silole-containing polymers have been synthesized and studied. Especially polymers with TS and BS building blocks present an emerging class of functional materials, the electronic and optical properties of which open good perspectives for creation of highly thermal and environmentally stable organic electronics devices with outstanding performance.

7 Conclusions and Outlook

The analysis of different conjugated organosilicon structures revealed that silicon may be incorporated into the structures of oligomeric, dendritic, HB, and polymeric semiconducting molecules by many ways to achieve quite different effects.

A number of brilliant examples exploit the electronic interaction of silicon with the π-systems to adjust HOMO and LUMO energy levels and modify (usually lower) the band gap. The incorporation of silicon may be combined with the attachment of other groups with similar function to achieve synergistic effects. Attachment of silicon-containing bulky groups will hinder aggregation, therefore raise the solubility, and have an impact on electronic properties associated with the formation of aggregates.

Many silicon-containing organic semiconductors define the state of the art in their target application like organic electronic and photonic devices. Among them are silicon-modified oligoacenes (TES-ADT-F2) with a hole mobility greater than $1.0\,cm^2\,V^{-1}\,s^{-1}$ processed from solutions [53] and $6\,cm^2\,V^{-1}\,s^{-1}$ made from single crystals [54]. Oligothiophenes with silicon-containing anchor groups for the first time yielded SAMFETs with a mobility of $0.04\,cm^2\,V^{-1}\,s^{-1}$ and on/off ratio of 1×10^8 at 40 µm channel length devices [25] as well as functional integrated circuits containing over 300 SAMFETS working simultaneously [28]. Other organosilicon semiconductors based on siloles-containing oligomers and polymers yielded highly efficient blue OLEDs with external quantum yield 8% and the power efficiency of $20\,lm\,W^{-1}$ [70] or superior thermal and devices stability [206, 217]. Improved solar cells were prepared from silafluorene copolymers and many other examples having a PCE up to 5.4% [222]. Most of the organosilicon materials considered above possess high thermal, electrical and environmental stability lacking today in conventional organic electronics. Bearing these achievements we foresee an increasing interest in this class of compounds which might result in numerous publications and successful innovation in the nearest future.

References

1. Forrest SR (2004) The path to ubiquitous and low-cost organic electronic appliances on plastic. Nature 428:911–918
2. Klauk H (ed) (2006) Organic electronics: materials, manufacturing and applications. Wiley-VCH, Weinheim
3. Facchetti A (2007) Semiconductors for organic transistors. Mater Today 10:28–38
4. Braun D (2002) Semiconducting polymer LEDs. Mater Today 5:32–39
5. Brabec C, Dyakonov C, Scherf U (eds) (2008) Organic photovoltaics. Wiley-VCH, Weinheim
6. Mayer AC, Scully SR, Hardin BE, Rowell MW, McGehee MD (2007) Polymer-based solar cells. Mater Today 10:28–33
7. Lloyd MT, Anthony JE, Malliaras GG (2007) Photovoltaics from soluble small molecules. Mater Today 10:34–41
8. Sokolov AN, Roberts ME, Bao Z (2009) Fabrication of low-cost electronic biosensors. Mater Today 12:12–20
9. Sun Y, Liu Y, Zhu D (2005) Advances in organic field-effect transistors. J Mater Chem 15: 53–65
10. Murphy AR, Fréchet JMJ (2007) Organic semiconducting oligomers for use in thin film transistors. Chem Rev 107:1066–1096
11. Sauvajol JL, Lère-Porte JP, Moreau JJE (1997) Silicon-containing thiophene oligomers and polymers: synthesis, characterization and properties. In: Nalwa NS (ed) Conductive polymers. Handbook of organic conductive molecules and polymers, vol 2. Wiley, New York

12. Herrema JK, Hutten PF, Gill RE, Wildeman J, Wieringa RH, Hadziioannou G (1995) Tuning of the luminescence in multiblock alternating copolymers. 1. synthesis and spectroscopy of poly [(silanylene)thiophenels. Macromolecules 28:8102–8116
13. Tour JM, Wu R (1992) Synthesis and UV-visible properties of soluble α-thiophene oligomers. Monomer to octamer. Macromolecules 25:1901–1907
14. Hapiot P, Gaillon L, Audebert P, Moreau JJE, Lère-Porte JP, Wong Chi Man M (1995) Solvent effects on the polymerization kinetics of some alfa-sylulated thiophene oligomers. Special influence of the α-silyl group. Synth Met 72:129–134
15. Lere-Porte JP, Moreau JJE, Torreilles C, Bouachrine M, Sauvajol JL, Serein-Spirau F (1999) Oxidative polymerisation of silyl monomers. Applications and limits. Synth Met 101:15–16
16. Barbarella G, Ostoja P, Maccagnani P, Pudova O, Antolini L, Casarini D, Bongini A (1998) Structural and electrical characterization of processable bis-silylated thiophene oligomers. Chem Mater 10:3683–3689
17. Halik M, Klauk H, Zschieschang U, Schmid G, Radlik W, Ponomarenko S, Kirchmeyer S, Weber W (2003) High-mobility organic thin-film transistors based on α,α'-didecyloligothiophenes. J Appl Phys 93:2977–2981
18. Halik M, Klauk H, Zschieschang U, Schmid G, Ponomarenko S, Kirchmeyer S, Weber W (2003) Relationship between molecular structure and electrical performance of oligothiophene organic thin film transistors. Adv Mater 15:917–922
19. Yassar A, Garnier F, Deloffre F, Horowitz G, Ricard L (1994) Crystal structure of α,ω-bis(triisopropylsylyl)-sexithiophene: unusual conjugated chain distortion induced by interchain steric effects. Adv Mater 6:660–663
20. Kim DH, Ohshita J, Kosuge T, Kunugi A, Kunai A (2006) Synthesis of silicon-bridged oligothiophenes and applications to thin film transistors. Chem Lett 35:266–267
21. Ohshita J, Izumi Y, Kim DH, Kunai A, Kosuge T, Kunugi Y, Naka A, Ishikawa M (2007) Applications of silicon-bridged oligothiophenes to organic FET materials. Organometallics 26:6150–6154
22. Facchetti A, Mushrush M, Yoon MH, Hutchison GR, Ratner MA, Marks TJ (2004) Building blocks for n-type molecular and polymeric electronics. perfluoroalkyl- versus alkyl-functionalized oligothiophenes (nT; n = 2–6). Systematics of thin film microstructure, semiconductor performance, and modeling of majority charge injection in field-effect transistors. J Am Chem Soc 126:13859–13874
23. Meyer-Friedrichsen T, Elschner A, Keohan F, Lövenich W, Ponomarenko SA (2009) Conductors and semiconductors for advanced organic electronics. Proc SPIE 7417:741704
24. Ponomarenko SA, Borshchev OV, Setayesh S, Smits ECP, Mathijssen SGJ, Pleshkova AP, Meyer-Friedrichsen T, Kirchmeyer S, Muzafarov AM, de Leeuw DM (2010) Synthesis of monochlorosilyl derivatives of dialkyloligothiophenes for self-assembling monolayer field-effect transistors. Organometallics (submitted)
25. Mathijssen SGJ, Smits ECP, van Hal PA, Wondergem HJ, Ponomarenko SA, Moser A, Resel R, Bobbert PA, Kemerink M, Janssen RAJ, de Leeuw DM (2009) Monolayer coverage and channel length set the mobility in self-assembled monolayer field-effect transistors. Nat Nanotechnol 4:674–680
26. Gholamrezaie F, Mathijssen SGJ, Smits ECP, Geuns TCT, van Hal PA, Ponomarenko SA, Cantatore E, Blom PWM, de Leeuw DM (2010) Ordered semiconducting self-assembled monolayers on polymeric surfaces applied in organic integrated circuits. Nano Lett (accepted)
27. Mottaghi M, Lang P, Rodriguez F, Rumyantseva A, Yassar A, Horowitz G, Lenfant S, Tondelier D, Vuillaume D (2007) Adv Funct Mater 17:597–604
28. Smits ECP, Mathijssen SGJ, van Hal PA, Setayesh S, Geuns TCT, Mutsaers KAHA, Cantatore E, Wondergem HJ, Werzer O, Resel R, Kemerink M, Kirchmeyer S, Muzafarov AM, Ponomarenko SA, de Boer B, Blom PWM, de Leeuw DM (2008) Bottom up organic integrated circuits. Nature 455:956–959
29. Anthony JE (2006) Functionalized acenes and heteroacenes for organic electronics. Chem Rev 106:5028–5048

30. Landis CA, Parkin SR, Anthony JE (2005) Silylethynylated anthracene derivatives for use in organic light-emitting diodes. Jpn J Appl Phys 44:3921–3922
31. Odom SA, Parkin SR, Anthony JE (2003) Tetracene derivatives as potential red emitters for organic LEDs. Org Lett 5:4245–4248
32. Karatsu T, Hazuku R, Asuke M, Nishigaki A, Yagai S, Suzuri Y, Kita H, Kitamura A (2007) Blue electroluminescence of silyl substituted anthracene derivatives. Org Electron 8:357–366
33. Kelley TW, Muyres DV, Baude PF, Smith TP, Jones TD (2003) High performance organic thin film transistors. Mater Res Soc Symp Proc 771:169-179
34. Allen CFH, Bell A (1942) Action of Grignard reagents on certain pentacenequinones, 6,13-diphenylpentacene. J Am Chem Soc 64:1253–1260
35. Anthony JE, Brooks JS, Eaton DL, Parkin SR (2001) Functionalized pentacene: improved electronic properties from control of solid-state order. J Am Chem Soc 123:9482–9483
36. Anthony JE, Eaton DL, Parkin S.R (2002) A road map to stable, soluble, easily crystallized pentacene derivatives. Org Lett 4:15–18
37. Sheraw CD, Jackson TN, Eaton DL, Anthony JE (2003) Functionalized pentacene active layer organic thin-film transistors. Adv Mater 15:2009–2011
38. Park SK, Jackson TN, Anthony JE, Mourey DA (2007) High mobility solution processed 6,13-bis(triisopropyl-silylethynyl) pentacene organic thin film transistors. Appl Phys Lett 91:063514
39. Troisi A, Orlandi G, Anthony JE (2005) Electronic interactions and thermal disorder in molecular crystals containing cofacial pentacene units. Chem Mater 17:5024–5031
40. Lobanova Griffith O, Gruhn NE, Anthony JE, Purushothaman B, Lichtenberger DL (2008) Electron transfer parameters of triisopropylsilylethynyl-substituted oligoacenes. J Phys Chem C 112:20518–20524
41. Lloyd MT, Mayer AC, Tayi AS, Bowen AM, Kasen TG, Herman DJ, Mourey DA, Anthony JE, Malliaras GG (2006) Photovoltaic cells from a soluble pentacene derivative. Org Electron 7:243–248
42. Miller GP, Briggs J, Mack J, Lord PA, Olmstead MM, Balch AL (2003) Fullerene–acene chemistry: single-crystal X-ray structures for a [60]fullerene–pentacene monoadduct and a cis-bis[60]fullerene adduct of 6,13-diphenylpentacene. Org Lett 5:4199–4202
43. Sakamoto Y, Suzuki T, Kobayashi M, Gao Y, Fukai Y, Inoue Y, Sato F, Tokito S (2004) Perfluoropentacene: high-performance p-n junctions and complementary circuits with pentacene. J Am Chem Soc 126:8138–8140
44. Inoue Y, Sakamoto Y, Suzuki T, Kobayashi M, Gao Y, Tokito S (2005) Organic thin-film transistors with high electron mobility based on perfluoropentacene. Jpn J Appl Phys 44:3663–3668
45. Swartz CR, Parkin SR, Bullock JE, Anthony JE, Mayer AC, Malliaras GG (2005) Synthesis and characterization of electron-deficient pentacenes. Org Lett 7:3163–3166
46. Wolak MA, Melinger JS, Lane PA, Palilis LC, Landis CA, Delcamp J, Anthony JE, Kafafi ZH (2006) Photophysical properties of dioxolane-substituted pentacene derivatives dispersed in tris(quinolin-8-olato)aluminum(III). J Phys Chem B 110:7928–7937
47. Wolak MA, Delcamp J, Landis CA, Lane PA, Anthony J, Kafafi Z (2006) High-performance organic light-emitting diodes based on dioxolane-substituted pentacene derivatives. Adv Funct Mater 16:1943–1949
48. Chiang CL, Wu MF, Dai CC, When YS, Wang JK, Chen CT (2005) Red-emitting fluorenes as efficient emitting hosts for non-doped, organic red-light-emitting diodes. Adv Funct Mater 15:231–238
49. Laquindanum JG, Katz HE, Lovinger AJ (1998) Synthesis, morphology, and field-effect mobility of anthradithiophenes. J Am Chem Soc 120:664–672
50. Payne MM, Parkin SR, Anthony JE, Kuo CC, Jackson TN (2005) Organic field-effect transistors from solution-deposited functionalized acenes with mobilities as high as 1 cm^2/vs. J Am Chem Soc 127:4986–4987
51. Dickey KC, Smith TJ, Stevenson KJ, Subramanian S, Anthony JE, Loo YL (2007) Establishing efficient electrical contact to the weak crystals of triethylsilylethynyl anthradithiophene. Chem Mater 19:5210–5215

52. Lloyd MT, Mayer AC, Subramanian S, Mourey DA, Herman DJ, Bapat AV, Anthony JE, Malliaras GG (2007) Efficient solution-processed photovoltaic cells based on an anthradithiophene/fullerene blend. J Am Chem Soc 129:9144–9149
53. Subramanian S, Park SK, Parkin SR, Podzorov V, Jackson TN, Anthony JE (2008) Chromophore fluorination enhances crystallization and stability of soluble anthradithiophene semiconductors. J Am Chem Soc 130:2706–2707
54. Jurchescu OD, Subramanian S, Kline RJ, Hudson SD, Anthony JE, Jackson TN, Gundlach DJ (2008) Organic single-crystal field-effect transistors of a soluble anthradithiophene. Chem Mater 20:6733–6737
55. Platt AD, Day J, Subramanian S, Anthony JE, Ostroverkhova O (2009) Optical, fluorescent, and (photo)conductive properties of high-performance functionalized pentacene and anthradithiophene derivatives. J Phys Chem C 113:14006–14014
56. Payne MM, Parkin SR, Anthony JE (2005) Functionalized higher acenes: hexacene and heptacene. J Am Chem Soc 127:8028–8029
57. Payne MM, Odom SA, Parkin SR, Anthony JE (2004) Stable, crystalline acenedithiophenes with up to seven linearly fused rings. Org Lett 6:3325–3328
58. Yamaguchi S, Tamao K (1998) Silole-containing σ- and π-conjugated compounds. J Chem Soc Dalton Trans:3693–3702, Doi: http://dx.doi.org/10.1039/a804491k
59. Tamao K, Yamaguchi S, Shiro M (1994) Oligosiloles: first synthesis based on a novel endo-endo mode intramolecular reductive cyclization of diethynylsilanes. J Am Chem Soc 116:11715–11722
60. Yamaguchi S, Jin RZ, Tamao K, Shiro M (1997) Silicon-catenated silole oligomers: oligo(1,1-silole)s. Organometallics 16:2486–2488
61. Kanno K, Ichinohe M, Kabuto C, Kira M (1998) Synthesis and structure of a series of oligo[1,1-(2,3,4,5-tetramethylsilole)]s. Chem Lett 27:99–100
62. Tamao K, Yamaguchi S, Ito Y, Matsuzaki Y, Yamabe T, Fukushima M, Mori S (1995) Silole-containing n-conjugated systems. 3. Series of silole-thiophene cooligomers and copolymers: synthesis, properties, and electronic structures. Macromolecules 28:8668–8675
63. Tamao K, Ohno S, Yamaguchi S (1996) Silole–pyrrole co-oligomers: their synthesis, structure and UV-VIS absorption spectra. Chem Commun:1873–1874
64. Tamao K, Uchida M, Izumizawa T, Furukawa K, Yamaguchi S (1996) Silole derivatives as efficient electron transporting materials. J Am Chem Soc 118:11974–11975
65. Murata H, Kafafi ZH, Uchida M (2002) Efficient organic light-emitting diodes with undoped active layers based on silole derivatives. Appl Phys Lett 80:189–191
66. Palilisa LC, Mäkinen AJ, Uchida M, Kafafi ZH (2003) Highly efficient molecular organic light-emitting diodes based on exciplex emission. Appl Phys Lett 82:2209–2214
67. Yamaguchi S, Endo T, Uchida M, Izumizawa T, Furukawa K, Tamao K (2000) Toward new materials or organic electroluminescent devices: synthesis, structures, and properties of a series of 2,5-diaryl-3,4-dippenylsiloles. Chem Eur J 6:1683–1692
68. Lee SH, Jang BB, Kafafi ZH (2005) Highly fluorescent solid-state asymmetric spirosilabifluorene derivatives. J Am Chem Soc 127:9071–9078
69. Braye EH, Hübel W, Caplier I (1961) New unsaturated heterocyclic systems I. J Am Chem Soc 83:4406–4413
70. Luo J, Xie Z, Lam JWY, Cheng L, Chen H, Qiu C, Kwok HS, Zhan X, Liu Y, Zhu D, Tang BZ (2001) Aggregation-induced emission of 1-methyl-1,2,3,4,5-pentaphenylsilole. Chem Commun 1740–1741
71. Yu G, Yin S, Liu Y, Chen J, Xu X, Sun X, Ma D, Zhan X, Peng Q, Shuai Z, Tang B, Zhu D, Fang W, Luo Y (2005) Structures, electronic states, photoluminescence, and carrier transport properties of 1,1-disubstituted 2,3,4,5-tetraphenylsiloles. J Am Chem Soc 127:6335–6346
72. Chen J, Law CCW, Lam JWY, Dong Y, Lo SMF, Williams ID, Zhu D, Tang BZ (2003) Synthesis, light emission, nanoaggregation, and restricted intramolecular rotation of 1,1-substituted 2,3,4,5-tetraphenylsiloles. Chem Mater 15:1535–1546
73. Son HJ, Han WS, Chun JY, Lee CJ, Han JI, Ko J, Kang SO (2007) Spiro-silacycloalkyl tetraphenylsiloles with a tunable exocyclic ring: preparation, characterization, and device application of 1,1'-silacycloalkyl-2,3,4,5-tetraphenylsiloles. Organometallics 26:519–526

74. Zeng Q, Li Z, Dong Y, Di C, Qin A, Hong Y, Ji L, Zhu Z, Jim CKW, Yu G, Li Q, Li Z, Liu Y, Qin J, Tang BZ (2007) Fluorescence enhancements of benzene-cored luminophors by restricted intramolecular rotations: AIE and AIEE effects. Chem Commun 70–72
75. Tang BZ, Zhan X, Yu G, Lee PPS, Liu Y, Zhu D (2001) Efficient blue emission from siloles. J Mater Chem 11:2974–2978
76. Mi B, Dong Y, Li Z, Lam JWY, Häußler M, Sung HHY, Kwok HS, Dong Y, Williams ID, Liu Y, Luo Y, Shuai Z, Zhu D, Tang BZ (2005) Making silole photovoltaically active by attaching carbazolyl donor groups to the silolyl acceptor core. Chem Commun 3583–3585
77. Gilman H, Gorsich RD (1955) A silicon analog of 9,9-diphenylfluorene. J Am Chem Soc 77:6380–6381
78. Gilman H, Gorsich RD (1958) Cyclic organosilicon compounds. I. Synthesis of compounds containing the dibenzosilole nucleus. J Am Chem Soc 80:1883–1886
79. Ohshita J, Nodono M, Watanabe T, Ueno Y, Kunai A, Harima Y, Yamashita K, Ishikawa M (1998) J Organomet Chem 553:487–491
80. Ohshita J, Nodono M, Kai H, Watanabe T, Kunai A, Komaguchi K, Shiotani M, Adachi A, Okita K, Harima Y, Yamashita K, Ishikawa M (1999) Synthesis and optical, electrochemical, and electron-transporting properties of silicon-bridged bithiophenes. Organometallics 18:1453–1459
81. Ohshita J, Kai H, Takata A, Iida T, Kunai K, Ohta N, Komaguchi K, Shiotani M, Adachi A, Sakamaki K, Okita K (2001) Effects of conjugated substituents on the optical, electrochemical, and electron-transporting properties of dithienosiloles. Organometallics 20:4800–4805
82. Lee IS, Kim SJ, Kwak YW, Choi MC, Park JW, Ha CS (2008) Synthesis of 2,6-diaryl-4,4-diphenyldithienosiloles and their luminescent properties. J Ind Eng Chem 14:344–349
83. Kim DH, Ohshita J, Lee KH, Kunugi Y, Kunai A (2006) Synthesis of π-conjugated oligomers containing dithienosilole units. Organometallics 25:1511–1516
84. Shimizu M, Tatsumi H, Mochida K, Oda K, Hiyama T (2008) Silicon-bridge effects on photophysical properties of silafluorenes. Chem Asian J 3:1238–1247
85. Ilies L, Tsuji H, Sato Y, Nakamura E (2008) Modular synthesis of functionalized benzosiloles by tin-mediated cyclization of (o-alkynylphenyl)silane. J Am Chem Soc 130:4240–4241
86. Ilies L, Tsuji H, Nakamura E (2009) Synthesis of benzo[b]siloles via KH-promoted cyclization of (2-alkynylphenyl)silanes. Org Lett 11:3966–3968
87. Shimizu M, Mochida K, Hiyama T (2008) Modular approach to silicon-bridged biaryls: palladium-catalyzed intramolecular coupling of 2-(arylsilyl)aryl triflates. Angew Chem Int Ed 47:9760–9764
88. Yamaguchi S, Xu C, Tamao K (2003) Bis-silicon-bridged stilbene homologues synthesized by new intramolecular reductive double cyclization. J Am Chem Soc 125:13662–13663
89. Xu C, Wakamiya A, Yamaguchi S (2005) Ladder oligo(*p*-phenylenevinylene)s with silicon and carbon bridges. J Am Chem Soc 127:1638–1639
90. Yamaguchi S, Xu C, Yamada H, Wakamiya A (2005) Synthesis, structures, and photophysical properties of silicon and carbon-bridged ladder oligo(*p*-phenylenevinylene)s and related π-electron systems. J Organomet Chem 690:5365–5377
91. Fukazawa A, Li Y, Yamaguchi S, Tsuji H, Tamao K (2007) Coplanar oligo(*p*-phenylenedisilenylene)s based on the octaethyl-substituted s-hydrindacenyl groups. J Am Chem Soc 129:14164–14165
92. Guay J, Diaz A, Wu R, Tour JM (1993) Electrochemical and electronic properties of neutral and oxidized soluble orthogonally fused thiophene oligomers. J Am Chem Soc 115:1869–1874
93. Aviram A (1988) Molecules for memory, logic, and amplification. J Am Chem Soc 110: 5687–5692
94. Tour JM, Wu R, Schumm JS (1991) Extended orthogonally fused conducting oligomers for molecular electronic devices. J Am Chem Soc 113:7064–7066
95. Lee SH, Jang BB, Kafafi ZH (2005) Highly fluorescent solid-state asymmetric spirosilabifluorene derivatives. J Am Chem Soc 127:9071–9078

96. Shumilkina EA, Borschev OV, Ponomarenko SA, Surin NM, Pleshkova AP, Muzafarov AM (2007) Synthesis and optical properties of linear and branched bithienylsilanes. Mendeleev Commun 17:34–36
97. Lukevics E, Ryabova V, Arsenyan P, Belyakov S, Popelis J, Pudova O (2000) Bithienylsilanes: unexpected structure and reactivity. J Organomet Chem 610:8–15
98. Schwarzer A, Schilling IC, Seichter W, Weber E (2009) Synthesis and X-ray crystal structures of new tetrahedral arylethynyl substituted silanes. Silicon 1:3–12
99. Tang H, Zhu L, Harima Y, Yamashita K, Lee KK, Naka A, Ishikawa M (2000) Strong fluorescence of nano-size star-like molecules. J Chem Soc Perkin Trans 2:1976–1979
100. Ishikawa M, Lee KK, Schneider W, Naka A, Yamabe T, Harima Y, Takeuchi T (2000) Synthesis and properties of nanosize starlike silicon compounds. Organometallics 19:2406–2407
101. Ishikawa M, Teramura H, Lee KK, Schneider W, Naka A, Kobayashi H, Yamaguchi Y, Kikugawa M, Ohshita J, Kunai A, Tang H, Harima Y, Yamabe T, Takeuchi T (2001) Nanosized, starlike silicon compounds. synthesis and optical properties of tris[(tert-butyldimethylsilyl)oligothienylenedimethylsilyl] methylsilanes. Organometallics 20:5331–5341
102. Arsenyan P, Pudova O, Popelis J, Lukevics E (2004) Novel radial oligothienyl silanes. Tetrahedron Lett 45:3109–3111
103. Roncali J, Thobie-Gautier C, Brisset H, Favart JF, Guy A (1995) Electro-oxidation of tetra(terthienyl)silanes: towards 3D electroactive π-conjugated systems. J Electroanal Chem 381:257–260
104. Garnier F, Yassar A, Hajlaoui R, Horowitz G, Deloffre F, Servet B, Ries S, Alnot P (1993) Molecular engineering of organic semiconductors: design of self-assembly properties in conjugated thiophene oligomers. J Am Chem Soc 115:8716–8721
105. Roquet S, de Bettignies R, Leriche P, Cravino A, Roncali J (2006) Three-dimensional tetra(oligothienyl)silanes as donor material for organic solar cells. J Mater Chem 16:3040–3045
106. Kleimyuk EA, Luponosov YN, Troshin PA, Khakina EA, Moskvin YL, Egginger M, Peregudova SM, Babenko SD, Razumov VF, Sariciftci NS, Muzafarov AM, Ponomarenko SA (2010) Three dimensional quater- and quinquethiophensilanes as promising electron donor materials for bulk heterojunction photovoltaic cells. J Mater Chem (submitted)
107. Ponomarenko SA, Tatarinova EA, Muzafarov AM, Kirchmeyer S, Brassat L, Mourran A, Moeller M, Setayesh S, de Leeuw DM (2006) Star-shaped oligothiophenes for solution-processible organic electronics: flexible aliphatic spacers approach. Chem Mater 18:4101–4108
108. Kirchmeyer S, Meyer-Friedrichsen T, Elschner A, Gaiser D, Lövenich W, Jonas F, Ponomarenko SA, Jang J (2008) Materials for organic electronics: conductors and semiconductors designed for wet processing. Proc SPIE 7054:705402
109. Mourran A, Defaux M, Luponosov YN, Ponomarenko SA, Muzafarov AM, Moeller M (2010) Film-formation of quaterthiophene derivatives and its multipods having branched 2-ethylhexyl end-groups. Thin Solid Films (submitted)
110. Troshin PA, Ponomarenko SA, Luponosov YN, Khakina EA, Egginger M, Meyer-Friedrichsen T, Elschner A, Peregudova SM, Buzin MI, Razumov VF, Sariciftci NS, Muzafarov AM (2010) Efficient solution-processible organic solar cells utilizing quaterthiophene-based multipods as electron donor materials. Solar Energy Materials & Solar Cells (submitted)
111. Kim C, Kim M (1998) Synthesis of carbosilane dendrimers based on tetrakis (phenylethynyl)silane. J Organomet Chem 563:43–51
112. Apperloo JJ, Janssen RAJ, Malenfant PRL, Fréchet JMJ (2000) Concentration-dependent thermochromism and supramolecular aggregation in solution of triblock copolymers based on lengthy oligothiophene cores and poly(benzyl ether) dendrons. Macromolecules 33:7038–7043
113. Adronov A, Malenfant PRL, Fréchet JMJ (2000) Synthesis and steady-state photophysical properties of dye-labeled dendrimers having novel oligothiophene cores: a comparative study. Chem Mater 12:1463–1472

114. Wang F, Kon AB, Rauh RD (2000) Synthesis of a terminally functionalized bromothiophene polyphenylene dendrimer by a divergent method. Macromolecules 33:5300–5302
115. Deng S, Locklin J, Patton D, Baba A, Advincula RC (2005) Thiophene dendron jacketed poly(amidoamine) dendrimers: nanoparticle synthesis and adsorption on graphite. J Am Chem Soc 127:1744–1751
116. Sebastian RM, Caminade AM, Majoral JP, Levillain E, Huchet L, Roncali J (2000) Electrogenerated poly(dendrimers) containing conjugated poly(thiophene) chains. Chem Commun 507–508
117. Zhang Y, Zhao C, Yang J, Kapiamba M, Haze O, Rothberg LJ, Ng MK (2006) Synthesis, optical, and electrochemical properties of a new family of dendritic oligothiophenes. J Org Chem 71:9475–9483
118. Mitchell WJ, Kopidakis N, Rumbles G, Ginley DS, Shaheen SE (2005) The synthesis and properties of solution processable phenyl cored thiophene dendrimers. J Mater Chem 15:4518–4528
119. Xia C, Fan X, Locklin J, Advincula RC (2002) A first synthesis of thiophene dendrimers. Org Lett 4:2067–2070
120. Xia C, Fan X, Locklin J, Advincula RC, Gies A, Nonidez W (2004) Characterization, supramolecular assembly, and nanostructures of thiophene dendrimers. J Am Chem Soc 126:8735–8743
121. Ma CQ, Mena-Osteritz E, Debaerdemaeker T, Wienk MM, Janssen RAJ, Bäuerle P (2007) Functionalized 3D oligothiophene dendrons and dendrimers: novel macromolecules for organic electronics. Angew Chem Int Ed 46:1679–1683
122. Ma CQ, Fonrodona M, Schikora MC, Wienk MM, Janssen RAJ, Bäuerle P (2008) Solution-processed bulk-heterojunction solar cells based on monodisperse dendritic oligothiophenes. Adv Funct Mater 18:3323–3331
123. Nakayama J, Lin JS (1997) An organosilicon dendrimer composed of 16 thiophene rings. Tetrahedron Lett 38:6043–6046
124. Ponomarenko SA, Muzafarov AM, Borshchev OV, Vodopyanov EA, Demchenko NV, Myakushev VD (2005) Synthesis of bithiophenesilane dendrimer of the first generation. Russ Chem Bull 3:684–690
125. Borshchev OV, Ponomarenko SA, Surin NM, Kaptyug MM, Buzin MI, Pleshkova AP, Demchenko NV, Myakushev VD, Muzafarov AM (2007) Bithiophenesilane dendrimers: synthesis and thermal and optical properties. Organometallics 26:5165–5173
126. Luponosov YN, Ponomarenko SA, Surin NM, Muzafarov AM (2008) Facile synthesis and optical properties of bithiophenesilane monodendrons and dendrimers. Org Lett 10:2753–2756
127. Gunawidjaja R, Luponosov YN, Huang F, Ponomarenko SA, Muzafarov AM, Tsukruk VV (2009) Photoluminescence and molecular ordering of functionalized bithiophenesilane monodendrons. Langmuir 25:9270–9284
128. Surin NM, Borshchev OV, Luponosov YN, Ponomarenko SA, Muzafarov AM (2010) Spectral-luminescent properties of oligothiophenesilane dendritic macromolecules. Russ J Phys Chem A (accepted)
129. Luponosov YN, Ponomarenko SA, Surin NM, Borshchev OV, Shumilkina EA, Muzafarov AM (2009) The first organosilicon molecular antennas. Chem Mater 21:447–455
130. Borshchev OV, Ponomarenko SA, Shumilkina EA, Luponosov YN, Surin NM, Muzafarov AM (2010) Branched oligothiophenesilanes with effective non-radiative energy transfer between the fragments. Russ Chem Bull (4) (accepted)
131. Xu Z, Moore JS (1994) Design and synthesis of a convergent and directional molecular antenna. Acta Polymer 45:83–87
132. Borschev OV (2007) Oligothiophenesilane dendrimers of the first generation: synthesis, optical and thermal properties. PhD Thesis, Moscow
133. You Y, An C, Lee D, Kim J, Park SY (2006) Silicon-containing dendritic tris-cyclometalated Ir(III) complex and its electrophosphorescence in a polymer host. J Mater Chem 16:4706–4713

134. Ponomarenko SA, Tatarinova EA, Meyer-Friedrichsen T, Kirchmeyer S, Setayesh S, de Leeuw DM, Magonov SN, Muzafarov AM (2007) Solution processible quaterthiophene-containing carbosilane dendrimers. Polym Mater Sci Eng 96:298–299
135. Gao C, Yan D (2004) Hyperbranched polymers: from synthesis to applications. Prog Polym Sci 29:183–275
136. Yao J, Son DY (1999) Hyperbranched poly(2,5-silylthiophenes). The possibility of σ-π conjugation in three dimensions. Organometallics 18:1736–1740
137. Ponomarenko S, unpublished results
138. Xiao Y, Wong RA, Son DY (2000) Synthesis of a new hyperbranched poly(silylenevinylene) with ethynyl functionalization. Macromolecules 33:7232–7234
139. Yoon K, Son DY (1999) Syntheses of hyperbranched poly(carbosilarylenes). Macromolecules 32:5210–5216
140. Chen J, Peng H, Law CCW, Dong Y, Lam JWY, Williams ID, Tang BZ (2003) Hyperbranched poly(phenylenesilolene)s: synthesis, thermal stability, electronic conjugation, optical power limiting, and cooling-enhanced light emission. Macromolecules 36:4319–4327
141. Chen J, Xie Z, Lam JWY, Law CCW, Tang BZ (2003) Silole-containing polyacetylenes. synthesis, thermal stability, light emission, nanodimensional aggregation, and restricted intramolecular rotation. Macromolecules 36:1108–1117
142. Kirchmeyer S, Ponomarenko S, Muzafarov A (2008) Macromolecular compounds with a core-shell structure. US patent 7,420,645
143. Masuda T, Higashimura T (1989) Synthesis and properties of silicon-containing polyacetylenes. In: Zeigler JM, Fearon FWG (eds) Silicon-based polymer science. Advances in chemistry, vol 224, pp 641–661, chapter doi: 10.1021/ba-1990–0224.ch035
144. Masuda T, Isobe E, Higashimura T, Takada K (1983) Poly[1-(trimethylsilyl)-1-propyne]: a new high polymer synthesized with transition-metal catalysts and characterized by extremely high gas permeability. J Am Chem Soc 105:7473–7474
145. Savoca AC, Surnamer AD, Tien CF (1993) Gas transport in poly(silylpropynes): the chemical structure point of view. Macromolecules 26:6211–6216
146. Yampolskii YP, Korikov AP, Shantarovich VP, Nagai K, Freeman BD, Masuda T, Teraguchi M, Kwak G (2001) Gas permeability and free volume of highly branched substituted acetylene polymers. Macromolecules 34:1788–1796
147. Kusumota T, Hiyama T. (1988) Polymerization of monomers containing two ethynyldimethylsilyl groups. Chem Lett 1149–1152
148. Chen J, Xie Z, Lam JWY, Law CCW, Zhong B (2003) Tang silole-containing polyacetylenes. synthesis, thermal stability, light emission, nanodimensional aggregation, and restricted intramolecular rotation. Macromolecules 36:1108–1117
149. Lee YB, Shim HK, Ko SW (2003) Silyl-substituted poly(thienylenevinylene) via heteroaromatic dehydrohalogenation polymerization. Macromol Rapid Commun 24:522–526
150. Höger S, McNamara JJ, Schricker S, Wudl F (1994) Novel silicon-substituted, soluble poly(phenylenviny1ene)s: enlargement of the semiconductor bandgap. Chem Mater 6: 171–173
151. Zhang C, Höger S, Pakbaz K, Wudl F, Heeger AJ (1994) Improved efficiency in green polymer light-emitting diodes with air-stable electrodes. J Electron Mater 23:453–458
152. Hwang DH, Shim HK, Lee JI, Lee KS (1994) Synthesis and properties of multifunctional poly(2-trimethylsilyl-1,4-phenylenevinylene): a novel, silicon-substituted, soluble PPV derivative. J Chem Soc Chem Commun 2461–2462
153. Kim ST, Hwang DH, Li XC, Grüner J, Friend RH, Holmes AB, Shim HK (1996) Efficient green electroluminescent diodes based on poly(2-dimethyloctylsilyl-1,4-phenylenevinylene). Adv Mater 8:979–982
154. Greenham NC, Samuel IDW, Hayes GR, Philips RT, Kessener YARR, Moratti SC, Holmes AB, Friend RH (1995) Measurement of absolute photoluminescence quantum efficiencies in conjugated polymers. Chem Phys Lett 241:89–96
155. Hwang DH, Kim ST, Shim HK, Holmes AB, Moratti SC, Friend RH (1996) Green light-emitting diodes from poly(2-dimethyloctylsilyl-1,4-phenylenevinylene). Chem Commun 2241–2242

156. Kim ST, Hwang DH, Holmes AB, Friend RH, Shim HK (1997) Green electroluminescent characteristics of poly(2-dimethyloctylsilyl-1,4-phenylenevinylene). Synth Met 84:655–656
157. Hwang DH, Kim ST, Shim HK, Holmes AB, Moratti SC, Friend RH (1997) Highly efficient green light-emitting diodes with aluminium cathode. Synth Met 84:615–618
158. Pei Q, Yu G, Zhang C, Yang Y, Heeger AJ (1995) Polymer light-emitting electrochemical cells. Science 269:1086–1088
159. Ahn T, Ko SW, Lee J, Shim HK (2002) Novel cyclohexylsilyl- or phenylsilyl-substituted poly(*p*-phenylene vinylene)s via the halogen precursor route and gilch polymerization. Macromolecules 35:3495–3505
160. Hwang DH, Kang IN, Lee JI, Do LM, Chu HY, Zyung T, Shim HK (1998) Synthesis and properties of silyl-substituted PPV derivative through two different precursor polymers. Polymer Bull 41:275–283
161. Chen ZK, Wang LH, Kang ET, Huang W (1999) Intense green light from a silyl-substituted poly(*p*-phenylenevinylene)-based light-emitting diode with air-stable cathode. Phys Chem Chem Phys 1:3789–3792
162. Chen ZK, Huang W, Wang LH, Kang ET, Chen BJ, Lee CS, Lee ST (2000) Family of electroluminescent silyl-substituted poly(*p*-phenylenevinylene)s: synthesis, characterization, and structure-property relationships. Macromolecules 33:9015–9025
163. Chu HY, Hwang DH, Do LM, Chang JH, Shim HK, Holmes AB, Zyung T (1999) Electroluminescence from silyl-disubstitutd PPV derivative. Synth Met 101:216–217
164. Wang LH, Chen ZK, Kang ET, Meng H, Huang W (1999) Synthesis, spectroscopy and electrochemistry study on a novel di-silyl substituted poly(*p*-phenylenevinylene). Synth Met 105:85–89
165. Geneste F, Fischmeister C, Martin RE, Holmes AB (2001) Ortho-methallation as a key step to the synthesis of silyl-substituted poly(*p*-phenylenevinylene). Synth Met 121:1709–1710
166. Rost H, Chuah BS, Hwang DH, Moratti SC, Holmes AB, Wilson J, Morgado J, Halls JJM, de Mello JC, Friend RH (1999) Novel luminescent polymers. Synth Met 102:937–938
167. Martin RE, Geneste F, Riehn R, Chuah BS, Cacialli F, Holmes AB, Friend RH (2001) Efficient electroluminescent poly(*p*-phenylenevinylene) copolymers for application in LEDs. Synth Met 119:43–44
168. Martin RE, Geneste F, Chuah BS, Fischmeister C, Ma Y, Holmes AB, Riehn R, Cacialli F, Friend RH (2001) Versatile synthesis of various conjugated aromatic homo- and copolymers. Synth Met 122:1–5
169. Ahn T, Jang MS, Shim HK, Hwang DH, Zyung T (1999) Blue electroluminescent polymers: control of conjugation length by kink linkages and substituents in the poly(*p*-phenylenevinylene)-related copolymers. Macromolecules 32:3279–3285
170. Shim HK, Song SY, Ahn T (2000) Efficient and blue light-emitting polymers composed of conjugated main chain. Synth Met 111/112:409–412
171. Ahn T, Song SY, Shim HK (2000) Highly photoluminescent and blue-green electroluminescent polymers: new silyl- and alkoxy-substituted poly(*p*-phenylenevinylene) related copolymers containing carbazole or fluorene groups. Macromolecules 33:6764–6771
172. Lee JH, Yu HS, Kim W, Gal YS, Park JH, Jin SH (2000) Synthesis and characterization of a new green-emitting poly(phenylenevinylene) derivative containing alkylsilylphenyl pendant. J Polym Sci A Polym Chem 38:4185–4193
173. Jin SH, Jang MS, Suh HS, Cho HN, Lee JH, Gal YS (2002) Synthesis and characterization of highly luminescent asymmetric poly(*p*-phenylene vinylene) derivatives for light-emitting diodes. Chem Mater 14:643–665
174. Jin SH, Jung HH, Hwang CK, Koo DS, Shin WS, Kim YI, Lee JW, Gal YS (2005) High electroluminescent properties of conjugated copolymers from poly[9,9-dioctylfluorenyl-2,7-vinylene]-co-(2-(3-dimethyldodecylsilylphenyl)-1,4-phenylene vinylene)] for light-emitting diode applications. J Polym Sci A Polym Chem 43:5062–5071
175. Ko SW, Jung BJ, Ahn T, Shim HK (2002) Novel poly(*p*-phenylenevinylene)s with an electron-withdrawing cyanophenyl group. Macromolecules 35:6217–6223

176. Ishikawa M, Ohshita J (1997) Silicon and germanium containing conductive polymers. In: Nalwa NS (ed) Conductive polymers. Handbook of organic conductive molecules and polymers vol 2. Wiley, New York
177. Ohshita J, Kunai A (1998) Polymers with alternating organosilicon and π-conjugated units. Acta Polym 49:379–403
178. Nate K, Ishikawa M, Ni H, Watanabe H, Saheki Y (1987) Photolysis of polymeric organosilicon systems. 4. Photochemical behavior of poly[p-(disilanylene)phenylene]. Organometallics 6:1673–1679
179. Ohshita J, Kanaya D, Ishikawa M, Koike T, Yamanaka T (1991) Polymeric organosilicon systems. 10. Synthesis and conducting properties of poly[2,5-(disilanylene)thienylenes]. Macromolecules 24:2106–2107
180. Chichart P, Corriu RJP, Moreau JJE, Garnier F, Yassar A (1991) Selective synthetic routes to electroconductive organosilicon polymers containing thiophene units. Chem Mater 3:8–10
181. Yi SH, Nagase J, Sato H (1993) Synthesis and characterization of soluble organosilicon polymers containing regularly repeated thiophene or terthiophene units. Synth Met 58:353–365
182. Ohshita J, Watanabe T, Kanaya D, Ohsaki H, Ishikawa M, Ago H, Tanaka K, Yamabe T (1994) Polymeric organosilicon systems. 22. Synthesis and photochemical properties of poly[(disilanylene)oligophenylylenes] and poly[(silylene)biphenylylenes]. Organometallics 13:5002–5012
183. Kunai A, Ueda T, Horata K, Toyoda E, Nagamoto I, Ohshita J, Ishikawa M, Tanaka K (1996) Polymeric organosilicon systems. 26. Synthesis and photochemical and conducting properties of poly[(tetraethyldisilanylene)oligo(2,5-thienylenes)]. Organometallics 15:2000–2008
184. Yi SH, Ohashi S, Sato H, Nomori H (1993) Syntheses and electrical properties of organosilicon polymers containing thiophene and anthraquinone units bull. Chem Soc Jpn 66:1244–1247
185. Ohshita J, Kim DH, Kunugi Y, Kunai A (2005) Synthesis of organosilanylene-oligothienylene alternate polymers and their applications to EL and FET materials. Organometallics 24:4494–4496
186. Ohshita J, Sugimoto K, Kunai A, Harima Y, Yamashita K (1999) Electrochemical and optical properties of poly[(disilanylene)oligophenylenes], peculiar behavior in the solid state. J Organomet Chem 580:77–81
187. Adachi A, Manhart SA, Okita K, Kido J, Ohshita J, Kunai A (1997) Multilayer electroluminescent device using organosilicon polymer as hole transport layer. Synth Met 91:333–334
188. He G, Pfeiffer M, Leo K, Hofmann M, Birnstock J, Pudzich R, Salbeck J (2004) High-efficiency and low-voltage p-i-n electrophosphorescent organic light-emitting diodes with double-emission layers. Appl Phys Lett 85:3911–3913
189. Manhart SA, Adachi A, Sakamaki K, Okita K, Ohshita J, Ohno T, Hamaguchi T, Kunai A, Kido J (1999) Synthesis and properties of organosilicon polymers containing 9,10-diethynylanthracene units with highly hole-transporting properties. J Organomet Chem 592:52–60
190. Suzuki H, Satoh S, Kimata Y, Kuriyama A (1995) Synthesis and properties of poly(methylphenylsilane) containing anthracene units. Chem Lett 451–452
191. Ohshita J, Takata A, Kai H, Kunai A, Komaguchi K, Shiotani M, Adachi A, Sakamaki K, Okita K, Harima Y, Kunugi Y, Yamashita K, Ishikawa M (2000) Synthesis of polymers with alternating organosilanylene and oligothienylene units and their optical, conducting, and hole-transporting properties. Organometallics 19:4492–4498
192. Kunugi Y, Harima Y, Yamashita K, Ohshita J, Kunai A, Ishikawa M (1996) Electrochemical anion doping of poly[(tetraethyldisilanylene) oligo(2,5-thienylene)] derivatives and their p-type semiconducting properties. J Electroanal Chem 414:135–139
193. Malliaras GG, Hadziioannou G, Herrema JK, Wildeman J, Wieringa RH, Gill RE, Lampoura SS (1993) Tuning of the photo- and electroluminescence in multi-block copolymers of poly[(silanylene)thiophene]s via exciton confinement. Adv Mater 5:721–723
194. Ohshita J, Yoshimoto K, Hashimoto M, Hamamoto D, Kunai A, Harima Y, Kunugi Y, Yamashita K, Kakimoto M, Ishikawa M (2003) Synthesis of organosilanylene–pentathienylene alternating polymers and their application to the hole-transporting materials in double-layer electroluminescent devices. J Organomet Chem 665:29–32

195. Tang H, Zhu L, Harima Y, Kunugi Y, Yamashita K, Ohshita J, Kunai A (2000) Optical study on electrochemical and chemical doping of polymers of oligothienyls bridged by monosilyl. Electrochim Acta 45:2771–2780
196. Kunugi Y, Harima Y, Yamashita K, Ohshita J, Kunai A, Ishikawa M (1996) Electrochemical anion doping of poly[(tetraethyldisilanylene) oligo(2,5-thienylene)] derivatives and their p-type semiconducting properties. J Electroanal Chem 414:135–139
197. Harima Y, Zhu L, Tang H, Yamashita K, Takata A, Ohshita J, Kunai A, Ishikawa M (1998) Electrochemical cleavage of a Si–Si bond in poly[(tetraethyldisilanylene) oligo(2,5-thienylene)] films. Synth Met 98:79–81
198. Tang H, Zhu L, Harima Y, Yamashita K, Ohshita J, Kunai A, Ishikawa M (1999) Electrochemistry and spectroelectrochemistry of poly[(tetraethyldisilanylene)quinque (2,5-thienylene)]. Electrochim Acta 44:2579–2587
199. Bokria JG, Kumar A, Seshadri V, Tran A, Sotzing GA (2008) Solid-state conversion of processable 3,4-ethylenedioxythiophene (EDOT) containing poly(arylsilane) precursors to π-conjugated conducting polymers. Adv Mater 20:1175–1178
200. Sotzing GA (2007) Conductive polymers from precursor polymers, method of making, and use thereof. US Patent Application US20070191576
201. Ohshita J, Nodono M, Watanabe T, Ueno Y, Kunai A, Harima Y, Yamashita K, Ishikawa M (1998) Synthesis and properties of dithienosiloles. J Organomet Chem 55:487–491
202. Ohshita J, Nodono M, Takata A, Kai H, Adachi A, Sakamaki K, Okita K, Kunai A (2000) Synthesis and properties of alternating polymers containing 2,6-diaryldithienosilole and organosilicon units. Macromol Chem Phys 201:851–857
203. Usta H, Lu G, Facchetti A, Marks TJ (2006) Dithienosilole- and dibenzosilole-thiophene copolymers as semiconductors for organic thin-film transistors. J Am Chem Soc 128:9034–9035
204. Lu G, Usta H, Risko C, Wang L, Facchetti A, Ratner MA, Marks TJ (2008) Synthesis, characterization, and transistor response of semiconducting silole polymers with substantial hole mobility and air stability. experiment and theory. J Am Chem Soc 130:7670–7685
205. Ohshita J, Kimura K, Lee KH, Kunai A, Kwak YW, Son EC, Kunugi Y (2007) Synthesis of silicon-bridged polythiophene derivatives and their applications to EL device materials. J Polym Sci A Polym Chem 45:4588–4596
206. Chan KL, McKiernan MJ, Towns CR, Holmes AB (2005) Poly(2,7-dibenzosilole): a blue light emitting polymer. J Am Chem Soc 127:7662–7663
207. Liu MS, Luo J, Jen AKY (2003) Efficient green-light-emitting diodes from silole-containing copolymers. Chem Mater 15:3496–3500
208. Mo Y, Tian R, Shi W, Cao Y (2005) Ultraviolet-emitting conjugated polymer poly(9,9′-alkyl-3,6-silafluorene) with a wide band gap of 4.0 eV. Chem Commun 4925–4926
209. Yang W, Hou Q, Liu C, Niu Y, Huang J, Yang R, Cao Y (2003) Improvement of color purity in blue-emitting polyfluorene by copolymerization with dibenzothiophene. J Mater Chem 13:1351–1355
210. Janietz S, Bradley DDC, Grell M, Giebeler C, Inbasekaran M, Woo EP (1998) Electrochemical determination of the ionization potential and electron affinity of poly(9,9-dioctylfluorene). Appl Phys Lett 73:2453
211. Chan KL, Watkins SE, Mak CSK, McKiernan MJ, Towns CR, Pascu SI, Holmes AB (2005) Poly(9,9-dialkyl-3,6-dibenzosilole): a high energy gap host for phosphorescent light emitting devices. Chem Commun 5766–5768
212. Scherf U, List EJW (2002) Semiconducting polyfluorenes: towards reliable structure-property relationships. Adv Mater 14:477–487
213. van Dijken A, Bastiaansen JJAM, Kiggen NMM, Langeveld BMW, Rothe C, Monkman A, Bach I, Stössel P, Brunner K (2004) Carbazole compounds as host materials for triplet emitters in organic light-emitting diodes: polymer hosts for high-efficiency light-emitting diodes. J Am Chem Soc 126:7718–7727
214. S Yamaguchi, T Endo, M Uchida, T Izumizawa, K Furukawa, K Tamao (2000) Toward new materials for organic electroluminescent devices: synthesis, structures, and properties of a series of 2, 5-diaryl-3,4-diphenylsiloles. Chem Eur J 6:1683–1692

215. Kawamura Y, Yanagida S, Forrest SR (2002) Energy transfer in polymer electrophosphorescent light emitting devices with single and multiple doped luminescent layers. J Appl Phys 92:87
216. Wang E, Li C, Mo Y, Zhang Y, Ma G, Shi W, Peng J, Yang W, Cao Y (2006) Poly(3,6-silafluorene-co-2,7-fluorene)-based high-efficiency and color-pure blue light-emitting polymers with extremely narrow band-width and high spectral stability. J Mater Chem 16:4133–4140, Doi: http://dx.doi.org/10.1039/b609250k
217. Wang E, Li C, Peng J, Cao Y (2007) High-efficiency blue light-emitting polymers based on 3,6-silafluorene and 2,7-silafluorene. J Polym Sci A Polym Chem 45:4941–4949
218. Wang F, Luo J, Yang K, Chen J, Huang F, Cao Y (2005) Conjugated fluorene and silole copolymers: synthesis, characterization, electronic transition, light emission, photovoltaic cell, and field effect hole mobility. Macromolecules 38:2253–2260
219. Wang Y, Hou L, Yang K, Chen J, Wang F, Cao Y (2005) Conjugated silole and carbazole copolymers: synthesis, characterization, single-layer light-emitting diode, and field effect carrier mobility. Macromol Chem Phys 206:2190–2198
220. Wang E, Li C, Zhuang W, Peng J, Cao Y (2008) High-efficiency red and green light-emitting polymers based on a novel wide bandgap poly(2,7-silafluorene). J Mater Chem 18:797–801
221. Horst S, Evans NR, Bronstein HA, Williams CK (2009) Synthesis of fluoro-substituted silole-containing conjugated materials. J Polym Sci A Polym Chem 47:5116–5125
222. Wang E, Wang L, Lan L, Luo C, Zhuang W, Peng J, Cao Y (2008) High-performance polymer heterojunction solar cells of a polysilafluorene derivative. Appl Phys Lett 92:033307
223. Liao L, Dai L, Smith A, Durstock M, Lu J, Ding J, Tao Y (2007) Photovoltaic-active dithienosilole-containing polymers. Macromolecules 40:9406–9412
224. Hou J, Chen HY, Zhang S, Li G, Yang Y (2008) Synthesis, characterization, and photovoltaic properties of a low band gap polymer based on silole-containing polythiophenes and 2,1,3-benzothiadiazole. J Am Chem Soc 130:16144–16145
225. Huo L, Chen HY, Hou J, Chen TL, Yang Y (2009) Low band gap dithieno[3,2-b:2′,3′-d]silole-containing polymers, synthesis, characterization and photovoltaic application. Chem Commun 5570–5572
226. Ohshita J, Nodono M, Watanabe T, Ueno Y, Kunai A, Harima Y, Yamashita K, Ishikawa M (1998) Synthesis and properties of dithienosiloles. J Organomet Chem 553:487–491
227. Zhu Z, Waller D, Gaudiana R, Morana M, Mühlbacher D, Scharber M, Brabec C (2007) Panchromatic conjugated polymers containing alternating donor/acceptor units for photovoltaic applications. Macromolecules 40:1981–1986
228. Beaujuge PM, Pisula W, Tsao HN, Ellinger S, Müllen K, Reynolds JR (2009) Tailoring structure-property relationships in dithienosilole-benzothiadiazole donor-acceptor copolymers. J Am Chem Soc 131:7514–7515

http://www.springer.com/978-3-642-16047-9

Silicon Polymers
Muzafarov, A.M. (Ed.)
2011, XIV, 234 p. 210 illus., 15 illus. in color., Hardcover
ISBN: 978-3-642-16047-9